Spacecraft Relative Attitude Formation Tracking on SO(3) Based on Line-of-Sight Measurements

by Tse-Huai Wu

B.S. in Power Mechanical Engineering, May 2008, National Tsing Hua University

A Thesis submitted to

The Faculty of
The School of Engineering and Applied Science
of The George Washington University
in partial fulfillment of the requirements
for the degree of Master of Science

January 31, 2013

Thesis directed by

Taeyoung Lee
Assistant Professor of Engineering and Applied Science

Abstract of Thesis

Spacecraft Relative Attitude Formation Tracking On SO(3) Based on Line-of-Sight Measurements

This thesis investigates the use of line-of-sight (LOS) measurements for the control of relative attitude formation among multiple spacecraft. It is based on the fact that two pointing directions, referring to LOS measurements, from the spacecraft to distinct objects can determine the absolute attitude of spacecraft. With the same approach, LOS measurements from cost-effective vision-based sensors can be applied to obtain the relative attitude among spacecraft. In the proposed approach, high accuracy of attitude control and simpler control scheme can be constructed by designing the control law in terms of LOS measurements. In addition, the relative attitude controller provides almost global exponential stability on the nonlinear configuration manifold of relative attitude. The described properties are illustrated by numerical examples.

In conventional approaches, the absolute attitude is measured locally by using an inertial measurement unit, and they are compared to determine relative attitude, thereby causing the accumulation of measurement errors and complex controller structures.

Table of Contents

Abstract of Thesis **iii**

List of Figures **v**

1 Introduction **1**

1.1 Motivation 1

1.2 Literature Review 3

1.3 Thesis Outline 5

1.4 Contributions 6

2 Tracking control of A Spherical Pendulum on the Two-Sphere **9**

2.1 Equation of Motion 9

2.2 PD Tracking Control of a Spherical Pendulum on Two-Sphere 12

2.2.1 Error Dynamics 12

2.2.2 Control System Design 17

2.3 PID Tracking Control of a Spherical Pendulum on Two-Sphere 21

2.4 Numerical Example 23

3 Vision-based Spacecraft Attitude Control on $\mathsf{SO}(3)$ **28**

3.1 Problem Formulation 28

3.1.1 Attitude Dynamics on $\mathsf{SO}(3)$ 28

3.1.2 Vision-Based Attitude Control Problem 30

3.2 Almost Global Exponential Tracking Control on $\mathsf{SO}(3)$ 32

3.2.1 Error Variables 33
3.2.2 Control System Design 41
3.3 Numerical Example 48

4 Spacecraft Relative Attitude Formation Tracking on SO(3) Based on Line-Of-Sight Measurements 49

4.1 Problem Formulation 49
4.1.1 Spacecraft Attitude Formation Configuration 50
4.1.2 Spacecraft Attitude Dynamics 54
4.1.3 Kinematics of Relative Attitudes and Line-Of-Sight 55
4.2 Relative Attitude Tracking Between Two Spacecrafts 55
4.2.1 Kinematics of Relative Attitude 56
4.2.2 Relative Attitude Tracking 66
4.3 Relative Attitude Formation Tracking 72
4.3.1 Relative Attitude Tracking Between Three Spacecrafts 73
4.3.2 Relative Attitude Formation Tracking Between n Spacecrafts . 78
4.4 Numerical Example 83

5 Conclusions 85

5.1 Concluding Remarks 85
5.2 Future Work 86

Bibliography 88

A Hat Map Identities 93

B The Spectral Theorem 95

C MATLAB Codes 96

List of Figures

Figure2.1 Spherical pendulum 10

Figure2.2 Numerical results for spherical pendulum under PD controller without perturbation 25

Figure2.3 Numerical results for spherical pendulum under PD controller with fixed perturbation 26

Figure2.4 Numerical results for spherical pendulum under PID controller 27

Figure3.1 Single spacecraft attitude control with LOS measurements . . . 29

Figure3.2 Numerical results for single spacecraft attitude control 48

Figure4.1 Formation of four spacecrafts 53

Figure4.2 Relative attitude formation tracking for seven spacecrafts . . . 82

Figure4.3 Numerical results for seven spacecrafts in formation 84

Chapter 1 Introduction

This thesis investigates the use of Line-of-Sight (LOS) measurements for relative attitude formation between multiple spacecraft. Relative attitude is important in the multiple spacecraft formation since a constellation of spacecraft should have accurate relative motion to meet the goal of mission. Based on the approach of geometric control, the controller in this thesis exhibits exponential stability of the desired time-varying tracking command with a daisy-chaining structure of multiple spacecraft.

1.1 Motivation

Multiple spacecraft in mission Satellites technology has been widely applied for communication, navigation, outer space investigation, scientific research or military purposes. Multiple satellites flying as a group, working together to carry out assigned tasks, define formation. For instance, in the mission of the Space Technology 5 (ST-5), three micro-satellites successfully launched in 2006 to explore the magnetic field of Earth. The Cluster mission of European Space Agency (ESA) with the extend project Cluster II, cooperated with National Aeronautics and Space Administration (NASA), has four spacecraft to collect data.

Precise control of relative configuration between spacecraft is critical for many cooperative missions [1]. For example, the Space Technology 3 (ST-3) mission is a space-based interferometer consists of two spacecraft [2]. The interferometer is an array of telescopes acting jointly to probe structure by means of interferometry. If telescopes are carried by spacecraft operating in the outer space, various celestial

objects can be observed as the spacecraft translate, and high resolution images can be captured compare to the stationary interferometer on Earth affected by atmospheric distortion. Also, multiple telescopes can capture the target from different angles or at different times. Another example is the famous Darwin mission, directed by ESA and NASA, which is a constellation of four to five spacecraft searching for Earth-like planets. The images provided by each telescope are combined together such that Darwin would work as a single large telescope. To do so, the accuracy of relative position and attitude among spacecraft is critical. The telescopes and the hub must have stayed in formation with millimeter precision for Darwin to work [3].

Formation Control The spacecraft formation control can be categorized to control of relative position and relative attitude. Carrier-phase Differential GPS has been successfully applied to relative position control and estimation [4], [5]. It has been shown that high precision of GPS technology is effective for relative position control.

As for attitude control, combination of different inertial measurement unit (IMU), such as accelerometer, gyroscope, or magnetometer, is commonly applied to measure orientation of spacecraft [6]. There is also a hybrid system using camera and IMU jointly to perform rotation control [7]. Most of the relative attitude control systems are based on a common framework: the absolute attitude of the spacecraft, with respect to an inertial frame, is measured independently by using local inertial measurement units and then it is transformed to other vehicle to determine relative attitude. In other words, relative attitude is acquired by comparing the absolute attitude of each spacecraft.

Measurement errors are accumulated due to this indirect process, and the accuracy of attitude formation is impaired. When there are more spacecraft in the constellation, the accumulated error becomes larger. This error problem is not insuperable, but this approach requires high quality IMU sensors and sophisticated controllers that increase

the development cost substantially.

Vision-Based System In recent years, vision-based systems have been applied for the navigation of autonomous vehicles where optical sensors are used to extract visual features to locate a vehicle [8], [9]. Specifically, it has been shown that line-of-sight observations can be applied for relative attitude determination [10]. Optical sensors are cost-effective with high accuracies, and they have less noises compared with other inertial sensors. Also, they yield a long-term stability and it requires no frequent corrections in contrast to gyros.

Global and Unique Representation Typically, attitude control is studied by using Euler angles or quaternions [11], [12], [13], which are referred to as attitude parameterizations. None of these parameterizations can successfully represent attitude uniquely and globally. For instance, Euler angles have singularities, therefore, it is not possible to globally define the control law by using Euler angles. Quaternion representation does not the have the issue of singularity but there exists ambiguity since it is not unique in representing attitude. Hence, this thesis proposes to construct the control system in terms of rotation matrix to control the attitude globally and uniquely [14].

In summary, the goal of this thesis is to control attitude formation by using line-of-sight measurements to accomplish high level of performance and cost-effectiveness. It has desirable feature of accurate relative attitude determination, simple control structures, low-cost hardware requirement and robust stability.

1.2 Literature Review

Control of the direction of line-of-sight is similar to control the direction of a spherical pendulum since they evolve in the same configuration space. A spherical pendulum is a weight bob suspend from a pivot that allows to swing freely in 3-dimensional

space. As there is no rotation along the axis direction of the link of the pendulum, it has 2 rotational degrees of freedom. The direction from pivot to bob is analogous to the direction of line-of-sight measurements. The nonlinear dynamics of spherical pendulum has been studied in [15], [16], [17] by using local coordinate. In addition, Lagrangian mechanical systems on two-spheres has been studied in [18]. If the limitation of axial rotation is removed, the pendulum has 3 rotational degrees of freedom, which is called 3D pendulum. There is also research about 3D rigid pendulum with almost global asymptotic stabilization [19], [20].

Attitude control systems are developed in terms of Euler angles [21] or quaternions [12], [22], [23]. Quaternions do not have singularities like Euler angle. Therefore it may achieve global attitude tracking properties [24]. However, there is ambiguity in representing attitude [14]. A phenomenon called "unwinding", where the close-loop control input unnecessarily rotates the spacecraft through a large angle even if the initial attitude error is small, may happen if we do not deal with this ambiguity carefully [25]. Nevertheless, there are interesting contributions among these publications. There is a attitude controller designed for micro-satellite [21]. In [22], a controller without angular velocity is presented. In [23], control input in saturation is addressed.

Recently, attitude control on special orthogonal group $\mathsf{SO}(3)$, the set of three by three orthogonal matrices with determinant equal to one, has been studied [14], [26], [27], [28], [29]. The most important feature of this representation is that it the attitude is determined globally and uniquely.

The coordinated control of multiple spacecraft in formation has been studied extensively [30], [31]. Notable contributions on relative attitude can be categorized as leader-follower strategy [32], [13], behavior-based control [33], [34], and virtual structures [35], [36]. In the leader-follower scheme, one spacecraft on the reference orbit is assigned to be leader, other spacecraft are followers tracking the relative motion with respect to the leader. The behavior-based control defines the "behavior" for the

spacecraft as the purpose of tasks such as formation keeping or collision avoidance. Additionally, virtual structure control considers every spacecraft as an element of a larger, single entity. Some of research even combine two schemes in formation control [37]. A common drawback of strategy mentioned above, is absolute attitude of each vehicle must be observed before computing the relative attitude and the measurement error in each inertial measurement unit is accumulated during this process.

Vision-based sensors combined with image processing are applied in controlling end-effectors of robot manipulators to reduce positioning error and reduce the overall cost [38]. Recently, vision-based control systems have been widely applied for navigation of autonomous vehicles, flying or underwater [8], [39]. For instance, in [9], vision-based control are applied to stabilize a quadrotor. Moreover, the LOS observations are used for relative attitude determination of multiple vehicles [40], [41].

1.3 Thesis Outline

This thesis is concerned with development of relative attitude control system with vision based sensors. This is motivated by the fact that control of pointing direction of line-of-sight measurements on $\mathsf{SO}(3)$ is analogous to control the direction of a spherical pendulum on S^2. We start from control a spherical pendulum in the first step which is the subject of Chapter 2.

In chapter 3, we use vision-based method in the application of attitude control of single spacecraft. The basic properties and assumptions of vision-based control are described. The nonlinear structure of $\mathsf{SO}(3)$ are explicitly considered in the control system design, and proof of almost global exponential stability is proposed. These are extended to the relative attitude control between multiple spacecraft in the next chapter.

In Chapter 4, the structure of multiple spacecraft is outlined, and work of previous chapters are combined for relative attitude between multiple spacecraft. We first show

the relative attitude control between two spacecraft and then in three spacecraft. By observing the differences of these two solid examples, we generalized the controller to multiple spacecraft in the final stage and use the case of 7 spacecraft as an numerical example.

Each chapter comes with numerical simulations in the final section to demonstrate the properties of the controlled system.

1.4 Contributions

Vision-based Formation Control The presented control system uses line-of-sight measurements to control the relative attitude. In other words, the control inputs are expressed in terms of the direction measurements. Thus, we directly control the relative attitude without the need for estimating the absolute attitude of each spacecraft. This scheme is not only simpler than using the traditional inertia measurement units, but also provides a higher accuracy. Without comparing absolute attitude between each spacecraft, the issue of accumulated error does not exist in the vision-based control system which leads to higher accuracy.

In particular, vision-based sensors normally require complex image processing to extract the information and this causes high computational load. However, we only need the direction from optical sensors to determine the formation and it requires relatively low computational cost. Compare to gyroscopes, vision-based sensors do not need calibration as there is no drift or errors.

Resource sharing and Cost effectiveness As each spacecraft should be equipped with high accuracy sensors, the total development cost of multiple spacecraft may become extremely high. Several projects, such as TechSat 21 constellation of three spacecraft, directed by U.S. Air Force Research Laboratory (AFRL), were canceled due to cost over budget. From the aspect of allowance, vision-based sensors are

relatively inexpensive compare to other hardware systems. Therefore, it reduces the development cost significantly, especially in large number of spacecraft cluster. Additionally, as each spacecraft is equipped with onboard visual sensors, we do not need all of the measurements between them to estimate the corresponding relative attitude, hence the system can still function well even if some of the sensors break down.

Geometric nonlinear control on manifolds Special orthogonal group $\mathsf{SO(3)}$, the group for 3×3 rotation matrices with determinant equals to 1, represents the attitude of spacecraft both globally and uniquely. By using the geometric property $\mathsf{SO(3)}$, the proposed controller avoids singularity and ambiguity associated with local parameterization such as Euler angle or quaternion. On the other hand, two-sphere is the group of unit length vectors that describes the direction from the origin. By modeling the dynamic system of spherical pendulum directly on S^2 without using angles relative to basis axes, intricate trigonometric expressions are void. The equations of motion are expressed by a compact form that significantly reduces the complexity of the control system and computation loads in analysis. In summary, geometric control systems provide compact expressions and global representations in attitude formation control.

Almost Global Exponential stability for tracking control The relative attitude controller for multiple spacecraft and PD controller for spherical pendulum provide almost global exponential stability, which yields on exponential rate of convergence. Also, the equilibrium of exponential stability is robust with respect to perturbation with a linear growth bound. The term "almost global" implies that desired equilibrium configuration can be exponentially stabilized from almost all initial conditions. It has been shown that it is impossible to develop a continuous control system that globally asymptotically stabilize an equilibrium on a compact manifold

such as the two sphere S^2 or the special orthogonal group $\mathsf{SO}(3)$ due to their topological properties [42]. The almost global exponential stability is the best result for continuous control system.

Chapter 2 Tracking control of A Spherical Pendulum on the Two-Sphere

In this chapter, we analyze the dynamics of a spherical pendulum and we present a nonlinear control system for the time-varying tracking control problem. Pendulum model without linearization is a good source to accommodate the effect and characteristics of nonlinear dynamics. The control system is directly constructed on the two-sphere, which is a nonlinear manifold of the spherical pendulum.

The proportional-integral-derivative (PID) controller is the most commonly applied controller, however, the typical PID controllers are constructed on linear systems, and a PID controller on the two-sphere has not been studied.

2.1 Equation of Motion

Consider a spherical pendulum supported by a fixed and frictionless pivot that is connected to a mass m by a massless link l (Figure 2.1). The unit vector from the pivot to the center of bob is denoted by $q \in \mathbb{R}^3$ and the corresponding angular velocity is defined as $\omega \in \mathbb{R}^3$. Notice that ω is constrained to be normal to q, i.e. $\omega \cdot q = 0$. Since the pendulum lies in three dimensional space but with two dimensional degree of freedom in rotation, the configuration of the pendulum is in the space of two-sphere, a unit sphere in a three dimensional space, denoted by S^2. The mathematical

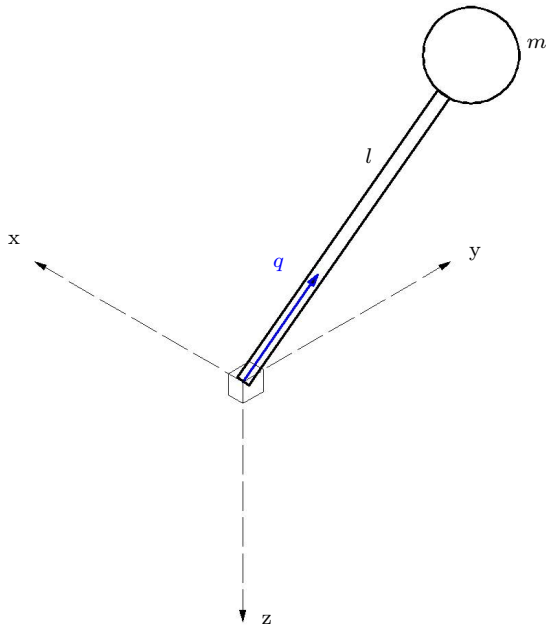

Figure 2.1: Spherical pendulum

definition of two-sphere is given by

$$\mathsf{S}^2 = \{q \in \mathbb{R}^3 \mid \|q\| = 1\}. \tag{2.1}$$

In particular, the kinematic equation on the two-sphere is

$$\dot{q} = \omega \times q. \tag{2.2}$$

Assume the pendulum is acting under a gravitational moment only. The angular momentum of the pendulum $\mathbf{H}$ is equal to the moment of inertia $I \in \mathbb{R}^3$ times angular velocity, namely the rate of change of the angular momentum is given by

$$\begin{aligned} H &= I\omega, \\ \dot{H} &= I\dot{\omega} = ml^2\dot{\omega}. \end{aligned} \tag{2.3}$$

The gravitational moment M_o is

$$M_o = r \times F = lq \times mge_3, \tag{2.4}$$

where r is the position vector which equals to the length times the unit vector, g denotes the gravitational constant and F represents the total force. Note that $e_3 = [0\ 0\ 1]^\mathsf{T}$ represents the unit vector along the direction of gravity according to the NED (North-East-Down) frame. Suppose that there is a control moment $u \in \mathbb{R}^3$ acting on the pivot. It is noteworthy that u is normal to q since any component of u along q does not have any effect on the pendulum dynamics. From Newton's second law, the rate of change of the angular momentum is equal to the sum of the moments, that is,

$$ml^2\dot{\omega} = M_o + u = lq \times mge_3 + u, \tag{2.5}$$

which implies the equation of motion:

$$\dot{\omega} = \frac{g}{l} q \times e_3 + \frac{1}{ml^2} u. \tag{2.6}$$

The projection of a vector $x \in \mathbb{R}^3$ to the plane normal to q is given by $-\hat{q}^2 x$, where the hat map $\hat{\cdot} : \mathbb{R}^3 \to \mathfrak{so}(3)$ is defined in Appendix A.

$$-\hat{q}^2 x = -q \times (q \times x) = -[(q \cdot x)q - (q \cdot q)x] = -(q \cdot x)q + x.$$

Considering the case $x \cdot q = 0$, above equation becomes $-\hat{q}^2 x = x$. Thus, for any $x \in \mathbb{R}^3$ that is noraml to q and any vector $y \in \mathbb{R}^3$, the following property holds:

$$x \cdot y = -\hat{q}^2 x \cdot y = -\hat{q}^2 y \cdot x. \tag{2.7}$$

2.2 PD Tracking Control of a Spherical Pendulum on Two-Sphere

We first drop the integral term to design a nonlinear proportional-derivative (PD) controller in this section. The characteristics of the two-sphere are carefully considered in the control system design, and we provide stronger convergent rate and almost global stability for the proposed control system.

2.2.1 Error Dynamics

Desired Trajectory Suppose that a smooth desired trajectory $q_d \in \mathbb{R}^3$ is given. It satisfies

$$\dot{q}_d = \omega_d \times q_d, \tag{2.8}$$

where $\omega_d \in \mathbb{R}^3$ is the desired angular velocity and it satisfies $\omega_d \cdot q_d = 0$. We can further obtain the following expressions:

$$\begin{aligned} \omega_d &= q_d \times \dot{q}_d, \\ \dot{\omega}_d &= q_d \times \ddot{q}_d. \end{aligned} \tag{2.9}$$

Furthermore, the desired angular velocity is assumed to be uniformly bounded by

$$\|\omega_d\| \leq B_{\omega d}, \ B_{\omega d} > 0.$$

Error Function To measure the difference between q and q_d, the error function of the state variable is introduced as:

$$\begin{aligned}\Psi(q, q_d) = \frac{1}{2}\|q - q_d\|^2 &= \frac{1}{2}(q - q_d)^{\mathsf{T}}(q - q_d) \\ &= \frac{1}{2}(q^{\mathsf{T}}q - q^{\mathsf{T}}q_d - {q_d}^{\mathsf{T}}q + {q_d}^{\mathsf{T}}q_d) \\ &= \frac{1}{2}[(\|q\|^2 + \|q_d\|^2) - 2q \cdot q_d] \\ &= 1 - q \cdot q_d. \end{aligned} \tag{2.10}$$

Note that $\|q\|^2 = \|q_d\|^2 = 1$, since both of q and q_d are unit vectors. Specifically, the range of the error function is $0 \leq \Psi(q, q_d) \leq 2$.

Direction Error Vector The variation of $q \in \mathsf{S}^2$ can be written as

$$q^{\epsilon} = \exp(\epsilon\hat{\xi})q,$$

where $\xi = [\xi_1 \ \xi_2 \ \xi_3]^{\mathsf{T}} \in \mathbb{R}^3$ is a vector and $\hat{\xi} \in \mathfrak{so}(3)$ is the skew-symmetric matrix defined as (A.1) in the appendix, which is rewritten as follows:

$$\hat{\xi} = \begin{bmatrix} 0 & -\xi_3 & \xi_2 \\ \xi_3 & 0 & -\xi_1 \\ -\xi_2 & \xi_1 & 0 \end{bmatrix}.$$

This represents the rotation of q about the axis ξ by the angle $\epsilon\|\xi\|$. There is a constraint that ξ is normal to q, i.e. $\xi \cdot q = 0$. Then, the corresponding infinitesimal variation is given by

$$\delta q = \left.\frac{d}{d\epsilon}\right|_{\epsilon=0} q^{\epsilon} = \xi \times q.$$

We can find the derivative of Ψ with respect to q along the direction of $\delta q = \xi \times q$ for $\xi \in \mathbb{R}^3$ with $\xi \cdot q = 0$ as follows:

$$\begin{aligned} D_q\Psi(q, q_d) \cdot \delta q &= \left.\frac{d}{d\epsilon}\right|_{\epsilon=0} \Psi(q^\epsilon, q_d) \\ &= -\delta q \cdot q_d = -(\xi \times q) \cdot q_d = (q_d \times q) \cdot \xi. \end{aligned}$$

From this, the configuration error vector is defined as:

$$e_q = q_d \times q. \tag{2.11}$$

Note that $e_q \cdot q = 0$.

Angular Velocity Error Vector In order to show the difference between q and q_d, the configuration error vector e_q is defined above. Similarly, the vector which links ω and ω_d is named as the angular velocity error vector and it is defined as

$$\begin{aligned} e_\omega &= \omega + \hat{q}^2\omega_d \qquad (2.12) \\ &= \omega + q \times (q \times \omega_d) \\ &= \omega + [(q \cdot \omega_d)q - (q \cdot q)\omega_d] \\ &= \omega - \omega_d + q(q \cdot \omega_d). \qquad (2.13) \end{aligned}$$

It is defined such that $e_\omega \cdot q = 0$.

Proposition 2.1. The tracking error dynamics is expressed by (2.10), (2.11) and (2.13), and they satisfies the following properties.

(i) $e_q \cdot q = e_\omega \cdot q = 0$.

(ii) $\frac{d}{dt}\Psi(q, q_d) = e_q \cdot e_\omega$.

(iii) $\dot{e}_q \cdot e_\omega \leq B_{\omega d}\|e_q\|\|e_\omega\| + \|e_\omega\|^2$.

(iv) $\frac{1}{2}\|e_q\|^2 \leq \Psi(q, q_d) \leq \frac{1}{2-\psi}\|e_q\|^2$, if $\Psi(q, q_d) \leq \psi < 2$.

Proof. Property (i) is from (2.13) and (2.11).

From (2.2) the time derivative of (2.10) is :

$$\begin{aligned}\dot{\Psi}(q, q_d) &= -\dot{q} \cdot q_d - q \cdot \dot{q_d} \\ &= -(\omega \times q) \cdot q_d - q \cdot (\omega_d \times q_d) \\ &= -\omega \cdot (q \times q_d) - \omega_d \cdot (q_d \times q) \\ &= (\omega - \omega_d) \cdot (e_q). \end{aligned} \tag{2.14}$$

Also, from (2.13)

$$\begin{aligned} e_q \cdot e_\omega &= e_q \cdot [\omega - \omega_d + q(q \cdot \omega_d)] \\ &= e_q \cdot (\omega - \omega_d), \end{aligned} \tag{2.15}$$

since $e_q \cdot q = 0$. This shows the property (ii).

From (2.8) and (2.11), the time derivative of the direction error vector is expressed as

$$\begin{aligned} \dot{e}_q &= \dot{q}_d \times q + q_d \times \dot{q} \\ &= (\omega_d \times q_d) \times q + q_d \times (\omega \times q). \end{aligned} \tag{2.16}$$

Then we apply the vector identity $x \times (y \times z) = y(x \cdot z) - z(x \cdot y)$ for x, y, $z \in \mathbb{R}^3$ and substitute (2.13) to obtain

$$\begin{aligned} \dot{e}_q &= [(\omega_d \cdot q)q_d - (q_d \cdot q)\omega_d] + [(q_d \cdot q)\omega - (q_d \cdot \omega)q] \\ &= (\omega_d \cdot q)q_d + (q_d \cdot q)(\omega - \omega_d) - (q_d \cdot \omega)q \\ &= (\omega_d \cdot q)q_d + (q_d \cdot q)[e_\omega - (q \cdot \omega_d)q] - (q_d \cdot \omega)q. \end{aligned} \tag{2.17}$$

The projection of $\dot{e}_q$ to the plane normal to q is given as

$$\begin{aligned} -\hat{q}^2\dot{e}_q &= -(\omega_d \cdot q)\hat{q}^2 q_d - (q_d \cdot q)[\hat{q}^2 e_\omega - (q \cdot \omega_d)\hat{q}^2 q] - (q_d \cdot \omega)\hat{q}^2 q \\ &= (\omega_d \cdot q)\hat{q}e_q + (q_d \cdot q)e_\omega, \end{aligned} \tag{2.18}$$

since $-\hat{q}^2 q_d = -q \times (q \times q_d) = q \times e_q = \hat{q}e_q$ and $\hat{q}^2 q = 0$. Also, $-\hat{q}^2 e_\omega = e_\omega$ since $e_\omega \cdot q = 0$. Again, noticing that e_ω is normal to q, we use (2.7) to obtain

$$\begin{aligned} e_\omega \cdot \dot{e}_q = e_\omega \cdot (-\hat{q}^2\dot{e}_q) &= (\omega_d \cdot q)\hat{q}e_q \cdot e_\omega + (q \cdot q_d)\|e_\omega\|^2 \\ &\leq \|\omega_d\|\|e_q\|\|e_\omega\| + \|e_\omega\|^2 \\ &\leq B_{\omega d}\|e_q\|\|e_\omega\| + \|e_\omega\|^2, \end{aligned}$$

which shows property (iii).

The last property is about the bounds of the error function. Define a constant ψ and $D = \{q \in \mathsf{S}^2 \mid \Psi(q, q_d) \leq \psi < 2\}$. From (2.10), we have $\Psi(q, q_d) = 1 - \cos(\theta)$ where $\theta \in \mathsf{S}^1$ is the angle between q and q_d. This yields:

$$0 \leq 1 - \cos(\theta) \leq \psi,$$

We rearrange the equation to have

$$\frac{1}{2} \leq \frac{1}{1 + \cos\theta} \leq \frac{1}{2 - \psi},$$

which yields

$$\frac{1}{2}\|e_q\|^2 \leq \frac{1}{1 + \cos\theta}\|e_q\|^2 \leq \frac{1}{2 - \psi}\|e_q\|^2.$$

From (2.11), we have $\|e_q\|^2 = \sin^2\theta$. Therefore, $\frac{1}{1+\cos\theta}\|e_q\|^2 = 1 - \cos\theta = \Psi(q, q_d)$,

which shows property (iv). □

2.2.2 Control System Design

Using the properties derived in previous section, we design a continuous feedback controller that exponentially stabilizes the desired eqilibium.

Proposition 2.2. Consider the system is given by (2.6) and (2.2) with a tracking command given by (2.8). The control input is designed as follows:

$$u = ml^2[-k_\omega e_\omega - k_q e_q - \hat{q}^2\dot{\omega}_d - \dot{q}(q\cdot\omega_d) - \frac{g}{l}q\times e_3], \tag{2.19}$$

where k_ω and k_q are positive constants. The following properties are satisfied by the control input:

(i) Equilibrium configuration is given by $(q,\omega) = (\pm q_d, \omega_d)$.

(ii) The desired equilibrium point (q_d, ω_d) is almost globally exponentially stable with an estimate of the region of attraction given by

$$\Psi(q(0), q_d(0)) \leq \psi < 2, \tag{2.20}$$

$$\|e_\omega(0)\|^2 \leq 2k_q(\psi - \Psi(q(0), q_d(0))). \tag{2.21}$$

(iii) The undesired equilibrium $(-q_d, \omega_d)$ is unstable.

The controller we present in (2.19) is expressed in terms of unit vector q, angular velocity ω which is much simpler than using complicated trigonometric functions. More importantly, the manifold converges to unstable equilibrium has less dimension than the tangent bundle of the configuration space of S^2. Therefore, *almost* global exponential stability is achieved.

Proof. Property (i) is from the fact that the zero equilibrium of the tracking errors is $(e_q, e_\omega) = (0, 0)$.

To find the region of attraction, define

$$\mathcal{U} = \frac{1}{2} e_\omega \cdot e_\omega + k_q \Psi(q, q_d).$$

A Lyapunov candidate is specified as

$$\mathcal{V} = \frac{1}{2} e_\omega \cdot e_\omega + k_q \Psi(q, q_d) + c e_q \cdot e_\omega. \tag{2.22}$$

for a constant c satisfying

$$c < \min\{\sqrt{k_q}, \sqrt{\frac{2k_q}{2-\psi_1}}, \frac{4k_q k_\omega}{(k_\omega - B_{\omega d})^2 + 4kq}\}. \tag{2.23}$$

Then, from property (iv) of Proposition 2.1, we obtain

$$\frac{1}{2} e_\omega \cdot e_\omega + \frac{1}{2} k_q \|e_q\|^2 - c\|e_q\|\|e_\omega\| \leq \mathcal{V} \leq \frac{1}{2} e_\omega \cdot e_\omega + \frac{1}{2-\psi_1} k_q \|e_q\|^2 + c\|e_q\|\|e_\omega\|.$$

This equation can be further rewritten as

$$z^\mathsf{T} M_1 z \leq \mathcal{V} \leq z^\mathsf{T} M_2 z,$$
$$\lambda_{min}(M_1)\|z\|^2 \leq \mathcal{V} \leq \lambda_{max}(M_2)\|z\|^2. \tag{2.24}$$

where $z = \begin{bmatrix} \|e_q\| \\ \|e_\omega\| \end{bmatrix} \in \mathbb{R}^2$, $M_1 = \frac{1}{2}\begin{bmatrix} k_q & -c \\ -c & 1 \end{bmatrix} \in \mathbb{R}^{2\times 2}$, and $M_2 = \frac{1}{2}\begin{bmatrix} \frac{2k_q}{2-\psi_1} & c \\ c & 1 \end{bmatrix} \in \mathbb{R}^{2\times 2}$. The matrices M_1 and M_2 are guaranteed to be positive definite as long as the constant c satisfying(2.23).

Next, we will prove the time-derivative of the Lyapunov function is negative definite. To show this, we start from deriving the time-derivative of e_ω. The time

derivative of (2.13) is

$$\dot{e}_\omega = \dot{\omega} - \dot{\omega}_d + \dot{q}(q \cdot \omega_d) + q(\dot{q} \cdot \omega_d) + q(q \cdot \dot{\omega}_d). \tag{2.25}$$

Substituting (2.19) into (2.6), we have

$$\dot{\omega} = -k_\omega e_\omega - k_q e_q + \dot{\omega}_d - \dot{q}(q \cdot \omega_d). \tag{2.26}$$

Then substituting (2.26) into (2.25), we obtain

$$\dot{e}_\omega = -k_\omega e_\omega - k_q e_q + q(\dot{q} \cdot \omega_d) + q(q \cdot \dot{\omega}_d). \tag{2.27}$$

From the property (ii) of Proposition 2.1, and (2.27), the time-derivative of $\mathcal{V}$ is given by:

$$\begin{aligned}
\dot{\mathcal{V}} &= e_\omega \cdot \dot{e}_\omega + k_q e_q \cdot e_\omega + c\dot{e}_q \cdot e_\omega + c e_q \cdot \dot{e}_\omega \\
&= (e_\omega + c e_q) \cdot (-k_\omega e_\omega - k_q e_q) + k_q e_q \cdot e_\omega + c\dot{e}_q \cdot e_\omega \\
&= -k_\omega \|e_\omega\|^2 - c k_\omega e_q \cdot e_\omega - c k_q \|e_q\|^2 + c\dot{e}_q \cdot e_\omega \\
&\leq -k_\omega \|e_\omega\|^2 + c k_\omega \|e_q\| \|e_\omega\| - c k_q \|e_q\|^2 + c\dot{e}_q \cdot e_\omega.
\end{aligned} \tag{2.28}$$

Notice that $e_\omega \cdot q = e_q \cdot q = 0$ since both of e_q and e_ω are normal to q. Moreover, By applying property (iii) of propositon 1, the time-derivative of Lyapunov function is bounded by

$$\begin{aligned}
\dot{\mathcal{V}} &\leq -[(k_\omega - c)\|e_\omega\|^2 - c(k_\omega - B_{\omega d})\|e_q\|\|e_\omega\| + c k_q \|e_q\|^2] = -z^\mathsf{T} Q z \\
&\leq -\lambda_{min}(Q)\|z\|^2,
\end{aligned} \tag{2.29}$$

where the matrix $Q \in \mathbb{R}^{2\times 2}$ is defined by

$$Q = \begin{bmatrix} ck_q & -\frac{c(k_\omega + B_{\omega d})}{2} \\ -\frac{c(k_\omega + B_{\omega d})}{2} & k_\omega - c \end{bmatrix}. \tag{2.30}$$

The matrix Q is positive definite if the leading principle minors of Q are positive, that is,

$$ck_q(k_\omega - c) - \frac{c^2(k_\omega - B_{\omega d})^2}{4} > 0, \tag{2.31}$$

which implies the last condition in (2.23),

$$c < \frac{4k_q k_\omega}{(k_\omega - B_{\omega d})^2 + 4kq}. \tag{2.32}$$

We now conclude that the zero equilibrium is exponentially stable under the designed control input.

To show (iii), The undesired equilibrium $(q, \omega) = (-q_d, \omega_d)$ implies $e_q = e_\omega = 0$ and $\Psi(q, q_d) = \Psi(-q_d, q_d) = 2$, thus the Lyapunov function, i.e., (2.22) equals to $2k_q$. And we can further define

$$\mathcal{W} = 2k_q - \mathcal{V} = -\frac{1}{2}e_\omega \cdot e_\omega + (2k_q - k_q\Psi(q, q_d)) - ce_q \cdot e_\omega, \tag{2.33}$$

Now, at the undesired equilibrium $\mathcal{W} = 0$, we can write

$$\mathcal{W} \geq -\frac{1}{2}\|e_\omega\|^2 + k_q(2 - \Psi(q, q_d)) - c\|e_q\|\|e_\omega\|, \tag{2.34}$$

We can choose q that is arbitrary close to $-q_d$ such that $2 - \Psi(q, q_d)$ is still positive. If $\|e_\omega\|$ is sufficiently small, we know $\mathcal{W} > 0$ at some points, i.e., at any small

neighborhood of $(-q_d, 0)$, there exists a domain such that

$$\dot{\mathcal{W}} = -\dot{\mathcal{V}} > 0. \tag{2.35}$$

As stated by Theorem 4.3 of [43], the undesired equilibrium is unstable. Property (iii) is verified. □

It has been shown that a lower dimensional manifold $\mathcal{M}_r$ can be defined such that closed-loop solutions starting in $\mathcal{M}_r$ will converge to the undesired equilibrium and all other solutions converges to the desired equilibrium [14]. Particularly, the dimension of $\mathcal{M}_r$ is less than the tangent space of the configuration manifold. Therefore, the desired equilibrium is exponentially stabilized for almost every initial condition except $\mathcal{M}_r$.

2.3 PID Tracking Control of a Spherical Pendulum on Two-Sphere

All of the control systems are subjected to disturbances and uncertainties. If we consider the disturbances and uncertainties, the equation of motion of the pendulum system now can be written as:

$$\dot{\omega} = \frac{g}{l} q \times e_3 + \frac{1}{ml^2} u - \hat{q}^2 \Delta, \tag{2.36}$$

where Δ is the fixed perturbation.

In the PD controller, the proportional term e_q is about present error, while the derivative error e_ω stands for the prediction of future error. Here we introduce the integral term, representing the accumulation of past error, denoted by

$$e_i = \int_0^t (ce_q + e_\omega) d\tau. \tag{2.37}$$

Using the properties derived before, we select a continuous feedback controller

that stabilizes the desired equilibrium.

Proposition 2.3. Consider the system is given by Eq. (2.36) and (2.2) with a tracking command given at Eq. (2.8). The control input is designed as follows:

$$u' = ml^2[-k_\omega e_\omega - k_q e_q + k_i \hat{q}^2 e_i - \hat{q}^2 \dot{\omega}_d - \dot{q}(q \cdot \omega_d) - \frac{g}{l} q \times e_3], \tag{2.38}$$

where k_ω, k_q and k_i are positive constants. The following properties are satisfied by the PID controller: the zero equilibrium of the tracking errors, namely $(e_q, e_\omega, e_i) = (0, 0, \frac{\Delta}{k_i})$ is stable. The present controller is robust with fixed perturbation Δ with the aid of integrator e_i.

Proof. A Lyapunov candidate is specified as

$$\mathcal{V}' = \frac{1}{2} e_\omega \cdot e_\omega + k_q \Psi(q, q_d) + c e_q \cdot e_\omega + \frac{1}{2k_i}(k_i e_i - \Delta)^2. \tag{2.39}$$

Then, applying property (iv) of Proposition 2.1 into (2.22) leads to

$$\begin{aligned} \mathcal{V}' &\geq \frac{1}{2}\|e_\omega\|^2 + \frac{1}{2} k_q \|e_q\|^2 - c\|e_q\|\|e_\omega\| + \frac{1}{2k_i}(k_i e_i - \Delta)^2 \\ &= z^\intercal M_1 z + \frac{1}{2k_i}(k_i e_i - \Delta)^2, \end{aligned}$$

Thus, the Lyapunov function $\mathcal{V}'$ is guaranteed to be positive definite.

$$\mathcal{V}' \geq \lambda_{min}(M_1)\|z\|^2 + \frac{1}{2k_i}(k_i e_i - \Delta)^2. \tag{2.40}$$

Substitute (2.38) into (2.36) and then apply the new form of $\dot{\omega}$ to (2.25). We have

$$\dot{e}_\omega = -k_w e_\omega - k_q e_q + k_i \hat{q}^2 e_i + k_i q(q \cdot e_i) + q(\dot{q} \cdot \omega_d) - \hat{q}^2 \Delta. \tag{2.41}$$

And the time-derivative of $\mathcal{V}'$ is expressed as

$$\begin{aligned}
\dot{\mathcal{V}}' &= e_\omega \cdot \dot{e}_\omega + k_q e_q \cdot e_\omega + c\dot{e}_q \cdot e_\omega + ce_q \cdot \dot{e}_\omega + \frac{1}{k_i}(k_i e_i - \Delta) \cdot (k_i \dot{e}_i) \\
&= (e_\omega + ce_q)\dot{e}_\omega + k_q e_q \cdot e_\omega + c\dot{e}_q \cdot e_\omega + (k_i e_i - \Delta) \cdot (ce_q + e_\omega) \\
&= (e_\omega + ce_q)[-k_w e_\omega - k_q e_q - k_i e_i + k_i q(q \cdot e_i) + q(\dot{q} \cdot \omega_d) - q(q \cdot \Delta) + \Delta] \\
&\quad + k_q e_q \cdot e_\omega + c\dot{e}_q \cdot e_\omega + ck_i e_i \cdot e_q + k_i e_i \cdot e_\omega - c\Delta \cdot e_q - \Delta \cdot e_\omega.
\end{aligned}$$

Using $e_q \cdot q = e_\omega \cdot q = 0$, the related terms can be eliminated. Finally, we have

$$\begin{aligned}
\dot{\mathcal{V}}' &= (e_\omega + ce_q)[-k_w e_\omega - k_q e_q - k_i e_i + \Delta] + k_q e_q \cdot e_\omega + c\dot{e}_q \cdot e_\omega + ck_i e_i \cdot e_q \\
&\quad + k_i e_i \cdot e_\omega - c\Delta \cdot e_q - \Delta \cdot e_\omega \\
&= -k_w e_\omega \cdot e_\omega - ck_w e_q \cdot e_\omega - ck_q e_q \cdot e_q + c\dot{e}_q \cdot e_\omega \\
&= \dot{\mathcal{V}}. \qquad (2.42)
\end{aligned}$$

All of the terms with the fixed perturbation are annihilated, hence the time-derivative of the Lyapunov function of PID controller is exactly same with our previous work about the PD tracking control. Since there exists a new state e_i in the PID case, $\dot{\mathcal{V}}$ is semi-negative definite and we can only conclude that the equilibrium $(e_q, e_\omega, e_i) = (0, 0, \frac{\Delta}{k_i})$ is stable.

□

2.4 Numerical Example

We present numerical examples for a spherical pendulum on S^2 corresponding to Proposition 2.2 and Proposition 2.3. The initial conditions $q = [0\ 0\ 1]^\mathsf{T}$ and $\omega = [0\ 0\ 0]^\mathsf{T}$ imply that the pendulum is in rest at the stable equilibrium. The length of the link and weight of the bob is 0.2m and 1kg, respectively. In addition, the control gain are chosen as $k_q = 10$ and $k_w = 10.1$. The desired direction of the pendulum q_d

can be a continuous function of time and must satisfies $\|q_d\|^{\mathsf{T}} = 1$ since it is a unit vector, thus we select

$$q_d = [\cos(\alpha t)\cos(\beta t) \;\; \cos(\alpha t)\sin(\beta t) \;\; \sin(\alpha t)]^{\mathsf{T}}, \tag{2.43}$$

where $\alpha = 0.5$ and $\beta = 2$. The corresponding numerical distributions are described at Figure 2.2.

The feature of PID controller is eliminating the effect of fixed perturbation where $\Delta = [7\ 1\ -3]^{\mathsf{T}}$. We then add the perturbation and execute the simulation on PD and PID controller so the effect of integral term can be distinctly observed. The numerical results for PD and PID controller with respect to fixed perturbation are illustrated at Figure 2.3 and Figure 2.4, respectively.

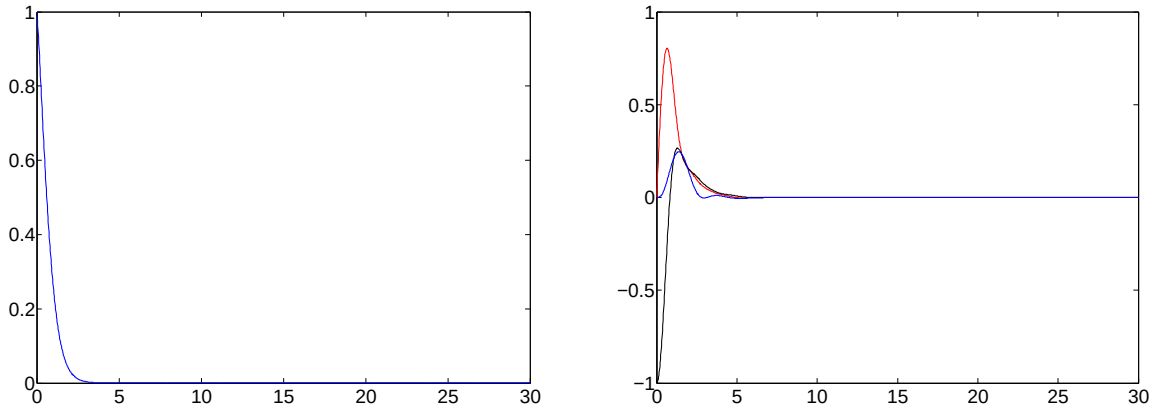

(a) Direction error function Ψ

(b) Direction error vector e_q

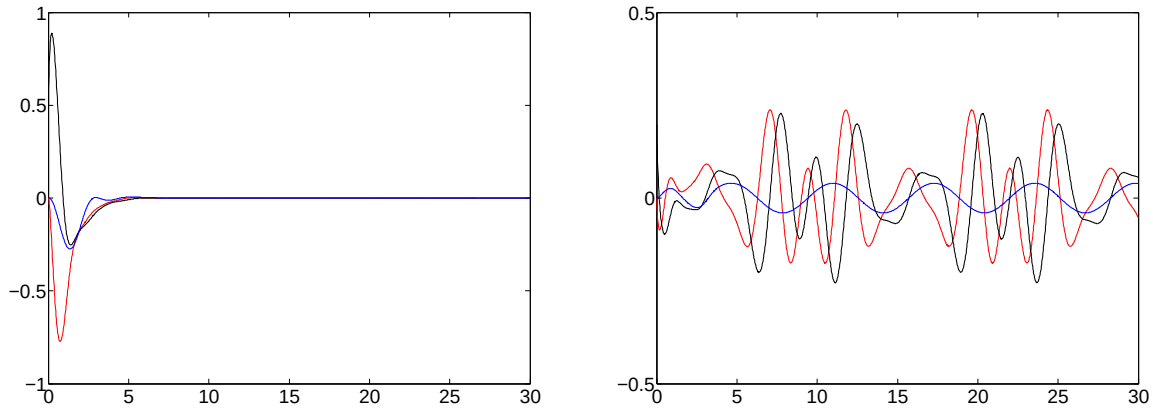

(c) Angular velocity error vector e_ω

(d) Control input u

Figure 2.2: Numerical results for spherical pendulum under PD controller without perturbation

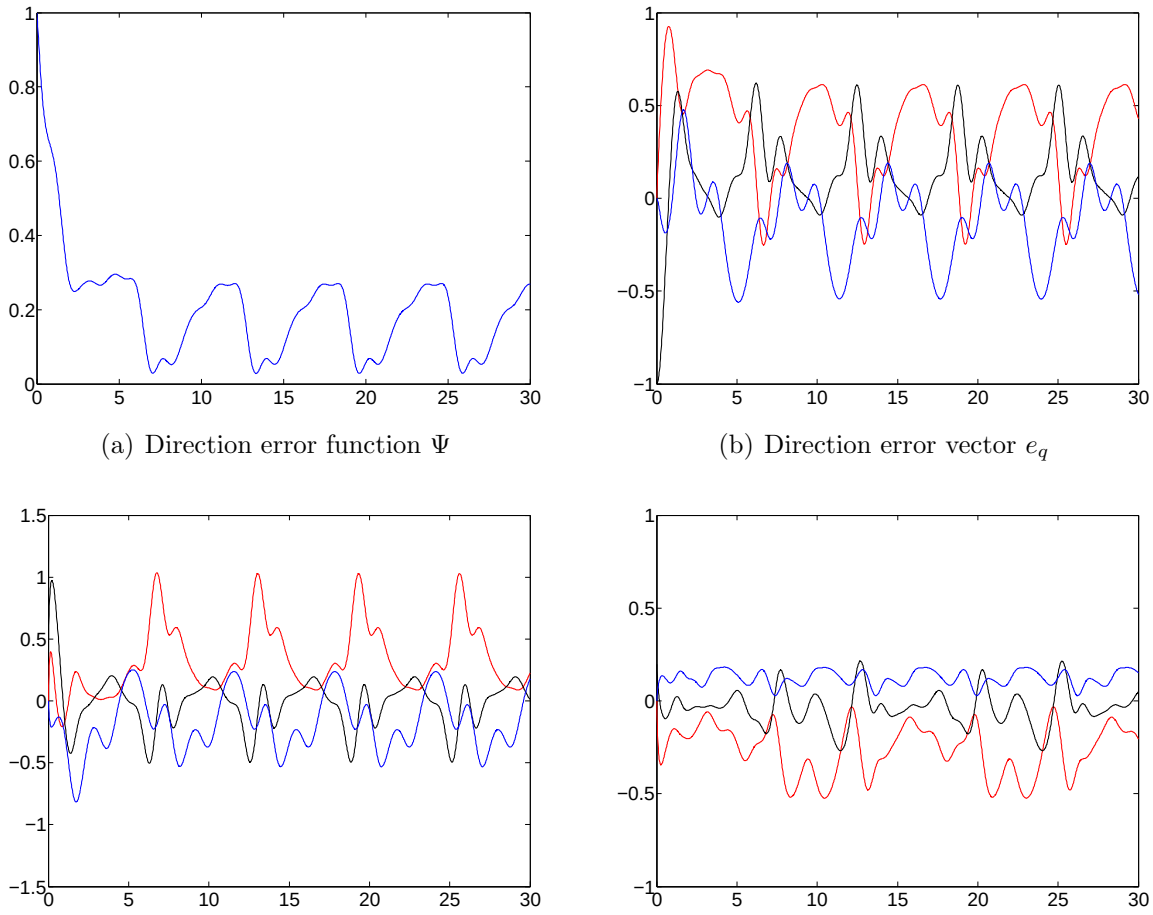

(a) Direction error function Ψ

(b) Direction error vector e_q

(c) Angular velocity error vector e_ω

(d) Control input u

Figure 2.3: Numerical results for spherical pendulum under PD controller with fixed perturbation, the error variables do not converge to zero due to the effect of perturbation.

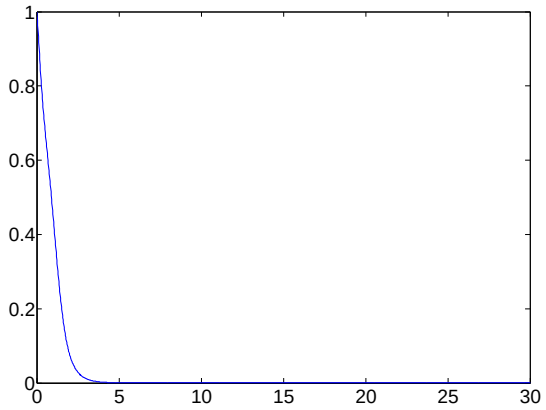

(a) Direction error function Ψ

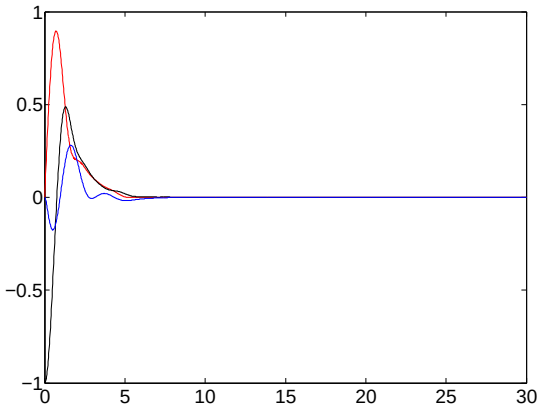

(b) Direction error vector e_q

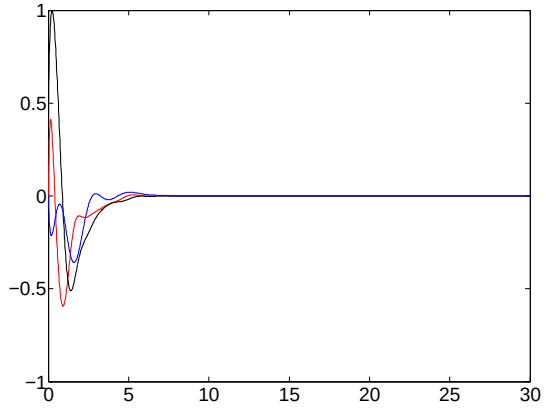

(c) Angular velocity error vector e_ω

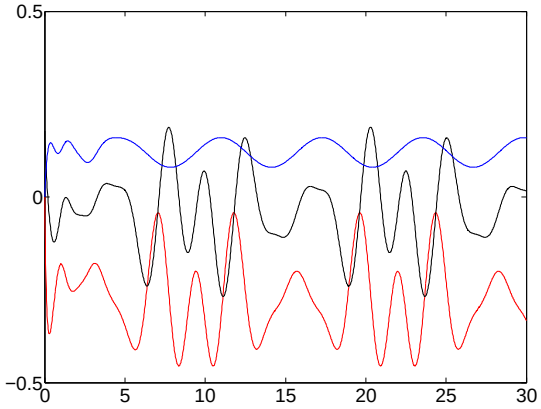

(d) Control input u

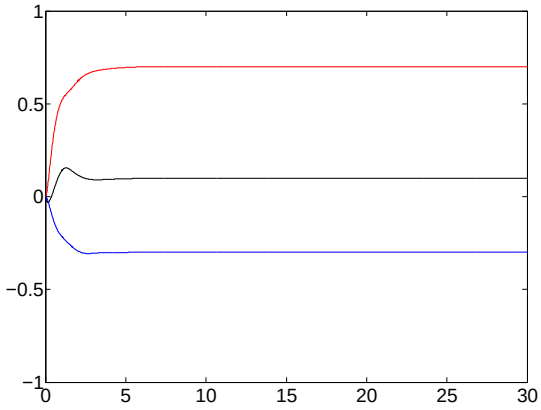

(e) Integral error u

Figure 2.4: Numerical results for spherical pendulum under PID controller with fixed perturbation(red, black and blue in ascending order), the integral term successfully eliminates the effect of perturbation.

Chapter 3 Vision-based Spacecraft Attitude Control on $\mathsf{SO}(3)$

This chapter presents a control strategy to rotate single spacecraft by using the information provided by a vision system. To be more specific, we select two distinct point objects as visual features, and use optical devices to obtain the line-of-sight (LOS) measurements to determine the absolute attitude of the spacecraft. The LOS observation is represented by a unit vector in two-sphere, which is analogous to the control system of a spherical pendulum we have presented in the preceding chapter.

We will explore the advantage the LOS observations in the next chapter to develop a relative attitude control system for multiple spacecrafts.

3.1 Problem Formulation

3.1.1 Attitude Dynamics on $\mathsf{SO}(3)$

Consider a spacecraft modeled as a rigid body. The origin of the body-fixed frame $\mathcal{B}$ are defined at the mass center of the spacecraft. A inertial reference frame or world frame $\mathcal{W}$ is also defined. Each frame is is constructed by three orthogonal unit basis vectors ordered according to the right-hand rule. A rotation matrix $R \in \mathsf{SO}(3)$ represents the physical attitude of the spacecraft where $\mathsf{SO}(3)$ is the special orthogonal group which denotes the set of all rotation matrices, that is

$$\mathsf{SO}(3) = \{R \in \mathbb{R}^{3\times 3} \mid R^{\mathsf{T}}R = I,\ \det(R) = 1\}. \tag{3.1}$$

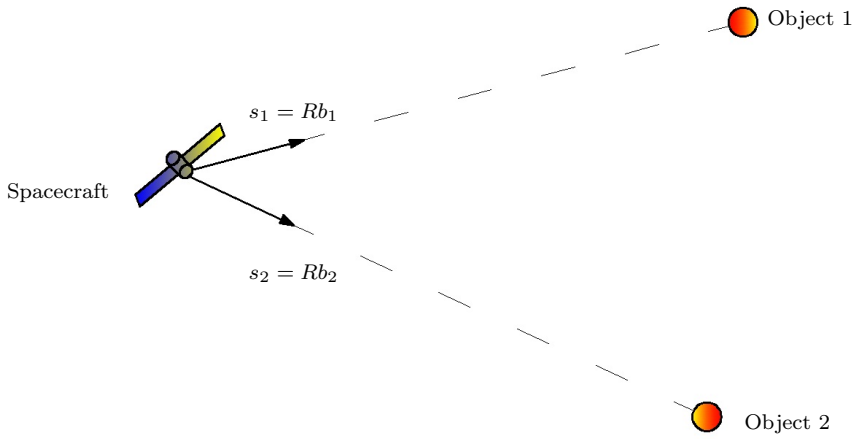

Figure 3.1: Problem definition: directions from spacecraft toward two distinct objects are given by s_1 and $s_2 \in \mathsf{S}^2$ with respect to the inertial reference frame. The corresponding line-of-sight measurements, b_1 and $b_2 \in \mathsf{S}^2$ are represented with respect to the body-fixed frame. They are related by the rotation matrix R representing the attitude of the spacecraft.

The rotation matrix represents the linear transformation from the body-fixed frame to the inertial reference frame. Furthermore, its transpose indicate the inverse mapping because of the orthogonality $R^{\mathsf{T}} = R^{-1}$,

$$ {}^{W}r = R({}^{B}r), \quad {}^{B}r = R^{\mathsf{T}}({}^{W}r), \tag{3.2} $$

where ${}^{B}r$ is a vector quantity r with respected to the body fixed frame and ${}^{W}r$ is the same vector with respect to the inertial reference frame. Notice that the full transformation between the two coordinate system also includes the the position transformation. However, the discussion about relative position is neglected in this thesis since we only care about the relative orientation.

The equation of motions for the spacecraft are given by

$$J\dot{\Omega} + \Omega \times J\Omega = u, \tag{3.3}$$

$$\dot{R}(t) = R(t)\hat{\Omega}, \tag{3.4}$$

where $J \in \mathbb{R}^{3\times3}$ is the inertia matrix, $\Omega \in \mathbb{R}^3$ represents the angular velocity of the body-fixed frame with respect to the inertial reference frame expressed in the body-fixed frame, and u denotes the total external moments applied to the aircraft expressed in the body-fixed frame. Assume that the desired angular velocity is uniformly bounded. In other words, for any $t \geq 0$, there exists a known constant $B_{\Omega d} > 0$ such that

$$\|\Omega(t)\| \leq B_{\Omega d}. \tag{3.5}$$

3.1.2 Vision-Based Attitude Control Problem

Suppose that there are two distinct objects, such as distant stars, whose location in the inertia reference frame is available. Let s_1, $s_2 \in \mathbb{R}^3$ be the unit vectors showing the direction from the spacecraft to the first object and the second object expressed in the inertial reference frame, respectively. Since each of these two vectors has unit length, they lie in the two-sphere S^2. The relative positions of objects with respect to the spacecraft are assumed to be fixed and they are non-parallel with each other, i.e., the following properties are satisfied:

$$\dot{s}_1 = \dot{s}_2 = 0, \quad s_1 \times s_2 \neq 0. \tag{3.6}$$

Assume the spacecraft is equipped with an onboard camera which can capture the direction to two distinct objects. These two line-of-sight (LOS) measurements from spacecraft toward the objects are defined as b_1, $b_2 \in \mathsf{S}^2$ (Figure 3.1). Since s_1, s_2 and

b_1, b_2 are referred to the same vectors with respect to different reference frames, they are related by the rotation matrix. From (3.2), we can write

$$s_1 = R(t)b_1(t), \quad s_2 = R(t)b_2(t), \tag{3.7}$$

$$b_1(t) = R(t)^{\mathsf{T}} s_1, \quad b_2(t) = R(t)^{\mathsf{T}} s_2. \tag{3.8}$$

Additionally, (3.4) shows that

$$\dot{R}(t)^{\mathsf{T}} = (R(t)\hat{\Omega})^{\mathsf{T}} = \hat{\Omega}^{\mathsf{T}} R(t)^{\mathsf{T}} = -\hat{\Omega} R(t)^{\mathsf{T}}. \tag{3.9}$$

From (3.9), (3.8) and the assumption $\dot{s}_i = 0$, we can obtain the kinematic equations for b_1, b_2,

$$\begin{aligned} \dot{b}_i(t) &= \dot{R}(t)^{\mathsf{T}} s_i + R(t)^{\mathsf{T}} \dot{s}_i = -\hat{\Omega} R(t)^{\mathsf{T}} s_i \\ &= -\hat{\Omega} b_i(t) = -\Omega(t) \times b_i(t) = b_i(t) \times \Omega(t), \end{aligned} \tag{3.10}$$

for $i \in \{1, 2\}$.

Suppose that the desired attitude trajectory $R_d(t) \in \mathsf{SO(3)}$ is given, It satisfies the following kinematic equation

$$\dot{R}_d(t) = R_d(t)\hat{\Omega}_d(t), \tag{3.11}$$

where $\Omega_d(t) \in \mathsf{SO(3)}$ is the desired angular velocity. The corresponding desired line-of-sight measurements are given by

$$b_{i_d}(t) = R_d(t)^{\mathsf{T}} s_i, \quad i = 1, 2. \tag{3.12}$$

Similar with (3.10), the kinematic equations for desired line-of-sight measurements

are denoted by

$$\dot{b}_{i_d}(t) = b_{i_d}(t) \times \Omega_d(t). \tag{3.13}$$

According to the rigid body assumption, the angle between b_1 and b_2 is always same as the angle between s_1 and s_2 and the angle between .

$$\begin{aligned} b_1(t) \cdot b_2(t) &= R(t)^{\mathsf{T}} s_1 \cdot R(t)^{\mathsf{T}} s_2 = [R(t)^{\mathsf{T}} s_1]^{\mathsf{T}} [R(t)^{\mathsf{T}} s_2] \\ &= s_1^{\mathsf{T}} R(t) R(t)^{\mathsf{T}} s_2 = s_1^{\mathsf{T}} s_2 = s_1 \cdot s_2. \end{aligned}$$

Since b_{1_d} and b_{2_d} are elements of b_1 and b_2, respectively, the foregoing property is also valid, i.e., $b_{1_d}(t) \cdot b_{2_d}(t) = s_1 \cdot s_2$.

The goal is to design a control input u in terms of the line-of-sight measurements $b_1(t)$, $b_2(t)$ and the angular velocity $\Omega(t)$ such that the spacecraft attitude $R(t)$ asymptotically follows the desired attitude $R_d(t)$.

3.2 Almost Global Exponential Tracking Control on $\mathsf{SO(3)}$

In order to let the spacecraft follow the desired trajectory, the desired attitude is assigned, and the difference of the current and desired attitude are characterized by smooth positive function called *error function*. Moreover, we are able to define *error vectors*, representing the difference of current angular velocity and LOS measurements between the desired ones, from the tangent space of the error function since we are dealing with a nonlinear manifold. We then construct the controller directly by the error vectors based on Lyapunov stability analysis so that the spacecraft can exponentially track the desired motion even though the initial attitude errors are significantly large.

3.2.1 Error Variables

First, we choose error functions that represent the distance between the desired attitude and the current attitude. The configuration error functions are defined as

$$\Psi_1(b_1, b_{1_d}) = 1 - b_1 \cdot b_{1_d}, \quad \Psi_2(b_2, b_{2_d}) = 1 - b_2 \cdot b_{2_d}, \tag{3.14}$$

$$\Psi(b_1, b_2, b_{1_d}, b_{2_d}) = k_{b_1}\Psi_1(b_1, b_{1_d}) + k_{b_2}\Psi_2(b_2, b_{2_d}). \tag{3.15}$$

For simplicity, hereafter we will use Ψ and Ψ_i as the short note of $\Psi(b_1, b_2, b_{1_d}, b_{2_d})$ and $\Psi_i(b_i, b_{i_d})$, respectively. For each object i, Ψ_i refers to the corresponding error of LOS measurements while Ψ involves the LOS error of the complete control system. Once the error of each line-of-sight measurements goes to zero, the error of the complete control system goes to zero as well.

Substituting (3.8), the error function Ψ_i can be written as

$$\Psi_i(R) = 1 - R^{\mathsf{T}} s_i \cdot R_d^{\mathsf{T}} s_i. \tag{3.16}$$

Since we have the assumption that s_i is fixed and R_d is given, Ψ_i can be considered as a function of R. Furthermore, the infinitesimal variation of a rotation matrix R can be expressed in terms of the exponential map as follows

$$\delta R = \frac{d}{d\epsilon}\bigg|_{\epsilon=0} R\exp(\epsilon\hat{\eta}) = R\hat{\eta}, \tag{3.17}$$

for a vector $\eta \in \mathbb{R}^3$. Thus, from (3.16) and substituting (3.17), the variation of Ψ_i is expressed by

$$\begin{aligned}\delta\Psi_i &= \frac{d}{d\epsilon}\bigg|_{\epsilon=0} \Psi_i(R\exp(\epsilon\hat{\eta})) = -(R\hat{\eta})^{\mathsf{T}} s_i \cdot R_d^{\mathsf{T}} s_i = \hat{\eta} b_i \cdot b_{id} = b_{id} \cdot (\eta \times b_i) \\ &= \eta \cdot (b_i \times b_{i_d}).\end{aligned} \tag{3.18}$$

According to (3.18), the configuration error vectors are defined as

$$e_{b_1} = b_1 \times b_{1_d}, \quad e_{b_2} = b_2 \times b_{2_d}, \tag{3.19}$$

$$e_b = k_{b_1} e_{b_1} + k_{b_2} e_{b_2}. \tag{3.20}$$

Notice that since b_i and b_{i_d} are unit vectors, the magnitude of e_{b_i} is bounded, i.e. $\|e_{b_i}\| \leq 1$, which leads to

$$\|e_b\| \leq k_{b_1}\|e_{b_1}\| + k_{b_2}\|e_{b_2}\| \leq k_{b_1} + k_{b_2}. \tag{3.21}$$

The angular velocity error vector is defined as

$$e_\Omega = \Omega - \Omega_d. \tag{3.22}$$

The properties of error variables mentioned above are summarized as follows.

Proposition 3.1. The error variables (3.14)-(3.22) satisfy the following properties

(i) $\frac{d}{dt}\Psi_i(b_i, b_{i_d}) = e_{b_i} \cdot e_\Omega$ for $i = 1, 2$.

(ii) $\|\dot{e}_b\| \leq (k_{b_1} + k_{b_2})\|e_\Omega\| + B_{\Omega d}\|e_b\|$.

(iii) Define a matrix $K \equiv= k_{b_1} s_1 s_1^\mathsf{T} + k_{b_2} s_2 s_2^\mathsf{T} \in \mathbb{R}^{3\times 3}$ and let g_1, $g_2 \in \mathbb{R}$ be two positive eigenvalues of K. If $\Psi < \psi < h_1 \equiv 2\min\{g_1, g_2\}$, the following inequality holds:

$$\frac{h_1}{h_2 + h_3}\|e_b\|^2 \leq \Psi \leq \frac{h_1 h_4}{h_5(h_1 - \psi)}\|e_b\|^2, \tag{3.23}$$

where the constants are defined as

$$
\begin{aligned}
h_1 &= 2\min\{g1, g2\}, \\
h_2 &= 4\max\{(g_1 - g_2)^2, g_1^2, g_2^2\}, \\
h_3 &= 4(g_1 + g_2)^2, \\
h_4 &= 2(g_1 + g_2), \\
h_5 &= 4\min\{g_1^2, g_2^2\},
\end{aligned}
$$

Proof. From (3.14) and (3.10), we can show (i) by

$$
\begin{aligned}
\dot{\Psi}_i &= -\dot{b}_i \cdot b_{i_d} - b_i \cdot \dot{b}_{i_d} \\
&= -(b_i \times \Omega) \cdot b_{i_d} - b_i \cdot (b_{i_d} \times \Omega_d) \\
&= -\Omega(b_{i_d} \times b_i) - \Omega_d(b_i \times b_{i_d}) \\
&= (\Omega - \Omega_d) \cdot (b_i \times b_{i_d}) \\
&= e_\Omega \cdot e_{b_i},
\end{aligned}
$$

and the time-derivative of Ψ is defined by

$$
\dot{\Psi} = k_{b_1}\dot{\Psi}_1 + k_{b_2}\dot{\Psi}_2 = k_{b_1} e_\Omega \cdot e_{b_1} + k_{b_2} e_\Omega \cdot e_{b_2} = e_\Omega \cdot (k_{b_1} e_{b_1} + k_{b_1} e_{b_1}) = e_\Omega \cdot e_b.
$$

From $e_{b_i} = b_i \times b_{i_d}$, $\dot{e}_{b_i}$ is given by

$$\begin{aligned}
\dot{e}_{b_i} &= \dot{b}_i \times b_{i_d} + b_i \times \dot{b}_{i_d} \\
&= (b_i \times \Omega) \times b_{i_d} + b_i \times (b_{i_d} \times \Omega_d) \\
&= -b_{i_d} \times (b_i \times \Omega) + b_i \times (b_{i_d} \times \Omega_d) \\
&= -[b_i(b_{i_d} \cdot \Omega) - \Omega(b_{i_d} \cdot b_i)] + b_{i_d}(b_i \cdot \Omega_d) - \Omega_d(b_i \cdot b_{i_d}) \\
&= (\Omega - \Omega_d)(b_{i_d} \cdot b_i) + b_{i_d}(b_i \cdot \Omega_d) - b_i(b_{i_d} \cdot \Omega). \qquad (3.24)
\end{aligned}$$

Substituting $\Omega = e_\Omega - \Omega_d$ then applying (A.3) in the appendix, above equation becomes

$$\begin{aligned}
\dot{e}_{b_i} &= e_\Omega(b_{i_d} \cdot b_i) + b_{i_d}(b_i^\mathsf{T})\Omega_d - b_i(b_{i_d}^\mathsf{T})(e_\Omega + \Omega_d) \\
&= e_\Omega(b_{i_d} \cdot b_i) + [b_{i_d}(b_i^\mathsf{T}) - b_i(b_{i_d}^\mathsf{T})]\Omega_d - b_i(b_{i_d}^\mathsf{T})e_\Omega \\
&= e_\Omega(b_{i_d} \cdot b_i) - b_i(b_{i_d} \cdot e_\Omega) + (\widehat{b_i \times b_{i_d}})\Omega_d \\
&= b_{i_d} \times (e_\Omega \times b_i) + (b_i \times b_{i_d}) \times \Omega_d \\
&= -b_{i_d} \times (b_i \times e_\Omega) + e_{b_i} \times \Omega_d, \qquad (3.25)
\end{aligned}$$

which leads to

$$\|\dot{e}_{b_i}\| \leq \|e_\Omega\| + B_{\Omega d}\|e_{b_i}\|, \qquad (3.26)$$

and

$$\|\dot{e}_b\| \leq k_{b_1}(\|e_\Omega\| + B_{\Omega d}\|e_{b_1}\|) + k_{b_2}(\|e_\Omega\| + B_{\Omega d}\|e_{b_2}\|) = (k_{b_1} + k_{b_2})\|e_\Omega\| + B_{\Omega d}\|e_b\|, \qquad (3.27)$$

where $\|e_b\| = k_{b_1}\|e_{b_1}\| + k_{b_2}\|e_{b_2}\|$. Hence property (ii) is proved.

To show property (iii), we introduce alternative expressions for Ψ and e_b

$$\begin{aligned}
\Psi &= k_{b_1}\Psi_1 + k_{b_2}\Psi_2 \\
&= k_{b_1}(1 - b_1 \cdot b_{1_d}) + k_{b_2}(1 - b_2 \cdot b_{2_d}) \\
&= k_{b_1} + k_{b_2} - k_{b_1} b_1^T b_{1_d} - k_{b_2} b_2^T b_{2_d} \\
&= k_{b_1} + k_{b_2} - \mathrm{tr}[k_{b_1} b_1 b_{1_d}^T + k_{b_2} b_2 b_{2_d}^T] \\
&= k_{b_1} + k_{b_2} - \mathrm{tr}[k_{b_1}(R^T s_1)(R_d^T s_1)^T + k_{b_2}(R^T s_2)(R_d^T s_2)^T] \\
&= k_{b_1} + k_{b_2} - \mathrm{tr}[k_{b_1}(R^T s_1)(s_1^T) R_d + k_{b_2}(R^T s_2)(s_2^T) R_d] \\
&= k_{b_1} + k_{b_2} - \mathrm{tr}[R^T(k_{b_1} s_1 s_1^T + k_{b_2} s_2 s_2^T) R_d] \\
&\triangleq k_{b_1} + k_{b_2} - \mathrm{tr}[R^T K R_d],
\end{aligned} \tag{3.28}$$

where we just appied $x^T y = \mathrm{tr}[xy^T]$ for any x, $y \in \mathbb{R}^3$. Let $\mu_i \in \mathbb{R}$ and $\nu_i \in \mathbb{R}^3$ be the i-th eigenvalue and normalized eigenvector of K, respectively. According to the spectral theorem addressed in appendix B, the matrix K can be factored to

$$K \equiv UGU^T, \tag{3.29}$$

where $U = [\nu_1\ \nu_2\ \nu_3] \in \mathsf{SO(3)}$, $G = \mathrm{diag}[\mu_1\ \mu_2\ \mu_3] \in \mathbb{R}^{3\times 3}$. In particular, it is ordered that $\mu_3 = 0$ and $\nu_3 = \nu_1 \times \nu_2$ such that U lies in $\mathsf{SO(3)}$. Alternatively, we have

$$k_{b_1} + k_{b_2} = \mathrm{tr}[K] = \mathrm{tr}[UGU^T] = \mathrm{tr}[GU^T U] = \mathrm{tr}[G]. \tag{3.30}$$

The first equality comes from $K = k_{b_1} s_1 s_1^T + k_{b_2} s_2 s_2^T$, where $\mathrm{tr}[s_i s_i^T] = s_i^T s_i = \|s_i\|^2 = 1$ for $i = 1, 2$. The rest comes from the trace identities $\mathrm{tr}[xy] = \mathrm{tr}[yx] = \mathrm{tr}[x^T y^T] = \mathrm{tr}[y^T x^T]$ for any x, $y \in \mathbb{R}^3$.

Thus, using (3.30), we can rewrite (3.28) as

$$\begin{aligned}\Psi &= \mathrm{tr}[G] - \mathrm{tr}[R^{\mathsf{T}}(UGU^{\mathsf{T}})R_d] \\ &= \mathrm{tr}[G] - \mathrm{tr}[(R_d^{\mathsf{T}}UGU^{\mathsf{T}})R] \\ &= \mathrm{tr}[G] - \mathrm{tr}[(GU^{\mathsf{T}}R)(R_d^{\mathsf{T}}U)] \qquad (3.31) \\ &= \mathrm{tr}[G(I - U^{\mathsf{T}}RR_d^{\mathsf{T}}U)]. \qquad (3.32)\end{aligned}$$

This is an alternative expression of Ψ.

From (3.31), we differentiate Ψ with respect to R along the direction $\delta R = R\hat{\eta}$ to obtain

$$\mathbf{D}_R\Psi \cdot R\hat{\eta} = -\mathrm{tr}[GU^{\mathsf{T}}R\hat{\eta}R_d^{\mathsf{T}}U] = -\mathrm{tr}[(\hat{\eta}R_d^{\mathsf{T}}U)(GU^{\mathsf{T}}R)] = -\mathrm{tr}[(R_d^{\mathsf{T}}KR)\hat{\eta}]. \qquad (3.33)$$

From (A.9), we have

$$\begin{aligned}\mathbf{D}_R\Psi \cdot R\hat{\eta} &= \eta^{\mathsf{T}}[R_d^{\mathsf{T}}KR - (R_d^{\mathsf{T}}KR)^{\mathsf{T}}]^{\vee} \qquad (3.34) \\ &= \eta \cdot [R_d^{\mathsf{T}}(k_{b_1}s_1s_1^{\mathsf{T}} + k_{b_2}s_2s_2^{\mathsf{T}})R - R^{\mathsf{T}}(k_{b_1}s_1s_1^{\mathsf{T}} + k_{b_2}s_2s_2^{\mathsf{T}})R_d]^{\vee} \\ &= \eta \cdot [k_{b_1}(R_d^{\mathsf{T}}s_1s_1^{\mathsf{T}}R) + k_{b_2}(R_d^{\mathsf{T}}s_2s_2^{\mathsf{T}}R) - k_{b_1}(R^{\mathsf{T}}s_1s_1^{\mathsf{T}}R_d) - k_{b_2}(R^{\mathsf{T}}s_2s_2^{\mathsf{T}}R_d)]^{\vee} \\ &= \eta \cdot [k_{b_1}(b_{1_d}b_1^{\mathsf{T}}) + k_{b_2}(b_{2_d}b_2^{\mathsf{T}}) - k_{b_1}(b_1b_{1_d}^{\mathsf{T}}) - k_{b_2}(b_2b_{2_d}^{\mathsf{T}})]^{\vee} \\ &= \eta \cdot [k_{b_1}(b_{1_d}b_1^{\mathsf{T}} - b_1b_{1_d}^{\mathsf{T}}) + k_{b_2}(b_{2_d}b_2^{\mathsf{T}} - b_2b_{2_d}^{\mathsf{T}})]^{\vee}. \qquad (3.35)\end{aligned}$$

Substituting (A.3),

$$\begin{aligned}\mathbf{D}_R\Psi \cdot R\hat{\eta} &= \eta \cdot [k_{b_1}(\widehat{b_1 \times b_{1_d}})^{\vee} + k_{b_2}(\widehat{b_2 \times b_{2_d}})^{\vee}] \\ &= \eta \cdot [k_{b_1}(b_1 \times b_{1_d}) + k_{b_2}(b_2 \times b_{2_d})] \\ &= \eta \cdot (k_{b_1}e_{b_1} + k_{b_2}e_{b_2}) \\ &= \eta \cdot e_b. \qquad (3.36)\end{aligned}$$

Comparing (3.34) with (3.36), we obtain

$$e_b = [R_d^{\mathsf{T}} K R - (R^{\mathsf{T}} K R_d)]^{\vee}, \tag{3.37}$$

which is an alternative expression of e_b.

These alternative expressions can be compared with [44] to show the third property. The properties developed in [44] are summarized as follows

$$\Phi = \frac{1}{2}\mathrm{tr}[F(I-P)], \tag{3.38}$$

$$e_P = \frac{1}{2}(FP - P^{\mathsf{T}}F)^{\vee}, \tag{3.39}$$

$$\frac{h_1}{h_2+h_3}\|e_P\|^2 \leq \Phi \leq \frac{h_1 h_4}{h_5(h_1-\psi)}\|e_P\|^2, \tag{3.40}$$

where $P \in \mathsf{SO(3)}$, $F = \mathrm{diag}[f_1, f_2, f_3]$ and the constants h_i are given by

$$\begin{aligned}
h_1 &= \min\{f_1+f_2,\ f_2+f_3,\ f_3+f_1\},\\
h_2 &= \max\{(f_1-f_2)^2,\ (f_2-f_3)^2,\ (f_3-f_1)^2\},\\
h_3 &= \max\{(f_1+f_2)^2,\ (f_2+f_3)^2,\ (f_3+f_1)^2\},\\
h_4 &= \max\{f_1+f_2,\ f_2+f_3,\ f_3+f_1\},\\
h_5 &= \min\{(f_1+f_2)^2,\ (f_2+f_3)^2,\ (f_3+f_1)^2\},
\end{aligned}$$

and it is assumed that $\Phi < \psi < h_1$.

After comparing (3.38) with (3.32), we let $F = 2G$ and $P = U^{\mathsf{T}} R R_d^{\mathsf{T}} U$ so $\Phi = \Psi$.

Then (3.39) is equivalent to

$$\begin{aligned}\hat{e}_P &= GU^\mathsf{T}RR_d^\mathsf{T}U - U^\mathsf{T}R_dR^\mathsf{T}UG \\ &= (U^\mathsf{T}U)GU^\mathsf{T}RR_d^\mathsf{T}U - U^\mathsf{T}R_dR^\mathsf{T}UG(U^\mathsf{T}U) \\ &= U^\mathsf{T}(UGU^\mathsf{T}RR_d^\mathsf{T} - R_dR^\mathsf{T}UGU^\mathsf{T})U \\ &= U^\mathsf{T}(KRR_d^\mathsf{T} - R_dR^\mathsf{T}K)U, \end{aligned} \tag{3.41}$$

where we have multiplied the identity matrix $I = U^\mathsf{T}U \in \mathbb{R}^3$. Similarly, we now multiply $I = R_dR_d^\mathsf{T}$ and then apply (A.4) so that

$$\begin{aligned}\hat{e}_P &= U^\mathsf{T}[(R_dR_d^\mathsf{T})KRR_d^\mathsf{T} - R_dR^\mathsf{T}K(R_dR_d^\mathsf{T})]U \\ &= U^\mathsf{T}R_d(R_d^\mathsf{T}KR - R^\mathsf{T}KR_d)R_d^\mathsf{T}U \\ &= (U^\mathsf{T}R_d)\hat{e}_b(U^\mathsf{T}R_d)^\mathsf{T} \\ &= (U^\mathsf{T}R_de_b)^\wedge. \end{aligned} \tag{3.42}$$

Thus, $e_P = U^\mathsf{T}R_de_b$, which implies that $\|e_P\| = \|e_b\|$ since U and R_d are all orthogonal matrices. From (3.40), The bounds of Ψ are given as

$$\frac{h_1}{h_2 + h_3}\|e_b\|^2 \leq \Phi \leq \frac{h_1h_4}{h_5(h_1 - \psi)}\|e_b\|^2.$$

In particular, $f_1 = 2k_{b_1}$, $f_1 = 2k_{b_2}$, and $f_3 = 0$, the constants h_i now are valued as

$$\begin{aligned} h_1 &= \min\{2k_{b_1},\ 2k_{b_2}\}, \\ h_2 &= \max\{4(k_{b_1} - k_{b_2})^2,\ 4k_{b_2}^2,\ 4k_{b_1}^2\}, \\ h_3 &= 4(k_{b_1} + k_{b_2})^2, \\ h_4 &= 2(k_{b_1} + k_{b_2}), \\ h_5 &= \min\{4k_{b_2}^2,\ k_{b_1}^2\}, \end{aligned}$$

which shows (iii). Notice that the eigenvalues u_1 and u_2 defined in the Proposition 3.1 equal to k_{b_1} and k_{b_2}, respectively, according to the spectral theory. □

3.2.2 Control System Design

Based on the properties we derived in the previous section, a control input is designed. By applying the designed control input, the equilibrium of the controlled system is guaranteed to have exponential convergence.

Proposition 3.2. Consider the dynamic system (3.3) and (3.4) on $\mathsf{SO(3)}$ with the desired trajectory (3.11) and (3.12), a control input is chosen as

$$u = -e_b - k_\Omega e_\Omega + \hat{\Omega}_d J(e_\Omega + \Omega_d) + J\dot{\Omega}_d, \tag{3.43}$$

then the following properties are secured:

(i) There are four equilibrium configurations, give by

$$(R, \Omega) \in \{(R_d, \Omega_d), (UD_1U^\mathsf{T}R_d, \Omega_d), (UD_2U^\mathsf{T}R_d, \Omega_d), (UD_3U^\mathsf{T}R_d, \Omega_d)\}, \tag{3.44}$$

where $D_1 = \mathrm{diag}[1, -1, -1]$, $D_2 = \mathrm{diag}[-1, 1, -1]$, and $D_3 = \mathrm{diag}[-1, -1, 1]$ are diagonal matrices with trace equals to -1 and $U \in \mathsf{SO(3)}$ which is already defined in (3.29).

(ii) The desired equilibrium (R_d, Ω_d) is almost globally exponentially stable, with an estimate of region of attraction given by

$$\Psi(0) \leq \psi < h_1, \tag{3.45}$$

$$\|e_\Omega(0)\|^2 \leq \frac{2}{\lambda_M(J)}(\psi - \Psi(0)), \tag{3.46}$$

where $\Psi(0) \equiv \Psi(b_1(0), b_2(0), b_{1_d}(0), b_{2_d}(0))$ and $\lambda_M(J)$ denotes the maximum

eigenvalue of J.

(iii) The remaining three undesired equilibrium configurations are unstable.

Without using any IMU sensors, two distinct pointing direction, referring to LOS measurements, are used to determine the absolute attitude. And the control input is directly expressed by the LOS measurements. Besides, by showing the instability of three undesired configuration equilibrium, the region of attraction of the desired equilibrium is almost global.

Proof. The equilibrium configurations locate at $(e_\Omega, e_b) = (0, 0)$. Since $e_\Omega = \Omega - \Omega_d$, we know that $e_\Omega = 0$ leads to $\Omega = \Omega_d$. As for $e_b = 0$, recall (3.37) to write

$$\begin{aligned} e_b &= [R_d^\mathsf{T} K R - R^\mathsf{T} K R_d]^\vee \\ &= [R_d^\mathsf{T} K R (R_d^\mathsf{T} R_d) - (R_d^\mathsf{T} R_d) R^\mathsf{T} K R_d]^\vee \\ &= [R_d^\mathsf{T} (K R R_d^\mathsf{T} - R_d R^\mathsf{T} K) R_d]^\vee \\ &= \{R_d^\mathsf{T} [K (R R_d^\mathsf{T}) - (R R_d^\mathsf{T})^\mathsf{T} K] R_d\}^\vee, \end{aligned} \tag{3.47}$$

which implies that

$$K(RR_d^\mathsf{T}) - (RR_d^\mathsf{T})^\mathsf{T} K = 0. \tag{3.48}$$

In [29], it has been show that (3.48) reveals

$$RR_d^\mathsf{T} \in \{I, UD_1U^\mathsf{T}, UD_2U^\mathsf{T}, UD_3U^\mathsf{T}\} \tag{3.49}$$

where $D_1 = \text{diag}[1, -1, -1]$, $D_2 = \text{diag}[-1, 1, -1]$, and $D_3 = \text{diag}[-1, -1, 1]$. Hence we are now able to show the eqauilibria in terms of R and Ω, which is (i).

To show the exponential stability, We first rewrite (3.3) as follows,

$$J\dot{\Omega} + \Omega \times J\Omega - J\dot{\Omega}_d = u - J\dot{\Omega}_d, \tag{3.50}$$

which leads to

$$J\dot{e}_\Omega = J(\dot{\Omega} - \dot{\Omega}_d) = -\Omega \times J\Omega - J\dot{\Omega}_d + u. \tag{3.51}$$

Substituting $e_\Omega = \Omega - \Omega_d$ and (A.2), we have

$$\begin{aligned} J\dot{e}_\Omega &= -(e_\Omega + \Omega_d) \times J(e_\Omega + \Omega_d) - J\dot{\Omega}_d + u \\ &= -e_\Omega \times J(e_\Omega + \Omega_d) - \Omega_d \times J(e_\Omega + \Omega_d) - J\dot{\Omega}_d + u \\ &= [J(e_\Omega + \Omega_d)]^\wedge e_\Omega - \hat{\Omega}_d J(e_\Omega + \Omega_d) - J\dot{\Omega}_d + u. \end{aligned}$$

Now substitute the control input into this equation, and the error dynamics for the angular velocity is given by

$$J\dot{e}_\Omega = [J(e_\Omega + \Omega_d)]^\wedge e_\Omega - e_b - k_\Omega e_\Omega. \tag{3.52}$$

To show the exponential stability, we first define

$$U = \frac{1}{2} e_\Omega \cdot J e_\Omega + \Psi,$$

notice that $U \geq \Psi$. Then, the time-derivative of U is given by

$$\begin{aligned} \dot{U} &= e_\Omega \cdot J\dot{e}_\Omega + \dot{\Psi} \\ &= e_\Omega \cdot ([J(e_\Omega + \Omega_d)]^\wedge e_\Omega - e_b - k_\Omega e_\Omega) + e_\Omega \cdot e_b \\ &= -k_\Omega \|e_\Omega\|^2, \end{aligned}$$

which implies that $U(t)$ is a non-increasing function. To specify the initial condition of U, we have

$$U(0) = \frac{1}{2} e_\Omega(0) \cdot J e_\Omega(0) + \Psi(0) \ \leq \ \frac{1}{2} \lambda_M(J) \|e_\Omega(0)\|^2 + \Psi(0). \tag{3.53}$$

Substituting (3.45) and (3.46) to (3.53) yields to

$$\begin{aligned} U(0) &\leq \frac{1}{2} \lambda_M(J) \|e_\Omega(0)\|^2 + \Psi(0) \\ &\leq \frac{1}{2} \lambda_M(J) \frac{2}{\lambda_M(J)} (\psi - \Psi(0)) + \Psi(0) = \psi. \end{aligned} \tag{3.54}$$

Since $U(t)$ is non-increasing, the value of $U(t)$ must be less or equal than $U(0)$ and we already know $U(t) \geq \Psi(t)$. Combine (3.45) and (3.54) to obtain

$$\Psi(t) \leq U(t) \leq U(0) \leq \psi < h_1.$$

This inequality implies that $\Psi(t) < h_1$ for all $t > 0$, and (3.40) is also satisfied.

The Lyapunov candidate is given as

$$\mathcal{V} = \frac{1}{2} e_\Omega \cdot J e_\Omega + \Psi + c e_\Omega \cdot e_b = U + c e_\Omega \cdot e_b, \tag{3.55}$$

where c is a positive constant. Notice that

$$\lambda_m(J) \|e_\Omega\|^2 \leq {e_\Omega}^\mathsf{T} \cdot J e_\Omega \leq \lambda_M(J) \|e_\Omega\|^2 \tag{3.56}$$

$$-c \|e_\Omega\| \|e_b\| \leq c e_\Omega \cdot e_b \leq c \|e_\Omega\| \|e_b\|. \tag{3.57}$$

By combining the inequalities, (3.56), (3.57) with (3.40) we can obtain the upper and

lower bounds of $\mathcal{V}$ as follows

$$\mathcal{V} \leq \frac{1}{2}\lambda_M(J)\|e_\Omega\|^2 + \frac{h_1 h_4}{h_5(h_1-\psi)}\|e_b\|^2 + c\|e_\Omega\|\|e_b\|,$$
$$\mathcal{V} \geq \frac{1}{2}\lambda_m(J)\|e_\Omega\|^2 + \frac{h_1}{h_2+h_3}\|e_b\|^2 - c\|e_\Omega\|\|e_b\|,$$

which can be written in the following matrix form

$$z^\mathsf{T} M_1 z \leq \mathcal{V} \leq z^\mathsf{T} M_2 z, \tag{3.58}$$

where $z = \begin{bmatrix} \|e_b\| \\ \|e_\Omega\| \end{bmatrix}$, $M_1 = \frac{1}{2}\begin{bmatrix} \frac{2h_1}{h_2+h_3} & -c \\ -c & \lambda_m(J) \end{bmatrix}$ and $M_2 = \frac{1}{2}\begin{bmatrix} \frac{2h_1 h_4}{h_5(h_1-\psi)} & c \\ c & \lambda_M(J) \end{bmatrix}$.

To guarantee M_1 and M_2 to be positive definite, we have

$$c < \min\{\sqrt{\frac{2h_1\lambda_m(J)}{h_2+h_3}}, \sqrt{\frac{2h_1 h_4 \lambda_M(J)}{h_5(h_1-\psi)}}\} \tag{3.59}$$

The time-derivative of $\mathcal{V}$ is given as

$$\begin{aligned} \dot{\mathcal{V}} &= \dot{U} + c\dot{e}_\Omega \cdot e_b + c e_\Omega \cdot \dot{e}_b \\ &= -k_\Omega \|e_\Omega\|^2 + c\dot{e}_\Omega \cdot e_b + c e_\Omega \cdot \dot{e}_b. \end{aligned} \tag{3.60}$$

To obtain the upper bound of $\dot{e}_\Omega \cdot e_b$, we first use (3.52) to have

$$J^{-1}J\dot{e}_\Omega = \dot{e}_\Omega = J^{-1}[J(e_\Omega + \Omega_d)]^\wedge e_\Omega - J^{-1}e_b - k_\Omega J^{-1} e_\Omega,$$

and then

$$\begin{aligned}\dot{e}_\Omega \cdot e_b &= J^{-1}[J(e_\Omega + \Omega_d)]^\wedge e_\Omega \cdot e_b - J^{-1}\|e_b\|^2 - k_\Omega J^{-1} e_\Omega \cdot e_b \\ &\leq \lambda_M(J^{-1})\|[\lambda_M(J)(e_\Omega + \Omega_d)]^\wedge e_\Omega\|\|e_b\| - \lambda_m(J^{-1})\|e_b\|^2 + k_\Omega \lambda_m(J^{-1})\|e_\Omega\|\|e_b\| \\ &\leq \frac{\|e_b\|}{\lambda_m(J)}(\|\lambda_M(J)\|e_\Omega\|^2 + \lambda_M(J)B_{\Omega d}\|e_\Omega\|) - \frac{1}{\lambda_M(J)}\|e_b\|^2 + k_\Omega \frac{1}{\lambda_m(J)}\|e_\Omega\|\|e_b\| \\ &= \frac{\|e_b\|}{\lambda_m}(\|\lambda_M\|e_\Omega\|^2 + \lambda_M B_d\|e_\Omega\|) - \frac{1}{\lambda_M}\|e_b\|^2 + k_\Omega \frac{1}{\lambda_m}\|e_\Omega\|\|e_b\|. \end{aligned} \tag{3.61}$$

Furthermore, by using property (ii) of Proposition 3.1, the upper bound of $e_\Omega \cdot \dot{e}_b$ is given by

$$\|e_\Omega\|\|\dot{e}_b\| \leq (k_{b_1} + k_{b_2})\|e_\Omega\|^2 + B_{\Omega d}\|e_b\|\|e_\Omega\|. \tag{3.62}$$

Substituting (3.61) and (3.62) into (3.60), we obtain

$$\begin{aligned}\dot{\mathcal{V}} \leq &-[k_\Omega - c(k_{b_1} + k_{b_2})(1 + \frac{\lambda_M(J)}{\lambda_m(J)})]\|e_\Omega\|^2 - \frac{c}{\lambda_M(J)}\|e_b\|^2 \\ &+ \frac{c}{\lambda_m}(\bar{\lambda}(J)B_{\Omega d} + k_\Omega)\|e_b\|\|e_\Omega\|. \end{aligned} \tag{3.63}$$

where $\bar{\lambda}(J) = \lambda_M(J) + \lambda_m(J)$. Again, this equation can be written in matrix form

$$\dot{\mathcal{V}} \leq -z^\mathsf{T} M_3 z, \tag{3.64}$$

where

$$M_3 = \begin{bmatrix} \frac{c}{\lambda_M(J)} & -\frac{c}{2\lambda_m}(\bar{\lambda}(J)B_{\Omega d} + k_\Omega) \\ -\frac{c}{2\lambda_m}(\bar{\lambda}(J)B_{\Omega d} + k_\Omega) & k_\Omega - c(k_{b_1} + k_{b_2})(1 + \frac{\lambda_M(J)}{\lambda_m(J)}) \end{bmatrix} \in \mathbb{R}^{2\times 2}.$$

To ensure M_3 is positive definite, we have the following limitation

$$c < \frac{4\lambda_m(J)^2 k_\Omega}{4\lambda_m(J)(k_{b_1}+k_{b_2})\bar{\lambda}(J) + \lambda_M(B_{\Omega d}\bar{\lambda}(J)+k_\Omega)^2}. \tag{3.65}$$

In summary, the constant c is chosen such that (3.59) and (3.65) are satisfied, then the matrices M_1, M_2 and M_3 are positive definite, which show that the desired equilibrium configuration is exponentially stable.

Finally, for (iii), substitute the first type of undesired equilibrium configurations, $(R,\Omega) = (UD_1U^\mathsf{T}R_d, \Omega_d)$, to obtain the Lyapunov function $\mathcal{V} = \Psi$. Form (3.32), we have

$$\Psi = \mathrm{tr}[G(I - U^\mathsf{T}(UD_1U^\mathsf{T}R_d)R_d^\mathsf{T}U)] = \mathrm{tr}[G(I-D_1)] = 2\mu_2. \tag{3.66}$$

Define

$$\mathcal{W} = 2\mu_2 - \mathcal{V} = -\frac{1}{2}e_\Omega \cdot Je_\Omega + (2\mu_2 - \Psi) - ce_\Omega \cdot e_b, \tag{3.67}$$

then at the first type undesired equilibrium, $\mathcal{W} = 0$, we have

$$\mathcal{W} \geq -\frac{\lambda_M(J)}{2}\|e_\Omega\|^2 + (2\mu_2 - \Psi) - c\|e_\Omega\|\|e_b\| \tag{3.68}$$

Since Ψ is a continuous function, we are able to select R that is arbitrary close to $UD_1U^\mathsf{T}R_d$ such that $(2\mu_2 - \Psi) > 0$. Therefore, if $\|e_\Omega\|$ is sufficiently small, $\mathcal{W} > 0$ can be achieved at those points. Indeed, at arbitrarily small neighborhood of the undesired equilibrium, there exists a domain in which $\mathcal{W} > 0$, and $\dot{\mathcal{W}} = \dot{\mathcal{V}} > 0$ where we have shown $\dot{\mathcal{V}} > 0$ in the proof of exponential stability. From Theorem 4.3 of [43], this undesired equilibrium is unstable. In a similar manner, we can say the rest of undesired equlibirua are unstable, which ensure (iii).

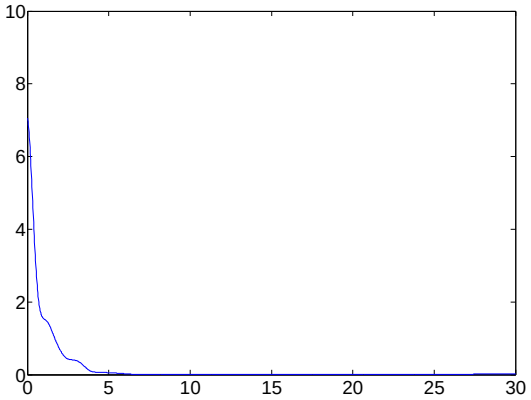

(a) Direction error function Ψ

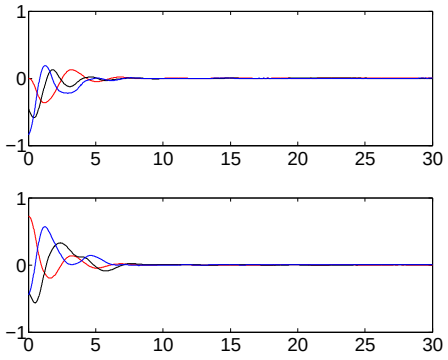

(b) Direction error vector e_{b_1} and e_{b_2}

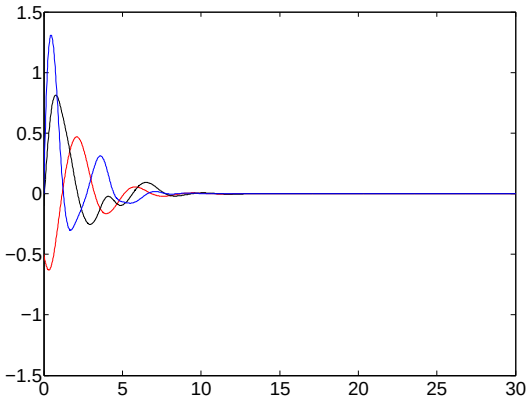

(c) Angular velocity error vector e_Ω

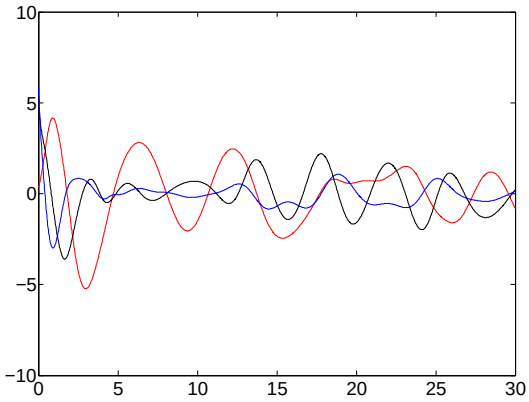

(d) Control input u

Figure 3.2: Numerical results for single spacecraft attitude control

□

3.3 Numerical Example

Consider a spacecraft with inertia matrix $J = \text{diag}[3, 2, 1]\,\text{kgm}^2$. The desired attitude is selected in terms of 3-2-1 Euler angles, that is $R_d = \exp(\alpha\hat{e}_3)\exp(\beta\hat{e}_2)\exp(\gamma\hat{e}_1)$ where $\alpha = \sin 0.5t$, $\beta = 0.1$, $\gamma = \cos t$, $e_1 = [1\ 0\ 0]^\mathsf{T}$, $e_2 = [0\ 1\ 0]^\mathsf{T}$, and $e_3 = [0\ 0\ 1]^\mathsf{T}$. Additionally, The direction to two distinctive objects are chosen as $s_1 = [1\ 0\ 0]^\mathsf{T}$ and $s_2 = [\cos(60^\circ)\ \ \sin(60^\circ)\ 0]^\mathsf{T}$ and the control gain are specified as $k_{b_1} = 5$, $k_{b_2} = 5.1$ and $k_\Omega = 3.13$. Fig 3.2 shows the corresponding simulation results.

Chapter 4 Spacecraft Relative Attitude Formation Tracking on $\mathsf{SO}(3)$ Based on Line-Of-Sight Measurements

This chapter is concerned with extending previous work to achieve the goal of this thesis, the control of relative attitude formation among multiple spacecraft by using LOS measurements.

As the relative control for an arbitrary number of spacecraft is quite challenging. We start from relative attitude between two spacecrafts and show the described properties explicitly. It is generalized for relative formation control among an arbitrary number of spacecraft.

4.1 Problem Formulation

Consider an arbitrary number n of spacecraft in formation. Each spacecraft is considered as a rigid body, and an inertial reference frame and corresponding n body-fixed frames are defined. The attitude of each spacecraft is the orientation of its body-fixed frame with respect to the inertial reference frame, and it is represented by a rotation matrix in the special orthogonal group, $\mathsf{SO}(3) = \{R \in \mathbb{R}^{3\times 3} \mid R^{\mathsf{T}}R = I,\ \det(R) = 1\}$. Each spacecraft measures the LOS from itself toward the other assigned spacecraft. A LOS observation is represented by a unit vector in the two-sphere, defined as $\mathsf{S}^2 = \{s \in \mathbb{R}^3 \mid \|s\| = 1\}$. The nonlinear properties of S^2 and $\mathsf{SO}(3)$ has been addressed in Chapter 2 and Chapter 3, respectively.

4.1.1 Spacecraft Attitude Formation Configuration

We hereby define the configuration variables as follows, for $i, j \in \{1, \ldots, n\}$ and $i \neq j$,

$R_i(t) \in \mathsf{SO(3)}$	the absolute attitude for the i-th spacecraft, representing the transformation from the i-th body-fixed frame to the inertial reference frame,
$s_{ij} \in \mathsf{S}^2$	the unit vector toward the j-th spacecraft from the i-th spacecraft, represented in the inertial frame,
$b_{ij}(t) \in \mathsf{S}^2$	the LOS direction observed from the i-th spacecraft to the j-th spacecraft, represented in the i-th body fixed frame,
$Q_{ij}(t) \in \mathsf{SO(3)}$	the relative attitude of the i-th spacecraft with respect to the j-th spacecraft,
$Q_{ij}^d(t) \in \mathsf{SO(3)}$	the desired relative attitude for Q_{ij}.

According to these definitions, the directions of the relative positions s_{ij} in the inertial reference frame are related to the LOS observation b_{ij} in the i-th body-fixed frame as follows:

$$s_{ij} = R_i b_{ij}, \quad b_{ij} = R_i^{\mathsf{T}} s_{ij}. \tag{4.1}$$

In short, b_{ij} represents the LOS observation of s_{ij}, observed from the i-th body. The relative attitude is given by

$$Q_{ij} = R_j^{\mathsf{T}} R_i, \tag{4.2}$$

which represents the transformation of the representation of a vector from the i-th body fixed frame to the j-th body-fixed frame. Note that

$$Q_{ij} = R_j^{\mathsf{T}} R_i = (R_i^{\mathsf{T}} R_j)^{\mathsf{T}} = Q_{ji}^{\mathsf{T}}. \tag{4.3}$$

To assign sets of LOS that should be measured for each spacecraft, a graph $(\mathcal{N}, \mathcal{E})$ and related sets are defined as follows.

$\mathcal{N} = \{1, \ldots, n\}$	the node set, hence each spacecraft is considered as a node,
$\mathcal{E} \subset \mathcal{N} \times \mathcal{N}$	the edge set. The relative attitude between the i-th spacecraft and the j-th spacecraft is directly controlled if $(i, j) \in \mathcal{E}$,
$\rho : \mathcal{E} \to \mathcal{N}$	the assignment map,
$\mathcal{A}$	the assignment set,
$\mathcal{L}_i$	the measurement set, the set of LOS measurements from the i-th spacecraft,
$\mathcal{C}_{ij}$	the communication set, the LOS transfered from the i-th spacecraft to the j-the spacecraft.

The graph $(\mathcal{N}, \mathcal{E})$ represents a set of LOS that should be measured for each spacecraft. Notice that $\mathcal{E}$ is symmetric, specifically, $(i, j) \in \mathcal{E} \Leftrightarrow (j, i) \in \mathcal{E}$. For each pair of spacecraft in the edge set $\mathcal{E}$, another third spacecraft is assigned by the assignment map ρ. Moreover, ρ is also a symmetric, i.e., $\rho(i, j) = \rho(j, i)$. The definition of the assignment set is given by

$$\mathcal{A} = \{(i, j, k) \in \mathcal{E} \times \mathcal{N} \mid (i, j) \in \mathcal{E},\ k = \rho(i, j)\}. \tag{4.4}$$

In particular, we have the following assumptions to describe the problem clearly:

Assumption 1. The configuration of the relative positions is fixed, i.e., $\dot{s}_{ij} = 0$ for all $i, j \in \mathcal{N}$ with $i \neq j$.

Assumption 2. The third spacecraft assigned to each edge does not lie on the line joining two spacecraft connected by the edge, i.e., $s_{ik} \times s_{jk} \triangleq s_{ijk} \neq 0$ for every $(i, j, k) \in \mathcal{A}$.

Assumption 3. The measurement set of the i-th spacecraft is given by

$$\mathcal{L}_i = \{b_{ij}, b_{ik} \in \mathsf{S}^2 \,|\, (i, j, k) \in \mathcal{A}\}. \tag{4.5}$$

Assumption 4. The communication set from the i-th spacecraft to the j-th spacecraft is given by

$$\mathcal{C}_{ij} = \begin{cases} \{b_{ij}, b_{i\rho(i,j)}\} & \text{if } (i, j) \in \mathcal{E}, \\ \emptyset & \text{otherwise.} \end{cases} \tag{4.6}$$

Assumption 5. In the edge set, spacecraft are paired serially by daisy-chaining.

The first assumption reflects the fact that this thesis does not consider the translational dynamics of spacecraft, and we focus on the rotational attitude dynamics only. The proposed control input does not depend on the values of s_{ij}, but its stability analyses is based on the first assumption that s_{ij} is fixed. The second assumption is required to determine the relative attitude between two spacecraft paired in the edge set from the assigned LOS measurements. The third assumption states that each spacecraft measures the LOS toward the paired spacecraft in the edge set, and the LOS toward the third spacecraft assigned to each pair by the assignment map. The fourth assumption implies that a spacecraft communicate only with the spacecraft paired with itself. The last assumption is made to simplify stability analysis while the proposed relative attitude formation control system can be extended for other network topologies.

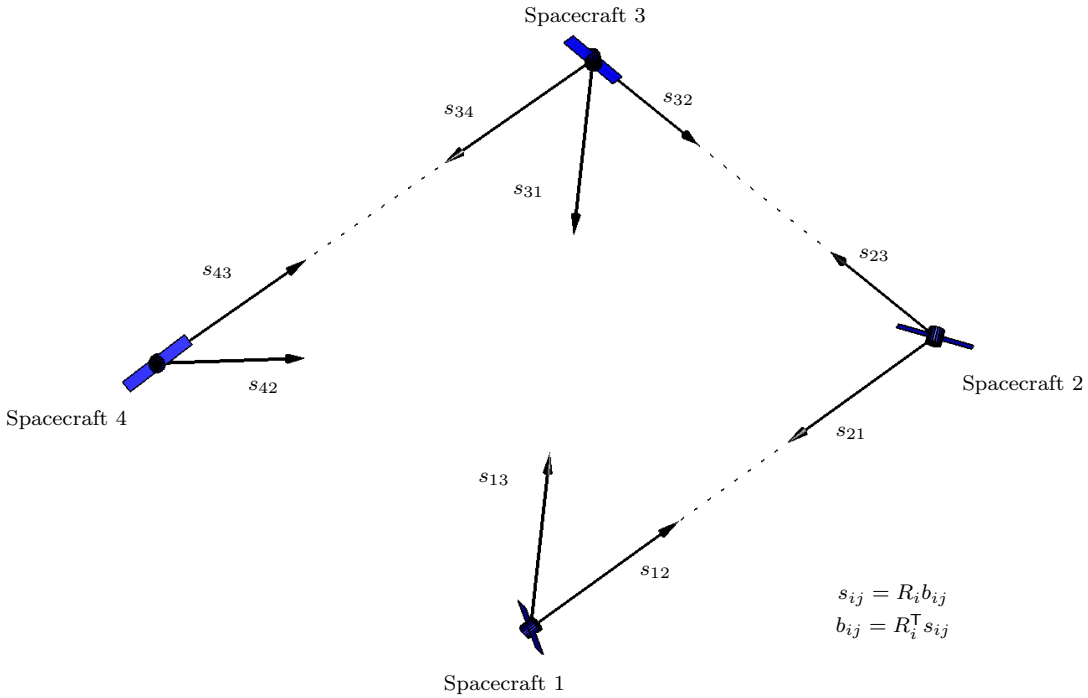

Figure 4.1: Formation of four spacecrafts: the direction along the relative position of the i-th body from the j-th body is denoted by s_{ij} in the inertial reference frame. The LOS observation of s_{ij} with respect the i-th body fixed frame, namely b_{ij} is obtained from (4.1).

An example for formation of four spacecraft satisfying these assumptions are illustrated at Figure 4.1, where

$$\mathcal{A} = \{(1,2,3),\ (2,1,3),\ (2,3,1),\ (3,2,1),\ (3,4,2),\ (4,3,2)\}.$$

The measurement sets and the communication sets can be determined by (4.5) and (4.6) from $\mathcal{A}$. For example, for the third spacecraft, we have $\mathcal{L}_3 = \{b_{31}, b_{32}, b_{34}\}$, $\mathcal{C}_{32} = \{b_{32}, b_{31}\}$, and $\mathcal{C}_{34} = \{b_{34}, b_{32}\}$.

4.1.2 Spacecraft Attitude Dynamics

Similar to (3.3) and (3.4), the equations of motion for the attitude dynamics of each spacecraft are given by

$$J_i\dot{\Omega}_i + \Omega_i \times J_i\Omega_i = u_i, \tag{4.7}$$

$$\dot{R}_i = R_i\hat{\Omega}_i, \tag{4.8}$$

where $J_i \in \mathbb{R}^{3\times 3}$ is the inertia matrix of the i-th spacecraft, and $\Omega_i \in \mathbb{R}^3$ and $u_i \in \mathbb{R}^3$ are the angular velocity and the control moment of the i-th spacecraft, represented with respect to its body-fixed frame, respectively. In particular, it is assumed that the desired angular velocities are bounded by known constants.

Assumption 6. For known positive constants B_d,

$$\|\Omega_i^d(t)\| \leq B^d,$$

for all $t \geq 0$.

4.1.3 Kinematics of Relative Attitudes and Line-Of-Sight

For any $i, j \in \mathcal{N}$, the time-derivative of the relative attitude is given, from (4.8) and (4.2), by

$$\begin{aligned}\dot{Q}_{ij} &= -\hat{\Omega}_j R_j^\mathsf{T} R_i + R_j^\mathsf{T} R_i \hat{\Omega}_i = Q_{ij}\hat{\Omega}_i - \hat{\Omega}_j Q_{ij} = Q_{ij}(\Omega_i - Q_{ij}^\mathsf{T}\Omega_j)^\wedge \\ &\triangleq Q_{ij}\hat{\Omega}_{ij}, \end{aligned} \tag{4.9}$$

where the relative angular velocity $\Omega_{ij} \in \mathbb{R}^3$ of the i-th spacecraft with respect to the j-th spacecraft is defined as

$$\Omega_{ij} = \Omega_i - Q_{ij}^\mathsf{T}\Omega_j. \tag{4.10}$$

From (4.1) and (4.8), the time-derivative of the LOS measurement b_{ij} is given by

$$\dot{b}_{ij} = \dot{R}_i^\mathsf{T} s_{ij} = -\hat{\Omega}_i R_i^\mathsf{T} s_{ij} = b_{ij} \times \Omega_i. \tag{4.11}$$

Define $b_{ijk} \in \mathbb{R}^3$ where $b_{ijk} \triangleq b_{ij} \times b_{ik}$. From (4.11) and (4.2), it can be shown that

$$\begin{aligned}\dot{b}_{ijk} &= (b_{ij} \times \Omega_i) \times b_{ik} + b_{ij} \times (b_{ik} \times \Omega_i) \\ &= -(\Omega_i \cdot b_{ik})b_{ij} + (\Omega_i \cdot b_{ij})b_{ik} \\ &= b_{ijk} \times \Omega_i. \end{aligned} \tag{4.12}$$

4.2 Relative Attitude Tracking Between Two Spacecrafts

As a concrete example, we develop a control system for the relative attitude between Spacecraft 1 and Spacecraft 2, namely $Q_{12} = R_2^\mathsf{T} R_1$ illustrated at Figure 4.1. The corresponding edge set, assignment set and measurement sets used in this section are

given by

$$\mathcal{E} = \{(1,2),(2,1)\}, \quad \mathcal{A} = \{(1,2,3),(2,1,3)\}, \tag{4.13}$$

$$\mathcal{L}_1 = \mathcal{C}_{12} = \{b_{12}, b_{13}\},\ \mathcal{L}_2 = \mathcal{C}_{21} = \{b_{21}, b_{23}\}. \tag{4.14}$$

Notice that we are controlling spacecraft 1 and 2, which are considered as nodes, while the spacecrafts 3 belongs to the assignment map. Spacecraft 3 is required because we need an object that can be measured from spacecraft 1 and 2.

Suppose that a desired relative attitude $Q_{12}^d(t)$ is given as a smooth function of time. It satisfies the following kinematic equation:

$$\dot{Q}_{12}^d = Q_{12}^d \hat{\Omega}_{12}^d, \tag{4.15}$$

where Ω_{12}^d is the desired relative angular velocity.

Our goal is to design control inputs u_1, u_2 in terms of the LOS measurements in $\mathcal{L}_1 \cup \mathcal{L}_2$ such that Q_{12} asymptotically follows Q_{12}^d, i.e., $Q_{12}(t) \to Q_{12}^d(t)$ as $t \to \infty$.

4.2.1 Kinematics of Relative Attitude

It has been shown that four LOS measurements in $\mathcal{L}_1 \cup \mathcal{L}_2$ completely determine the relative attitude Q_{12} from the following constraints [10]:

$$b_{12} = -Q_{12}^{\mathsf{T}} b_{21}, \tag{4.16}$$

$$\frac{b_{123}}{\|b_{123}\|} = -\frac{Q_{12}^{\mathsf{T}} b_{213}}{\|b_{213}\|}. \tag{4.17}$$

These are derived from the fact that four unit vectors, namely, s_{12}, s_{13}, s_{21} and s_{23}, lie on the sides of a triangle composed of three spacecraft. In particular, the first constraint (4.16) states that the unit vector from Spacecraft 1 to Spacecraft 2 is exactly opposite to the unit vector from Spacecraft 2 to Spacecraft 1, i.e., $s_{12} = -s_{21}$.

The second constraint (4.17) implies that the plane spanned by s_{12} and s_{13} should be co-planar with the plane spanned by s_{21} and s_{23}. These geometric constraints are simply expressed with respect to the first body-fixed frame to obtain (4.16) and (4.17). In consequence, the relative attitude Q_{12} is determined uniquely by the LOS measurements $\{b_{12}, b_{13}, b_{21}, b_{23}\}$ according to (4.16) and (4.17).

We develop a relative attitude tracking control system based on these two constraints. More explicitly, control inputs are chosen such that two constraints are satisfied when the relative attitude is equal to its desired value. As both constraints are conditions on unit vectors, controller design similar to tracking control on the two-sphere. From now on, variables related to the type of first constraint we just introduced, (4.16) are denoted by the sub- or super-script α while β refers to variables related to the second type constraint, (4.17).

The α-type configuration error function are defined as

$$\Psi_{12}^{\alpha} = \frac{1}{2}\|b_{21} + Q_{12}^{d} b_{12}\|^2 = 1 + b_{21} \cdot Q_{12}^{d} b_{12} \tag{4.18}$$

$$= 1 + (R_2^{\mathsf{T}} s_{21}) \cdot (Q_{12}^{d} R_1^{\mathsf{T}} s_{12}) = 1 + s_{21} \cdot R_2 Q_{12}^{d} R_1^{\mathsf{T}} s_{12}. \tag{4.19}$$

It is equivalent to $\Psi_{12}^{\alpha} = 1 - \cos(\theta_{12}^{\alpha})$, where θ_{12}^{α} is the angle between b_{21} and $-Q_d b_{12}$. The corresponding error vectors can be defined by using the direction derivative of Ψ_{ij}, i.e., (4.19). This process is analogous to preceding work in Chapter 3, expressly, from (3.16) to (3.18). By following the same approach, the α-type error vectors are defined as follows:

$$\begin{aligned} e_{12}^{\alpha} &= ({Q_{12}^{d}}^{\mathsf{T}} b_{21}) \times b_{12} = (Q_{21}^{d} b_{21}) \times b_{12}, \\ e_{21}^{\alpha} &= (Q_{12}^{d} b_{12}) \times b_{21}. \end{aligned} \tag{4.20}$$

The β-type error function are defined by

$$\Psi_{12}^{\beta} = 1 + \frac{1}{a_{12}} b_{213} \cdot Q_{12}^{d} b_{123}, \tag{4.21}$$

where $a_{12} = a_{21} \triangleq \|b_{213}\|\|b_{123}\| \in \mathbb{R}$. Since $\|b_{ijk}\| = \|b_{ij} \times b_{ik}\| = \|R_i^{\mathsf{T}} s_{ij} \times R_i^{\mathsf{T}} s_{ik}\| = \|s_{ij} \times s_{ik}\|$, the constant a_{12} is fixed according to Assumption 1, and it is non-zero from Assumption 2. In particular, Ψ_{12}^{β} stands for the error between $Q_d b_{123}$ and $-b_{213}$. Furthermore, the configuration error vectors are given as

$$e_{12}^{\beta} = \frac{1}{a_{12}} ({Q_{12}^{d}}^{\mathsf{T}} b_{213}) \times b_{123} = \frac{1}{a_{12}} (Q_{21}^{d} b_{213}) \times b_{123}, \tag{4.22}$$

$$e_{21}^{\beta} = \frac{1}{a_{21}} (Q_{12}^{d} b_{123}) \times b_{213}. \tag{4.23}$$

As b_{12}, b_{21} are unit vectors, and from the definition of a_{12}, a_{21}, we can show that the upper bound bonds of all the error vectors, $\|e_{12}^{\alpha}\|, \|e_{21}^{\alpha}\|, \|e_{12}^{\beta}\|, \|e_{21}^{\beta}\| \leq 1$.

We also define the angular velocity errors:

$$e_{\Omega_1} = \Omega_1 - \Omega_1^{d}, \quad e_{\Omega_2} = \Omega_2 - \Omega_2^{d}, \tag{4.24}$$

where the desired absolute angular velocities Ω_1^{d} and Ω_d^{2} are chosen such that

$$\Omega_{12}^{d} = \Omega_1^{d} - Q_{21}^{d} \Omega_2^{d}. \tag{4.25}$$

This corresponds to (4.10). Any desired absolute angular velocities satisfying (4.25) can be chosen. For example, they can be selected as

$$\Omega_{1_d} = \frac{1}{2} \Omega_{12}^{d}, \quad \Omega_{2_d} = \frac{1}{2} \Omega_{21}^{d} = -Q_{12}^{d} \Omega_{1_d}.$$

Using these desired angular velocities, the derivative of the desired relative attitude

can be rewritten as

$$\dot{Q}_{12}^d = Q_{12}^d \hat{\Omega}_1^d - \hat{\Omega}_2^d Q_{12}^d. \tag{4.26}$$

The properties of these error variables are summarized as follows.

Proposition 4.1. For positive constants $k_{12}^\alpha \neq k_{12}^\beta$, define

$$\Psi_{12} = k_{12}^\alpha \Psi_{12}^\alpha + k_{12}^\beta \Psi_{12}^\beta, \tag{4.27}$$

$$e_{12} = k_{12}^\alpha e_{12}^\alpha + k_{12}^\beta e_{12}^\beta, \tag{4.28}$$

$$e_{21} = k_{21}^\alpha e_{21}^\alpha + k_{21}^\beta e_{21}^\beta, \tag{4.29}$$

where $k_{21}^\alpha = k_{21}^\beta$, $k_{21}^\beta = k_{12}^\beta$. The following properties hold:

(i) $e_{12} = -Q_{21}^d e_{21}$, and $\|e_{12}\| = \|e_{21}\|$.

(ii) $\frac{d}{dt}\Psi_{12} = e_{12} \cdot e_{\Omega_1} + e_{21} \cdot e_{\Omega_2}$.

(iii) $\|\dot{e}_{12}\| \leq (k_{12}^\alpha + k_{12}^\beta)(\|e_{\Omega_1}\| + \|e_{\Omega_2}\|) + B^d \|e_{12}\|$,
$\|\dot{e}_{21}\| \leq (k_{12}^\alpha + k_{12}^\beta)(\|e_{\Omega_1}\| + \|e_{\Omega_2}\|) + B^d \|e_{21}\|$.

(iv) If $\Psi_{12} \leq \psi < 2\min\{k_{12}^\alpha, k_{12}^\beta\}$ for a constant ψ, then Ψ is quadratic with respect to $\|e_{12}\|$, i.e., the following inequality is satisfied:

$$\underline{\psi}_{12} \|e_{12}\|^2 \leq \Psi_{12} \leq \overline{\psi}_{12} \|e_{12}\|^2, \tag{4.30}$$

where the constants $\underline{\psi}_{12}, \overline{\psi}_{12}$ are given by

$$\underline{\psi}_{12} = \frac{\min\{k_{12}^\alpha, k_{12}^\beta\}}{2\max\{(k_{12}^\alpha)^2, (k_{12}^\beta)^2, (k_{12}^\alpha - k_{12}^\beta)^2\} + 2(k_{12}^\alpha + k_{12}^\beta)^2},$$
$$\overline{\psi}_{12} = \frac{\min\{k_{12}^\alpha, k_{12}^\beta\}(k_{12}^\alpha + k_{12}^\beta)}{\min\{(k_{12}^\alpha)^2, (k_{12}^\beta)^2\}(2\min\{k_{12}^\alpha, k_{12}^\beta\} - \varphi)}.$$

Proof. Throughout this proof, we use the symbolic representation for property 1 and 2 to show that this proposition can be applied to arbitrary spacecraft i and j. From (4.20), e_{ij}^{α} is given by

$$e_{ij}^{\alpha} = (Q_{ji}^{d} b_{ji}) \times b_{ij} = Q_{ji}^{d}(b_{ji} \times Q_{ij}^{d} b_{ij}) = -Q_{ji}^{d} e_{ji}^{\alpha}.$$

Likewise, $e_{ij}^{\beta} = -Q_{ji}^{d} e_{ji}^{\beta}$. The symbolic form of (4.28) and (4.29) can be denoted by

$$e_{ij} = k_{ij}^{\alpha}(-Q_{ji}^{d} e_{ji}^{\alpha}) + k_{ij}^{\beta}(-Q_{ji}^{d} e_{ji}^{\beta}) = -Q_{ji}^{d}(k_{ji}^{\alpha} e_{ji}^{\alpha} + k_{ji}^{\beta} e_{ji}^{\beta}) = -Q_{ji}^{d} e_{ji} \tag{4.31}$$

where we have applied $k_{ij}^{\alpha} = k_{ji}^{\beta}$ and $k_{ij}^{\alpha} = k_{ji}^{\beta}$. Since $Q_{ij}^{d} \in \mathsf{SO(3)}$, any vector multiplied by Q_{ij}^{d} may change its direction but not the magnitude, thus $\|e_{ij}\| = \|e_{ji}\|$. These show (i).

From (4.19), the time-derivative of Ψ_{ij}^{α} is given by

$$\dot{\Psi}_{ij}^{\alpha} = s_{ji} \cdot (\dot{R}_j Q_{ij}^{d} R_i^{\mathsf{T}} s_{ij}) + s_{ji} \cdot (R_j \dot{Q}_{ij}^{d} R_i^{\mathsf{T}} s_{ij}) + s_{ji} \cdot (R_j Q_{ij}^{d} \dot{R}_i^{\mathsf{T}} s_{ij}). \tag{4.32}$$

Define $\dot{\Psi}_{ij}^{\alpha} = A + B$ where

$$A = s_{ji} \cdot [\dot{R}_j Q_{ij}^{d}(R_i^{\mathsf{T}} s_{ij}) + R_j Q_{ij}^{d}(\dot{R}_i^{\mathsf{T}}) s_{ij}], \tag{4.33}$$

$$B = s_{ji} \cdot (R_j \dot{Q}_{ij}^{d} R_i^{\mathsf{T}} s_{ij}). \tag{4.34}$$

By applying $\dot{R}_i = R_i \hat{\Omega}_i$ and $\dot{s}_{ij} = \dot{s}_{ji} = 0$, A becomes

$$\begin{aligned} A &= s_{ji}^{\mathsf{T}} R_j \hat{\Omega}_j Q_{ij}^{d}(R_i^{\mathsf{T}} s_{ij}) + s_{ji}^{\mathsf{T}} R_j Q_{ij}^{d}(R_i \hat{\Omega}_i)^{\mathsf{T}} s_{ij} \\ &= (R_j^{\mathsf{T}} s_{ji})^{\mathsf{T}} \hat{\Omega}_j Q_{ij}^{d}(R_i^{\mathsf{T}} s_{ij}) + (R_j^{\mathsf{T}} s_{ji})^{\mathsf{T}} Q_{ij}^{d} \hat{\Omega}_i^{\mathsf{T}}(R_i^{\mathsf{T}} s_{ij}) \\ &= b_{ji} \cdot \hat{\Omega}_j Q_{ij}^{d} b_{ij} - b_{ji} \cdot Q_{ij}^{d} \hat{\Omega}_i b_{ij} \\ &= b_{ji} \cdot [\Omega_j \times (Q_{ij}^{d} b_{ij})] - ({Q_{ij}^{d}}^{\mathsf{T}} b_{ji}) \cdot (\Omega_i \times b_{ij}) \end{aligned} \tag{4.35}$$

From the triple product expansion, $x \cdot (y \times z) = y \cdot (z \times z) = z(x \times y)$ for x, y, and $z \in \mathbb{R}^3$

$$A = \Omega_i \cdot [(Q_{ij}^{d\,\mathsf{T}} b_{ji}) \times b_{ij}] + \Omega_j \cdot [(Q_{ij}^d b_{ij}) \times b_{ji}] = \Omega_i \cdot e_{ij}^\alpha + \Omega_j \cdot e_{ji}^\alpha. \tag{4.36}$$

For B, we substitute (4.26) and obtain

$$B = s_{ji} \cdot (R_j \dot{Q}_{ij}^d R_i^\mathsf{T} s_{ij}) = s_{ji}^\mathsf{T} R_j (Q_{ij}^d \hat{\Omega}_i^d - \hat{\Omega}_j^d Q_{ij}^d) R_i^\mathsf{T} s_{ij}. \tag{4.37}$$

Then we apply (4.1), i.e., $R_i^\mathsf{T} s_{ij} = b_{ij}$ yield

$$\begin{aligned} B &= (Q_{ij}^{d\,\mathsf{T}} R_j^\mathsf{T} s_{ji})^\mathsf{T} \hat{\Omega}_i^d b_{ij} - b_{ji}^\mathsf{T} \hat{\Omega}_j^d (Q_{ij}^d b_{ij}) \\ &= (Q_{ij}^{d\,\mathsf{T}} b_{ji}) \cdot \hat{\Omega}_i^d b_{ij} - b_{ji} \cdot [\Omega_j^d \times (Q_{ij}^d b_{ij})] \\ &= \Omega_i^d \cdot [b_{ij} \times (Q_{ij}^{d\,\mathsf{T}} b_{ji})] - \Omega_j^d \cdot [(Q_{ij}^d b_{ij}) \times b_{ji}] \\ &= -\Omega_i^d \cdot e_{ij}^\alpha - \Omega_j^d \cdot e_{ji}^\alpha. \end{aligned} \tag{4.38}$$

Combine (4.36) with (4.38), to obtain

$$\dot{\Psi}_{ij}^\alpha = e_{ij}^\alpha \cdot (\Omega_i - \Omega_i^d) + e_{ji}^\alpha \cdot (\Omega_j - \Omega_j^d) = e_{ij}^\alpha \cdot e_{\Omega_i} + e_{ji}^\alpha \cdot e_{\Omega_j}. \tag{4.39}$$

Similarly, we can write

$$\dot{\Psi}_{ij}^\beta = e_{ij}^\beta \cdot e_{\Omega_i} + e_{ji}^\beta \cdot e_{\Omega_j}, \tag{4.40}$$

Then, substituting (4.39) and (4.40) into (4.27), (ii) is verified.

From (4.20), the time-derivative of e_{ij}^α is shown as

$$\dot{e}_{ij}^\alpha = \frac{d}{dt}(Q_{ij}^{d\,\mathsf{T}} b_{ji}) \times b_{ij} + (Q_{ij}^{d\,\mathsf{T}} b_{ji}) \times \dot{b}_{ij}. \tag{4.41}$$

First, we have

$$\frac{d}{dt}({Q_{ij}^d}^{\mathsf{T}} b_{ji}) = (\dot{Q}_{ij}^d)^{\mathsf{T}} b_{ji} + {Q_{ij}^d}^{\mathsf{T}} \dot{b}_{ji} = (Q_{ij}^d \hat{\Omega}_i^d - \hat{\Omega}_j^d Q_{ij}^d)^{\mathsf{T}} b_{ji} + {Q_{ij}^d}^{\mathsf{T}} (-\hat{\Omega}_j b_{ji}), \quad (4.42)$$

where we have applied (4.26), and (4.11). Then we can rearrange the equation as

$$\begin{aligned} \frac{d}{dt}({Q_{ij}^d}^{\mathsf{T}} b_{ji}) &= -\hat{\Omega}_i^d {Q_{ij}^d}^{\mathsf{T}} b_{ji} + {Q_{ij}^d}^{\mathsf{T}} (\hat{\Omega}_j^d - \hat{\Omega}_j) b_{ji} \\ &= -\hat{\Omega}_i^d {Q_{ij}^d}^{\mathsf{T}} b_{ji} + {Q_{ij}^d}^{\mathsf{T}} (\hat{\Omega}_j^d - \hat{\Omega}_j) Q_{ij}^d {Q_{ij}^d}^{\mathsf{T}} b_{ji}. \end{aligned} \quad (4.43)$$

Apply (A.4) at the second term. Then,

$$\begin{aligned} \frac{d}{dt}({Q_{ij}^d}^{\mathsf{T}} b_{ji}) &= -\hat{\Omega}_i^d {Q_{ij}^d}^{\mathsf{T}} b_{ji} + [{Q_{ij}^d}^{\mathsf{T}} (\Omega_j^d - \Omega_j)]^{\wedge} {Q_{ij}^d}^{\mathsf{T}} b_{ji} \\ &= -[\Omega_i^d + {Q_{ij}^d}^{\mathsf{T}} (\Omega_j - \Omega_j^d)]^{\wedge} {Q_{ij}^d}^{\mathsf{T}} b_{ji} \\ &= ({Q_{ij}^d}^{\mathsf{T}} b_{ji}) \times (\Omega_i^d + {Q_{ij}^d}^{\mathsf{T}} e_{\Omega_j}). \end{aligned} \quad (4.44)$$

Next, substituting (4.44) and (4.11) into (4.41),

$$\begin{aligned} \dot{e}_{ij}^{\alpha} &= \frac{d}{dt}(Q_d^{\mathsf{T}} b_{ji}) \times b_{ij} + (Q_d^{\mathsf{T}} b_{ji}) \times \dot{b}_{ij} \\ &= [({Q_{ij}^d}^{\mathsf{T}} b_{ji}) \times (\Omega_i^d + {Q_{ij}^d}^{\mathsf{T}} e_{\Omega_j})] \times b_{ij} + ({Q_{ij}^d}^{\mathsf{T}} b_{ji}) \times (b_{ij} \times \Omega_i) \\ &= -b_{ij} \times [({Q_{ij}^d}^{\mathsf{T}} b_{ji}) \times (\Omega_i^d + {Q_{ij}^d}^{\mathsf{T}} e_{\Omega_j})] + ({Q_{ij}^d}^{\mathsf{T}} b_{ji}) \times (b_{ij} \times \Omega_i). \end{aligned} \quad (4.45)$$

By applying $x \times (y \times z) = y(x \cdot z) - z(x \cdot y)$ for x, y, $z \in \mathbb{R}^3$, we obtain

$$\begin{aligned}
\dot{e}_{ij}^{\alpha} &= -({Q_{ij}^d}^{\mathsf{T}} b_{ji})[b_{ij} \cdot (\Omega_i^d + {Q_{ij}^d}^{\mathsf{T}} e_{\Omega_j})] + (\Omega_i^d + {Q_{ij}^d}^{\mathsf{T}} e_{\Omega_j})[b_{ij} \cdot ({Q_{ij}^d}^{\mathsf{T}} b_{ji})] \\
&\quad + b_{ij}[({Q_{ij}^d}^{\mathsf{T}} b_{ji}) \cdot \Omega_i] - \Omega_i[({Q_{ij}^d}^{\mathsf{T}} b_{ji}) \cdot b_{ij}] \\
&= -({Q_{ij}^d}^{\mathsf{T}} b_{ji})[b_{ij} \cdot (\Omega_i^d + {Q_{ij}^d}^{\mathsf{T}} e_{\Omega_j})] + b_{ij}[({Q_{ij}^d}^{\mathsf{T}} b_{ji}) \cdot \Omega_i] \\
&\quad + (\Omega_i^d + {Q_{ij}^d}^{\mathsf{T}} e_{\Omega_j} - \Omega_i)[({Q_{ij}^d}^{\mathsf{T}} b_{ji}) \cdot b_{ij}] \\
&= -({Q_{ij}^d}^{\mathsf{T}} b_{ji})(b_{ij}^{\mathsf{T}})(\Omega_i^d + {Q_{ij}^d}^{\mathsf{T}} e_{\Omega_j}) + b_{ij}[({Q_{ij}^d}^{\mathsf{T}} b_{ji})^{\mathsf{T}}(e_{\Omega_i} + \Omega_i^d)] \\
&\quad + [{Q_{ij}^d}^{\mathsf{T}} e_{\Omega_j} - (\Omega_i - \Omega_i^d)][({Q_{ij}^d}^{\mathsf{T}} b_{ji}) \cdot b_{ij}], \qquad (4.46)
\end{aligned}$$

where we have applied $\Omega_i = e_{\Omega_i} + \Omega_i^d$ from (4.24). Then, we expand every term in the equation.

$$\begin{aligned}
\dot{e}_{ij}^{\alpha} &= [-({Q_{ij}^d}^{\mathsf{T}} b_{ji})(b_{ij}^{\mathsf{T}})\Omega_i^d - ({Q_{ij}^d}^{\mathsf{T}} b_{ji})(b_{ij})^{\mathsf{T}}({Q_{ij}^d}^{\mathsf{T}} e_{\Omega_i})] + [b_{ij}({Q_{ij}^d}^{\mathsf{T}} b_{ji})^{\mathsf{T}} e_{\Omega_j} \\
&\quad + b_{ij}({Q_{ij}^d}^{\mathsf{T}} b_{ji})^{\mathsf{T}}\Omega_i^d] + ({Q_{ij}^d}^{\mathsf{T}} e_{\Omega_j} - e_{\Omega_i})[({Q_{ij}^d}^{\mathsf{T}} b_{ji}) \cdot b_{ij}] \\
&= b_{ij}({Q_{ij}^d}^{\mathsf{T}} b_{ji})^{\mathsf{T}}\Omega_i^d - ({Q_{ij}^d}^{\mathsf{T}} b_{ji})(b_{ij})^{\mathsf{T}}\Omega_i^d - ({Q_{ij}^d}^{\mathsf{T}} b_{ji})(b_{ij}^{\mathsf{T}})({Q_{ij}^d}^{\mathsf{T}} e_{\Omega_j}) \\
&\quad + b_{ij}({Q_{ij}^d}^{\mathsf{T}} b_{ji})^{\mathsf{T}} e_{\Omega_i} + {Q_{ij}^d}^{\mathsf{T}} e_{\Omega_j}[({Q_{ij}^d}^{\mathsf{T}} b_{ji}) \cdot b_{ij}] - e_{\Omega_i}[({Q_{ij}^d}^{\mathsf{T}} b_{ji}) \cdot b_{ij}]. \qquad (4.47)
\end{aligned}$$

Notice that we rearranged the equation such that (A.3) can be directly applied. The yields

$$\begin{aligned}
\dot{e}_{ij}^{\alpha} &= [({Q_{ij}^d}^{\mathsf{T}} b_{ji}) \times b_{ij}]^{\wedge}\Omega_i^d - ({Q_{ij}^d}^{\mathsf{T}} b_{ji})(b_{ij})^{\mathsf{T}}({Q_{ij}^d}^{\mathsf{T}} e_{\Omega_j}) \\
&\quad + b_{ij}({Q_{ij}^d}^{\mathsf{T}} b_{ji})^{\mathsf{T}} e_{\Omega_i} + ({Q_{ij}^d}^{\mathsf{T}} e_{\Omega_j}) b_{ij}^{\mathsf{T}}({Q_{ij}^d}^{\mathsf{T}} b_{ji}) - e_{\Omega_i}[({Q_{ij}^d}^{\mathsf{T}} b_{ji})^{\mathsf{T}}] b_{ij} \\
&= [({Q_{ij}^d}^{\mathsf{T}} b_{ji}) \times b_{ij}] \times \Omega_i^d + ({Q_{ij}^d}^{\mathsf{T}} e_{\Omega_j}) b_{ij}^{\mathsf{T}}({Q_{ij}^d}^{\mathsf{T}} b_{ji}) \\
&\quad - ({Q_{ij}^d}^{\mathsf{T}} b_{ji})(b_{ij})^{\mathsf{T}}({Q_{ij}^d}^{\mathsf{T}} e_{\Omega_j}) + b_{ij}({Q_{ij}^d}^{\mathsf{T}} b_{ji})^{\mathsf{T}} e_{\Omega_i} - e_{\Omega_i}[({Q_{ij}^d}^{\mathsf{T}} b_{ji})^{\mathsf{T}}] b_{ij} \\
&= e_{ij}^{\alpha} \times \Omega_i^d + b_{ij} \times [{Q_{ij}^d}^{\mathsf{T}} e_{\Omega_j}) \times ({Q_{ij}^d}^{\mathsf{T}} b_{ji})] + ({Q_{ij}^d}^{\mathsf{T}} b_{ji}) \times (b_{ij} \times e_{\Omega_i}). \qquad (4.48)
\end{aligned}$$

Consequently, we can further derive the upper bound of $\dot{e}_{ij}^{\alpha}$,

$$\|\dot{e}_{ij}^{\alpha}\| \leq B^d \|e_{ij}^{\alpha}\| + \|e_{\Omega_j}\| + \|e_{\Omega_i}\|. \tag{4.49}$$

Following the same approach,

$$\dot{e}_{ij}^{\beta} = e_{ij}^{\beta} \times \Omega_i^d + b_{ijk} \times [{Q_{ij}^d}^{\mathsf{T}} e_{\Omega_j}) \times ({Q_{ij}^d}^{\mathsf{T}} b_{jik})] + ({Q_{ij}^d}^{\mathsf{T}} b_{jik}) \times (b_{ijk} \times e_{\Omega_i}), \tag{4.50}$$

and

$$\|\dot{e}_{ij}^{\beta}\| \leq B^d \|e_{ij}^{\beta}\| + \|e_{\Omega_j}\| + \|e_{\Omega_i}\|. \tag{4.51}$$

Combine (4.49), (4.51) with $e_{ij} = k_{ij}^{\alpha} e_{ij}^{\alpha} + k_{ij}^{\beta} e_{ij}^{\beta}$ to obtain

$$\|\dot{e}_{ij}\| \leq (k_{ij}^{\alpha} + k_{ij}^{\beta})(\|e_{\Omega_i}\| + \|e_{\Omega_j}\|) + B^d \|e_{ij}\|, \tag{4.52}$$

which shows (iii).

The procedure to show (iv) is analogous to the proof of property (iii) of Proposition 3.1. We will skip the extensive derivations and only show the important equations. The alternative expression for Ψ_{ij} is as given follows

$$\begin{aligned} \Psi_{ij} &= k_{ij}^{\alpha} + k_{ij}^{\beta} - \mathrm{tr}[Q_{ij}^d R_i^{\mathsf{T}} (k_{ij}^{\alpha} s_{ij} s_{ij}^{\mathsf{T}} + k_{ij}^{\beta} \frac{1}{\|s_{ijk}\|} s_{ijk} s_{ijk}^{\mathsf{T}}) R_j], \\ &= \mathrm{tr}[G_{ij}(I - U_{ij}^{\mathsf{T}} R_j Q_{ij}^d R_i^{\mathsf{T}} U_{ij})], \end{aligned} \tag{4.53}$$

where

$$K_{ij} = K_{ji} \triangleq k_{ij}^{\alpha} s_{ij} s_{ij}^{\mathsf{T}} + k_{ij}^{\beta} \frac{1}{\|s_{ijk}\|} s_{ijk} s_{ijk}^{\mathsf{T}} \triangleq U_{ij} G_{ij} U_{ij}^{\mathsf{T}}. \tag{4.54}$$

The matrix G_{ij} is the diagonal matrix given by $G_{ij} = \mathrm{diag}[k_{ij}^{\alpha}, k_{ij}^{\beta}, 0] \in \mathbb{R}^3$, and U_{ij} is

an orthonormal matrix defined as $U_{ij} = [s_{ij}, \frac{s_{ijk}}{\|s_{ijk}\|}, \frac{s_{ij} \times s_{ijk}}{\|s_{ij} \times s_{ijk}\|}] \in \mathsf{SO(3)}$. Furthermore, the derivative of Ψ_{ij} with respect to R_i along the direction of $\delta R_i = R_i \hat{\eta}_i$ correspond to e_{ij} is expressed by

$$D_{R_i}\Psi \cdot R_i\hat{\eta}_i = -\eta_i \cdot (R_i^{\mathsf{T}} K_{ij} R_j Q_{ij}^d - {Q_{ij}^d}^{\mathsf{T}} R_j^{\mathsf{T}} K_{ij} R_i)^\vee = \eta_i \cdot e_{ij}, \tag{4.55}$$

which gives rise to an alternative expression for e_{ij}:

$$e_{ij} = ({Q_{ij}^d}^{\mathsf{T}} R_j^{\mathsf{T}} K_{ij} R_i - R_i^{\mathsf{T}} K_{ij} R_j Q_{ij}^d)^\vee. \tag{4.56}$$

From the Proposition 1 in [44], we have

$$\Phi_{ij} = \frac{1}{2}\mathrm{tr}[F_{ij}(I - P_{ij})], \tag{4.57}$$

$$e_{ij}^P = \frac{1}{2}(F_{ij}P_{ij} - P_{ij}^{\mathsf{T}} F_{ij})^\vee, \tag{4.58}$$

$$\frac{h_6}{h_7 + h_8}\|e_{ij}^P\|^2 \leq \Phi_{ij} \leq \frac{h_6 h_9}{h_{10}(h_6 - \varphi)}\|e_{ij}^P\|^2, \tag{4.59}$$

where $F_{ij} = [f_a, f_b, f_c] \in \mathbb{R}^{3\times 3}$ is a diagonal matrix with non-negative constants f_a, f_b and f_c, ad $P \in \mathsf{SO(3)}$ is a rotation matrix. If $\Phi_{ij} < \varphi < h_6$ for a constant φ, where h_6–h_{10} are given by

$$\begin{aligned}
h_6 &= \min\{f_a + f_b,\ f_b + f_c,\ f_c + f_a\},\\
h_7 &= \max\{(f_a - f_b)^2,\ (f_b - f_c)^2,\ (f_c - f_a)^2\},\\
h_8 &= \max\{(f_a + f_b)^2,\ (f_b + f_c)^2,\ (f_c + f_a)^2\},\\
h_9 &= \max\{f_a + f_b,\ f_b + f_c,\ f_c + f_a\},\\
h_{10} &= \min\{(f_a + f_b)^2,\ (f_b + f_c)^2,\ (f_c + f_a)^2\}.
\end{aligned}$$

Compare (4.53) with (4.57), we have $F_{ij} = 2G_{ij}$ and $P_{ij} = U_{ij}^{\mathsf{T}} R_j Q_{ij}^d R_i^{\mathsf{T}} U_{ij}$ which

leads to $\Psi_{ij} = \Phi$. Furthermore (4.58) can also be updated to

$$\hat{e}_{ij}^P = (U_{ij}^\mathsf{T} R_i {Q_{ij}^d}^\mathsf{T} e_{ji})^\wedge.$$

Thus, $e_{ij}^P = U_{ij}^\mathsf{T} R_i (Q_{ij}^d)^\mathsf{T} e_{ji}$, which implies that $\|e_{ij}^P\| = \|e_{ji}\| = \|e_{ij}\|$ since U_{ij}, R_i and Q_{ij}^d are all rotation matrices have unit magnitude, respectively.

Therefore, (4.59) can be rewrite as follows

$$\frac{h_6}{h_7 + h_8}\|e_{ij}\|^2 \leq \Phi_{ij} \leq \frac{h_6 h_9}{h_{10}(h_6 - \varphi)}\|e_{ij}\|^2. \tag{4.60}$$

Then, with $f_a = 2k_{ij}^\alpha$, $f_b = 2k_{ij}^\beta$, $f_c = 0$, we denote $\frac{h_6}{h_7+h_8}$ and $\frac{h_6 h_9}{h_{10}(h_6-\varphi)}$ by $\underline{\psi}_{ij}$ and $\overline{\psi}_{ij}$, respectively, which shows (iv). □

4.2.2 Relative Attitude Tracking

Using the properties derived in the preceding section, we develop a control system to track the given desired relative attitude as follows.

Proposition 4.2. Consider the attitude dynamics of spacecraft given by (4.7), (4.8) for $i \in \{1, 2\}$, with the LOS measurements specified at (4.13). A desired relative attitude trajectory is given by (4.15). For positive constants $k_{ij}^\alpha \neq k_{ij}^\beta, k_{ij}^\alpha = k_{ji}^\alpha, k_{ij}^\beta = k_{ji}^\beta, k_{\Omega_i}, k_{\Omega_j}$, control inputs are chosen as

$$u_i = -e_{ij} - k_{\Omega_i} e_{\Omega_i} + \hat{\Omega}_i^d J_i (e_{\Omega_i} + \Omega_i^d) + J\dot{\Omega}_i^d, \tag{4.61}$$

where $(i, j) \in \mathcal{E}$. Then, the following properties hold:

(i) There are four types of equilibrium, given by the desired equilibrium $(Q_{12}, \Omega_{12}) = (Q_{12}^d, \Omega_{12}^d)$, and the relative configurations represented by $Q_{12}^d = R_2^\mathsf{T} U D U^\mathsf{T} R_1$ and $\Omega_{12} = \Omega_{12}^d$ where $D \in \{\mathrm{diag}[1, -1, -1], \mathrm{diag}[-1, 1, -1], \mathrm{diag}[-1, -1, 1]\}$ and $U \in \mathsf{SO(3)}$ is the matrix composed of eigenvectors of K_{12} given at (4.54).

(ii) The desired equilibrium is almost globally exponentially stable, and a (conservative) estimate to the region of attraction is given by

$$\Psi_{12}(0) \leq \psi < 2\min\{k_{12}^{\alpha}, k_{12}^{\beta}\}, \tag{4.62}$$

$$\sum_{i=1,2} \lambda_{M_i} \|e_{\Omega_i}(0)\|^2 \leq 2(\psi - \Psi_{12}(0)), \tag{4.63}$$

where ψ is a positive constant satisfying $\psi < 2\min\{k_{12}^{\alpha}, k_{12}^{\beta}\}$, and λ_{M_i} denotes the maximum eigenvalue of J_i.

(iii) The undesired equilibria are unstable.

The overall feature of this controller is in a similar manner with Proposition 3.2, with the main difference that here we control the relative attitude between spacecraft. The absolute attitude of each spacecraft is not required in this proposition.

Proof. From (4.7), (4.61), and rearranging, the time-derivative of $J_i e_{\Omega_i}$ is given by

$$J_i \dot{e}_{\Omega_i} = -(e_{\Omega_i} + \Omega_i^d) \times J_i(e_{\Omega_i} + \Omega_i^d) + u_i - J_i \dot{\Omega}_i^d, \tag{4.64}$$

$$= (J_i e_{\Omega_i} + J\Omega_i^d)^{\wedge} e_{\Omega_i} - e_{ij} - k_{\Omega_i} e_{\Omega_i}. \tag{4.65}$$

The equilibrium configurations are where $e_{12} = e_{21} = e_{\Omega_1} = e_{\Omega_2} = 0$, which corresponds to the critical points of the configuration error function given by (4.53). In [45], it has been shown that there are four critical points:

$$R_1 Q_{21}^d R_2^{\mathsf{T}} \in \{I, UD_1U^{\mathsf{T}}, UD_2U^{\mathsf{T}}, UD_3U^{\mathsf{T}}\},$$

where $D_1 = \mathrm{diag}[1, -1, -1]$, $D_2 = \mathrm{diag}[-1, 1, -1]$, $D_3 = \mathrm{diag}[-1, -1, 1]$. This shows (i).

Next, we show exponential stability of the desired equilibrium. A sufficient condi-

tion on the initial conditions to satisfy (4.30) is obtained from the following variable:

$$\mathcal{U} = \frac{1}{2} e_{\Omega_1} \cdot J_1 e_{\Omega_1} + \frac{1}{2} e_{\Omega_2} \cdot J_2 e_{\Omega_2} + \Psi_{12}.$$

From (4.65) and the property (ii) of Proposition 4.1, the time-derivative of $\mathcal{U}$ is simply given by

$$\dot{\mathcal{U}} = e_{\Omega_1} \cdot (-e_{12} - k_{\Omega_1} e_{\Omega_1}) + e_{\Omega_1} \cdot (-e_{12} - k_{\Omega_1} e_{\Omega_1}) \tag{4.66}$$

$$+ e_{12} \cdot e_{\Omega_1} + e_{21} \cdot e_{\Omega_2} \tag{4.67}$$

$$= -k_{\Omega_1} \|e_{\Omega_1}\|^2 - k_{\Omega_2} \|e_{\Omega_2}\|^2 \leq 0, \tag{4.68}$$

which implies that $\mathcal{U}(t)$ is non-increasing. For the initial conditions satisfying (4.62), (4.63), we have

$$\mathcal{U}(0) \leq \frac{1}{2} \sum_{i=1,2} \lambda_{M_i} \|e_{\Omega_i}(0)\|^2 + \Psi_{12}(0) \leq \psi.$$

As $\mathcal{U}(0)$ is non-increasing,

$$\Psi_{12}(t) \leq \mathcal{U}(t) \leq \mathcal{U}(0) \leq \psi < 2 \min\{k_{12}^{\alpha}, k_{12}^{\beta}\}.$$

Therefore, $\Psi_{12}(t) \leq \psi < h_1$ for all $t \geq 0$, and the inequality (4.30) is satisfied.

Let a Lyapunov function be

$$\mathcal{V} = \mathcal{U} + c(e_{12} \cdot e_{\Omega_1} + e_{21} \cdot e_{\Omega_2}),$$

for a constant c. Using (4.30), it can be shown that

$$\sum_{i,j \in \mathcal{E}} z_{ij}^{\mathsf{T}} \underline{M}_{ij} z_{ij} \leq \mathcal{V} \leq \sum_{i,j \in \mathcal{E}} z_{ij}^{\mathsf{T}} \overline{M}_{ij} z_{ij}, \tag{4.69}$$

where $z_{ij} = [\|e_{ij}\|, \|e_{\Omega_i}\|] \in \mathbb{R}^2$, and the matrices $\underline{M}_{ij}, \overline{M}_{ij} \in \mathbb{R}^{2\times 2}$ are defined as

$$\underline{M}_{ij} = \frac{1}{2}\begin{bmatrix} \underline{\psi}_{ij} & -c \\ -c & \lambda_{m_i} \end{bmatrix}, \quad \overline{M}_{ij} = \frac{1}{2}\begin{bmatrix} \overline{\psi}_{ij} & c \\ c & \lambda_{M_i} \end{bmatrix}, \tag{4.70}$$

for $(i,j) \in \mathcal{E} = \{(1,2),(2,1)\}$, where it is assumed that $\underline{\psi}_{ij} = \underline{\psi}_{ji}$, $\overline{\psi}_{ij} = \overline{\psi}_{ji}$. From (4.68), we obtain

$$\dot{\mathcal{V}} = \sum_{i,j\in\mathcal{E}} -k_{\Omega_i}\|e_{\Omega_i}\|^2 + c(\dot{e}_{ij}\cdot e_{\Omega_i} + e_{ij}\cdot \dot{e}_{\Omega_i}). \tag{4.71}$$

For any vector x, $y \in \mathbb{R}^3$ and square matrix $J_i \in \mathbb{R}^{3\times 3}$, we have the following properties: $\lambda_{m_i} x \le J_i x \le \lambda_{M_i} x$ and $-x\cdot y \le \|x\|\|y\|$. From (4.65) and the two properties just mentioned, it can be shown that

$$\begin{aligned} \dot{e}_{\Omega_i}\cdot e_{ij} &= J_i^{-1}[J_i(e_{\Omega_i}+\Omega_i^d)]^\wedge e_{\Omega_i}\cdot e_{ij} - J_i^{-1}\|e_{ij}\|^2 - k_{\Omega_i}J_i^{-1}e_{\Omega_i}\cdot e_{ij} \\ &\le \lambda_{M_i^{-1}}\|[\lambda_{M_i}(e_{\Omega_i}+\Omega_i^d)]^\wedge e_{\Omega_i}\|\|e_i\| - \lambda_{m_i^{-1}}\|e_{ij}\|^2 + k_{\Omega_i}\lambda_{M_i^{-1}}\|e_{\Omega_i}\|\|e_{ij}\|, \end{aligned} \tag{4.72}$$

where $\lambda_{M_i^{-1}}$ and $\lambda_{M_i^{-1}}$ denote the maximum and the minimum eigenvalue of the matrix J_i^{-1}, respectively. Also, applying $\hat{x}y \le \|x\|\|y\|$ for x, $y \in \mathbb{R}^3$, $\lambda_{M_i^{-1}} = \frac{1}{\lambda_{m_i}}$ and $\lambda_{m_i^{-1}} = \frac{1}{\lambda_{M_i}}$ gives rise to

$$\begin{aligned} \dot{e}_{\Omega_i}\cdot e_{ij} &\le \frac{1}{\lambda_{m_i}}\|\lambda_{M_i}\hat{e}_{\Omega_i}e_{\Omega_i} + \lambda_{M_i}\hat{\Omega}_i^d e_{\Omega_i}\|\|e_{ij}\| - \frac{1}{\lambda_{m_i}}\|e_{ij}\|^2 + k_{\Omega_i}\frac{1}{\lambda_{m_i}}\|e_{\Omega_i}\|\|e_{ij}\| \\ &\le \frac{\|e_{ij}\|}{\lambda_{m_i}}(\lambda_{m_i}\|e_{\Omega_i}\|^2 + \lambda_{M_i}\|\Omega_i^d\|\|e_{\Omega_i}\|) - \frac{1}{\lambda_{M_i}}\|e_{ij}\|^2 + k_{\Omega_i}\frac{1}{\lambda_{m_i}}\|e_{\Omega_i}\|\|e_{ij}\| \\ &\le \frac{\|e_{ij}\|}{\lambda_{m_i}}(\lambda_{M_i}\|e_{\Omega_i}\|^2 + \lambda_{M_i}B^d\|e_{\Omega_i}\|) - \frac{1}{\lambda_{M_i}}\|e_{ij}\|^2 + k_{\Omega_i}\frac{1}{\lambda_{m_i}}\|e_{\Omega_i}\|\|e_{ij}\| \\ &= \frac{\|e_{ij}\|}{\lambda_{m_i}}(\|\lambda_{M_i}\|e_{\Omega_i}\|^2 + \lambda_{M_i}B^d\|e_{\Omega_i}\|) - \frac{1}{\lambda_{M_i}}\|e_{ij}\|^2 + k_{\Omega_i}\frac{1}{\lambda_{m_i}}\|e_{\Omega_i}\|\|e_{ij}\|. \end{aligned} \tag{4.73}$$

From the fact that $\|e_{ij}\| \leq k_{ij}^{\alpha} + k_{ij}^{\beta}$, we have

$$\begin{aligned}\dot{e}_{\Omega_i} \cdot e_{ij} &\leq \frac{\lambda_{M_i}}{\lambda_{m_i}}(k_{ij}^{\alpha} + k_{ij}^{\beta})\|e_{\Omega_i}\|^2 + \frac{\lambda_{M_i} B^d}{\lambda_{m_i}}\|e_{ij}\|\|e_{\Omega_i}\| - \frac{1}{\lambda_{M_i}}\|e_{ij}\|^2 + k_{\Omega_i}\frac{1}{\lambda_{m_i}}\|e_{\Omega_i}\|\|e_{ij}\| \\ &= \frac{\lambda_{M_i}}{\lambda_{m_i}}(k_{ij}^{\alpha} + k_{ij}^{\beta})\|e_{\Omega_i}\|^2 + \frac{\lambda_{M_i} B^d + k_{\Omega_i}}{\lambda_{m_i}}\|e_{ij}\|\|e_{\Omega_i}\| - \frac{1}{\lambda_{M_i}}\|e_{ij}\|^2. \end{aligned} \tag{4.74}$$

Together with the property (iii) of Proposition 4.1, this yields the following inequality:

$$\begin{aligned}\dot{\mathcal{V}} \leq \sum_{i,j \in \mathcal{E}} &-(k_{\Omega_i} - c\bar{k}_{ij}(1 + \frac{\lambda_{M_i}}{\lambda_{m_i}}))\|e_{\Omega_i}\|^2 - \frac{c}{\lambda_{M_i}}\|e_{ij}\|^2 + c\bar{k}_{ij}\|e_{\Omega_i}\|\|e_{\Omega_j}\| \\ &+ \frac{c}{\lambda_{m_i}}(\bar{\lambda}_i B^d + k_{\Omega_i})\|e_{ij}\|\|e_{\Omega_i}\|, \end{aligned} \tag{4.75}$$

where $\bar{\lambda}_i$ denotes $\bar{\lambda}_i = \lambda_{M_i} + \lambda_{m_i}$, and $\bar{k}_{ij}$ denotes $\bar{k}_{ij} = k_{ij}^{\alpha} + k_{ij}^{\beta}$. Expanding the summation index, we now have

$$\begin{aligned}\dot{\mathcal{V}} \leq &-[k_{\Omega_1} - c\bar{k}_{12}(1 + \frac{\lambda_{M_1}}{\lambda_{m_1}})]\|e_{\Omega_1}\|^2 - \frac{c}{\lambda_{M_1}}\|e_{12}\|^2 + c\bar{k}_{12}\|e_{\Omega_1}\|\|e_{\Omega_2}\| \\ &+ \frac{c}{\lambda_{m_1}}(\bar{\lambda}_1 B^d + k_{\Omega_1})\|e_{12}\|\|e_{\Omega_1}\| \\ &- [k_{\Omega_2} - c\bar{k}_{21}(1 + \frac{\lambda_{M_2}}{\lambda_{m_2}})]\|e_{\Omega_2}\|^2 - \frac{c}{\lambda_{M_2}}\|e_{21}\|^2 + c\bar{k}_{21}\|e_{\Omega_2}\|\|e_{\Omega_1}\| \\ &+ \frac{c}{\lambda_{m_2}}(\bar{\lambda}_2 B^d + k_{\Omega_2})\|e_{21}\|\|e_{\Omega_2}\|, \end{aligned} \tag{4.76}$$

then, we can rearrange the equation to obtain

$$\begin{aligned}\dot{\mathcal{V}} \leq &-\{[\frac{1}{2}k_{\Omega_1} - c\bar{k}_{12}(1 + \frac{\lambda_{M_1}}{\lambda_{m_1}})]\|e_{\Omega_1}\|^2 + \frac{c}{\lambda_{M_1}}\|e_{12}\|^2 \\ &- \frac{c}{\lambda_{m_1}}(\bar{\lambda}_1 B^d + k_{\Omega_1})\|e_{12}\|\|e_{\Omega_1}\|\} - \{[\frac{1}{2}k_{\Omega_2} - c\bar{k}_{21}(1 + \frac{\lambda_{M_2}}{\lambda_{m_2}})]\|e_{\Omega_2}\|^2 \\ &+ \frac{c}{\lambda_{M_2}}\|e_{21}\|^2 - \frac{c}{\lambda_{m_2}}(\bar{\lambda}_2 B^d + k_{\Omega_2})\|e_{21}\|\|e_{\Omega_2}\|\} \\ &- \{\frac{1}{2}k_{\Omega_1}\|e_{\Omega_1}\|^2 + \frac{1}{2}k_{\Omega_2}\|e_{\Omega_2}\|^2 - 2c\bar{k}_{12}\|e_{\Omega_1}\|\|e_{\Omega_2}\|\}, \end{aligned} \tag{4.77}$$

which can be rewritten as the following matrix form:

$$\dot{\mathcal{V}} \leq -z_{12}^{\mathsf{T}} W_{12} z_{12} - z_{21}^{\mathsf{T}} W_{21} z_{21} - \zeta_{12}^{\mathsf{T}} Y_{12} \zeta_{12}, \tag{4.78}$$

where $\zeta_{12} = [\|e_{\Omega_1}\|, \|e_{\Omega_2}\|]^{\mathsf{T}} \in \mathbb{R}^2$ and the matrices $W_{12}, W_{21}, Y_{12} \in \mathbb{R}^{2\times 2}$ are given by

$$W_{ij} = \frac{1}{2}\begin{bmatrix} 2\frac{c}{\lambda_{M_i}} & -\frac{c}{\lambda_{m_i}}(\bar{\lambda}_i B^d + k_{\Omega_i}) \\ -\frac{c}{\lambda_{m_i}}(\bar{\lambda}_i B^d + k_{\Omega_i}) & k_{\Omega_i} - 2c\bar{k}_{ij}(1 + \frac{\lambda_{M_i}}{\lambda_{m_i}}) \end{bmatrix}, \tag{4.79}$$

$$Y_{12} = \frac{1}{2}\begin{bmatrix} k_{\Omega_1} & -2c\bar{k}_{12} \\ -2c\bar{k}_{12} & k_{\Omega_2} \end{bmatrix}. \tag{4.80}$$

for $(i,j) \in \mathcal{E}$. Thus, we choose the constant c such that

$$\begin{aligned} c < \min\{ & \sqrt{\underline{\psi}_{12}\lambda_{m_1}},\ \sqrt{\underline{\psi}_{21}\lambda_{m_2}},\ \sqrt{\overline{\psi}_{12}\lambda_{M_1}},\ \sqrt{\overline{\psi}_{21}\lambda_{M_2}},\ \frac{\sqrt{k_{\Omega_1}k_{\Omega_2}}}{2\bar{k}_{12}}, \\ & \frac{2k_{\Omega_1}\lambda_{m_1}^2}{4\bar{k}_{12}\lambda_{m_1}(\bar{\lambda}_1) + \lambda_{M_1}(B^d\bar{\lambda}_1 + k_{\Omega_1})^2},\ \frac{2k_{\Omega_2}\lambda_{m_2}^2}{4\bar{k}_{21}\lambda_{m_2}(\bar{\lambda}_2) + \lambda_{M_2}(B^d\bar{\lambda}_2 + k_{\Omega_2})^2}\} \end{aligned} \tag{4.81}$$

The first four conditions come from (4.69) and (4.70) to ensure the Lyapunov candidate to be a positive-definite function. The last three terms come from (4.79) and (4.80). Furthermore, it is chosen such that the time-derivative of the Lyapunov candidate is negative-definite. Therefore, the desired equilibrium is exponentially stable.

Next, we show (iii). At the first type of undesired equilibria given by $R_1 Q_{21}^d R_2^{\mathsf{T}} = UD_1U^{\mathsf{T}}$ and $e_{\Omega_1} = e_{\Omega_2} = 0$, the value of the Lyapunov function becomes $\mathcal{V} = 2k_{12}^{\beta}$. Define

$$\mathcal{W} = 2k_{12}^{\beta} - \mathcal{V}.$$

Then, $\mathcal{W} = 0$ at the undesired equilibrium, and we have

$$-\sum_{(i,j)\in\mathcal{E}} \{\frac{\lambda_{M_i}}{2}\|e_{\Omega_i}\|^2 + c\|e_{ij}\|\|e_{\Omega_i}\|\} + (2k_{12}^{\beta} - \Psi) \leq \mathcal{W}.$$

Due to the continuity of Ψ, we can choose R_1 and R_2 arbitrary close to the undesired equilibrium such that $(2k_2^{\beta} - \Psi) > 0$. Therefore, if $\|e_{\Omega_i}\|$ is sufficiently small, we obtain $\mathcal{W} > 0$. Therefore, at any arbitrarily small neighborhood of the undesired equilibrium, there exists a set in which $\mathcal{W} > 0$, and we have $\dot{\mathcal{W}} = -\dot{\mathcal{V}} > 0$ from (4.78). Therefore, the undesired equilibrium is unstable [43, Theorem 4.3]. The instability of other types of equilibrium can be shown similarly. This shows (iii).

The region of attraction to the desired equilibrium excludes the union of stable manifolds to the unstable equilibria. But, the union of stable manifolds has less dimension than the tangent bundle of the configuration manifold. Therefore, the measure of the stable manifolds to the unstable equilibria is zero. This implies the desired equilibrium is almost globally exponentially stable [14], which shows (ii). □

The result we presented in this section can be considered as a generalization of [10] with time-varying desired relative attitude tracking commands and stronger exponential stability.

4.3 Relative Attitude Formation Tracking

The ultimate goal in this thesis is relative attitude formation control between n spacecraft. The key idea of relative attitude control is illustrated in the previous section with two spacecraft, and we generate it into an arbitrary number of spacecraft in this section.

4.3.1 Relative Attitude Tracking Between Three Spacecrafts

We first consider relative attitude formation tracking between three spacecraft, given by Spacecraft 1, 2, and 3, illustrated at Figure 4.1. The corresponding edge set and the assignment set used in this subsection are given by

$$\mathcal{E} = \{(1,2),(2,1),(2,3),(3,2)\}, \tag{4.82}$$

$$\mathcal{A} = \{(1,2,3),(2,1,3),(2,3,1),(3,2,1)\}. \tag{4.83}$$

For given relative attitude commands, $Q_{12}^d(t), Q_{23}^d(t)$, the goal is to design control inputs such that $Q_{12}(t) \to Q_{12}^d(t)$ and $Q_{23}(t) \to Q_{23}^d(t)$ as $t \to \infty$.

The definition of error variables and their properties developed in the previous section for two spacecraft are readily generalized to any $(i,j,k) \in \mathcal{A}$ in this section. For example, the kinematic equation for the desired relative attitude Q_{23}^d is obtained from (4.15) as

$$\dot{Q}_{23}^d = Q_{23}^d \hat{\Omega}_{23}^d, \tag{4.84}$$

where Ω_{23}^d is the desired relative angular velocity. Other configuration error functions and error vectors between Spacecraft 2 and Spacecraft 3 are defined similarly.

The desired absolute angular velocities for each spacecraft, namely Ω_1^d, Ω_2^d, and Ω_3^d should be properly defined. For the given Ω_{12}^d, Ω_{23}^d, they can be arbitrarily chosen such that

$$\Omega_{12}^d(t) = \Omega_1^d(t) - Q_{21}^d(t)\Omega_2^d(t), \tag{4.85}$$

$$\Omega_{23}^d(t) = \Omega_2^d(t) - Q_{32}^d(t)\Omega_3^d(t). \tag{4.86}$$

For example, they can be chosen as $\Omega_1^d = \Omega_{12}^d$, $\Omega_2^d = 0$, $\Omega_3^d = -Q_{23}^d\Omega_{23}^d$. Assumption 6

is considered to be satisfied such that each of the desired angular velocity is bounded by a known constant B^d.

Proposition 4.3. Consider the attitude dynamics of spacecraft given by (4.7), (4.8) for $i \in \{1,2,3\}$, with the LOS measurements specified at (4.83). Desired relative attitudes are given by $Q_{12}^d(t)$, $Q_{23}^d(t)$. For positive constants $k_{ij}^\alpha, k_{ij}^\beta, k_{\Omega_i}$ with $k_{ij}^\alpha \neq k_{ij}^\beta$, $k_{ij}^\alpha = k_{ji}^\alpha$, $k_{ij}^\beta = k_{ji}^\beta$ for $(i,j) \in \mathcal{E}$,

$$u_1 = -e_{12} - k_{\Omega_1} e_{\Omega_1} + \hat{\Omega}_1^d J_1 (e_{\Omega_1} + \Omega_1^d) + J\dot{\Omega}_1^d, \tag{4.87}$$

$$u_2 = -\frac{1}{2}(e_{21} + e_{23}) - k_{\Omega_2} e_{\Omega_2} + \hat{\Omega}_2^d J_2 (e_{\Omega_2} + \Omega_2^d) + J\dot{\Omega}_2^d, \tag{4.88}$$

$$u_3 = -e_{32} - k_{\Omega_3} e_{\Omega_3} + \hat{\Omega}_3^d J_3 (e_{\Omega_3} + \Omega_3^d) + J\dot{\Omega}_3^d, \tag{4.89}$$

Then, the desired relative attitude configuration is almost globally exponentially stable, and a (conservative) estimate to the region of attraction is given by

$$\Psi_{12}(0) + \Psi_{23}(0) \leq \psi < 2\min\{k_{12}^\alpha, k_{12}^\beta, k_{23}^\alpha, k_{23}^\beta\}, \tag{4.90}$$

$$\lambda_{M_1}\|e_{\Omega_1}(0)\|^2 + 2\lambda_{M_2}\|e_{\Omega_2}(0)\|^2 + \lambda_{M_3}\|e_{\Omega_3}(0)\|^2 \leq 2(\psi - \Psi_{12}(0) - \Psi_{23}(0)), \tag{4.91}$$

where ψ is a positive constant satisfying $\psi < 2\min\{k_{12}^\alpha, k_{12}^\beta, k_{23}^\alpha, k_{23}^\beta\}$.

Proof. The time-derivative of $J_1 e_1$ and $J_3 e_3$ are given by (4.65), and the time-derivative of $J_2 e_2$ is given by

$$J_2 \dot{e}_{\Omega_2} = (J_2 e_{\Omega_2} + J\Omega_2^d)^\wedge e_{\Omega_2} - \frac{1}{2}(e_{21} + e_{23}) - k_{\Omega_2} e_{\Omega_2}. \tag{4.92}$$

Define

$$\mathcal{U} = \frac{1}{2} e_{\Omega_1} \cdot J_1 e_{\Omega_1} + e_{\Omega_2} \cdot J_2 e_{\Omega_2} + \frac{1}{2} e_{\Omega_3} \cdot J_3 e_{\Omega_3} + \Psi_{12} + \Psi_{23}. \tag{4.93}$$

From (4.65), (4.92), we have

$$\dot{\mathcal{U}} = -k_{\Omega_1}\|e_{\Omega_1}\|^2 - 2k_{\Omega_2}\|e_{\Omega_2}\|^2 - k_{\Omega_3}\|e_{\Omega_3}\|^2, \tag{4.94}$$

which implies that $\mathcal{U}(t)$ is non-increasing. For the initial conditions satisfying (4.90) and (4.91), we have $\mathcal{U}(0) \leq \psi$. Therefore,

$$\Psi_{12}(t) + \Psi_{23}(t) \leq \mathcal{U}(t) \leq \mathcal{U}(0) \leq \psi < 2\min\{k_{12}^{\alpha}, k_{12}^{\beta}, k_{23}^{\alpha}, k_{23}^{\beta}\}. \tag{4.95}$$

Therefore, the inequality (4.30) holds for both of Ψ_{12} and Ψ_{23}.

Let a Lyapunov function be

$$\mathcal{V} = \mathcal{U} + ce_{\Omega_1} \cdot e_{12} + ce_{\Omega_2} \cdot (e_{21} + e_{23}) + ce_{\Omega_3} \cdot e_{32}. \tag{4.96}$$

From (4.30), we can show that this Lyapunov function satisfies the inequality given by (4.69), that is,

$$\mathcal{V} \leq z_{12}^{\mathsf{T}}\overline{M}_{12}z_{12} + z_{21}^{\mathsf{T}}\overline{M}_{21}z_{21} + z_{23}^{\mathsf{T}}\overline{M}_{23}z_{23} + z_{32}^{\mathsf{T}}\overline{M}_{32}z_{32}, \tag{4.97}$$

$$\mathcal{V} \geq z_{12}^{\mathsf{T}}\underline{M}_{12}z_{12} + z_{21}^{\mathsf{T}}\underline{M}_{21}z_{21} + z_{23}^{\mathsf{T}}\underline{M}_{23}z_{23} + z_{32}^{\mathsf{T}}\underline{M}_{32}z_{32}. \tag{4.98}$$

where the matrices $\overline{M}_{ij}$ and $\underline{M}_{ij}$ are welled defined by (4.70). Moreover, the time-derive of Lyapunov function (4.96) is similar to (4.71). We will expand $\dot{\mathcal{V}}$ term by term in the coming paragraph so the the sequence of idea will be clear.

For $(i, j) \in \{(1, 2), (3, 2)\}$, the upper bound of $\dot{e}_{\Omega_i} \cdot e_{ij}$ is given by (4.74). Alternatively, from (4.92), with the similar procedure in (4.72) through (4.74), the upper

bound of $\dot{e}_{\Omega_2} \cdot (e_{21} + e_{23})$ is given by

$$\dot{e}_{\Omega_2} \cdot (e_{21} + e_{23}) \leq \frac{\lambda_{M_2}}{\lambda_{m_2}}(\overline{k}_{21} + \overline{k}_{23})\|e_{\Omega_2}\|^2 + \frac{\lambda_{M_2}B^d + k_{\Omega_2}}{\lambda_{m_2}}\|e_{21} + e_{23}\|\|e_{\Omega_2}\| - \frac{1}{2\lambda_{M_2}}\|e_{21} + e_{23}\|^2. \tag{4.99}$$

The upper bounds of $\|\dot{e}_{32}\|$ and $\|\dot{e}_{12}\|$ are given by the property (iii) of Proposition 4.1. Additionally, using (4.52), we can show that

$$\|\dot{e}_{21} + \dot{e}_{23}\| \leq (\overline{k}_{21} + \overline{k}_{23})(\|e_{\Omega_1}\| + 2\|e_{\Omega_2}\| + \|e_{\Omega_3}\|) + B^d\|e_{21} + e_{23}\|. \tag{4.100}$$

Applying these bounds to the expression of $\dot{\mathcal{V}}$ and rearranging, we obtain

$$\begin{aligned}
\dot{\mathcal{V}} \leq & -[k_{\Omega_1} - c\bar{k}_{12}(1 + \frac{\lambda_{M_1}}{\lambda_{m_1}})]\|e_{\Omega_1}\|^2 - \frac{c}{\lambda_{M_1}}\|e_{12}\|^2 + c\bar{k}_{12}\|e_{\Omega_1}\|\|e_{\Omega_2}\| \\
& - [k_{\Omega_3} - c\bar{k}_{32}(1 + \frac{\lambda_{M_3}}{\lambda_{m_3}})]\|e_{\Omega_3}\|^2 - \frac{c}{\lambda_{M_3}}\|e_{32}\|^2 + c\bar{k}_{32}\|e_{\Omega_3}\|\|e_{\Omega_2}\| \\
& + \frac{c}{\lambda_{m_1}}(\bar{\lambda}_1 B^d + k_{\Omega_1})\|e_{12}\|\|e_{\Omega_1}\| + \frac{c}{\lambda_{m_3}}(\bar{\lambda}_3 B^d + k_{\Omega_3})\|e_{32}\|\|e_{\Omega_3}\| \\
& - [k_{\Omega_2} - c\bar{k}_{213}(2 + \frac{\lambda_{M_2}}{\lambda_{m_2}})]\|e_{\Omega_2}\|^2 + \frac{c}{\lambda_{m_2}}(\bar{\lambda}_2 B^d + k_{\Omega_2})\|e_{21} + e_{23}\|\|e_{\Omega_2}\| \\
& - \frac{c}{2\lambda_{M_2}}\|e_{21} + e_{23}\|^2 + c\bar{k}_{213}\|e_{\Omega_1}\|\|e_{\Omega_2}\| + c\bar{k}_{213}\|e_{\Omega_2}\|\|e_{\Omega_3}\|,
\end{aligned} \tag{4.101}$$

This can be rearranged as

$$\begin{aligned}\dot{\mathcal{V}} \leq & -\{\frac{c}{\lambda_{M_1}}\|e_{12}\|^2 - \frac{c}{\lambda_{m_1}}(\bar{\lambda}_1 B^d + k_{\Omega_1})\|e_{12}\|\|e_{\Omega_1}\| + [\frac{1}{2}k_{\Omega_1} - c\bar{k}_{12}(1+\frac{\lambda_{M_1}}{\lambda_{m_1}})]\|e_{\Omega_1}\|^2\} \\ & - \{\frac{c}{\lambda_{M_3}}\|e_{32}\|^2 - \frac{c}{\lambda_{m_3}}(\bar{\lambda}_3 B^d + k_{\Omega_3})\|e_{32}\|\|e_{\Omega_3}\| + [\frac{1}{2}k_{\Omega_3} - c\bar{k}_{32}(1+\frac{\lambda_{M_3}}{\lambda_{m_3}})]\|e_{\Omega_3}\|^2\} \\ & - \{\frac{c}{2\lambda_{M_2}}\|e_{21}+e_{23}\|^2 - \frac{c}{\lambda_{m_2}}(\bar{\lambda}_2 B^d + k_{\Omega_2})\|e_{21}+e_{23}\|\|e_{\Omega_2}\| \\ & + [\frac{1}{2}k_{\Omega_2} - c\bar{k}_{213}(2+\frac{\lambda_{M_2}}{\lambda_{m_2}})]\|e_{\Omega_2}\|^2\} \\ & - \{\frac{1}{2}k_{\Omega_1}\|e_{\Omega_1}\|^2 + \frac{1}{4}k_{\Omega_2}\|e_{\Omega_2}\|^2 - c(2\bar{k}_{21}+\bar{k}_{23})\|e_{\Omega_1}\|\|e_{\Omega_2}\|\} \\ & - \{\frac{1}{4}k_{\Omega_2}\|e_{\Omega_2}\|^2 + \frac{1}{2}k_{\Omega_3}\|e_{\Omega_3}\|^2 - c(\bar{k}_{21}+2\bar{k}_{23})\|e_{\Omega_2}\|\|e_{\Omega_3}\|\}. \end{aligned} \tag{4.102}$$

The corresponding matrix form is

$$\dot{\mathcal{V}} \leq -z_{12}^{\mathsf{T}} W_{12} z_{12} - z_{213}^{\mathsf{T}} W_{213} z_{213} - z_{32}^{\mathsf{T}} W_{32} z_{32} - \zeta_{21}^{\mathsf{T}} Z_{21} \zeta_{21} - \zeta_{23}^{\mathsf{T}} Z_{23} \zeta_{23}, \tag{4.103}$$

where the matrix $W_{12}, W_{23} \in \mathbb{R}^{2\times 2}$ are given as (4.79), and $z_{213} = [\|e_{21}+e_{23}\|, \|e_{\Omega_2}\|]^{\mathsf{T}} \in \mathbb{R}^2$. The matrices W_{213}, Z_{21}, $Z_{23} \in \mathbb{R}^{2\times 2}$ are defined as

$$W_{213} = \frac{1}{2}\begin{bmatrix} \frac{c}{\lambda_{M_2}} & -\frac{c}{\lambda_{m_2}}(\bar{\lambda}_2 B^d + k_{\Omega_2}) \\ -\frac{c}{\lambda_{m_2}}(\bar{\lambda}_2 B^d + k_{\Omega_2}) & k_{\Omega_2} - 2c\bar{k}_{213}(2+\frac{\lambda_{M_2}}{\lambda_{m_2}}) \end{bmatrix}, \tag{4.104}$$

$$Z_{21} = \frac{1}{2}\begin{bmatrix} \frac{1}{2}k_{\Omega_2} & -c(2\bar{k}_{21}+\bar{k}_{23}) \\ -c(2\bar{k}_{21}+\bar{k}_{23}) & k_{\Omega_1} \end{bmatrix}, \tag{4.105}$$

$$Z_{23} = \frac{1}{2}\begin{bmatrix} \frac{1}{2}k_{\Omega_2} & -c(\bar{k}_{21}+2\bar{k}_{23}) \\ -c(\bar{k}_{21}+2\bar{k}_{23}) & k_{\Omega_3} \end{bmatrix}, \tag{4.106}$$

where $\bar{k}_{213} = \bar{k}_{12} + \bar{k}_{23}$. It can be shown that all of matrices at (4.97), (4.98) and (4.103) are positive definite if the constant c is sufficient small. In particular, the way to find the maximum value of c is in a similar manner with the proof of Proposition

2.2 and with (4.81) as well. Therefore, we now can write

$$\begin{aligned}\dot{\mathcal{V}} &\leq -\lambda_m(W_{12})(\|e_{12}\|^2 + \|e_{\Omega_1}\|^2) - \lambda_m(W_{213})(\|e_{21} + e_{23}\|^2 + \|e_{\Omega_2}\|^2) \\ &\quad - \lambda_m(W_{32})(\|e_{31}\|^2 + \|e_{\Omega_3}\|^2) \\ &\leq -\lambda_m(W_{12}) \left\{ \frac{1}{2}(\|e_{12}\|^2 + \|e_{21}\|^2) + \|e_{\Omega_1}\|^2 \right\} - \lambda_m(W_{213})\|e_{\Omega_2}\|^2 \\ &\quad - \lambda_m(W_{32}) \left\{ \frac{1}{2}(\|e_{32}\|^2 + \|e_{23}\|^2) + \|e_{\Omega_3}\|^2 \right\}, \end{aligned} \tag{4.107}$$

where $\lambda_m(\cdot)$ denotes the minimum eigenvalue of a matrix, and we use the fact that $\|e_{12}\| = \|e_{21}\|$, $\|e_{23}\| = \|e_{32}\|$. Therefore, the desired equilibrium is exponentially stable.

To show *almost* exponential stability, it is required that the fifteen types of the undesired equilibria, corresponding to the critical points of Ψ_{12} and Ψ_{23}, are unstable. This is similar to the proof of the property (iii) of Proposition 4.2, and it is omitted.

□

4.3.2 Relative Attitude Formation Tracking Between n Spacecrafts

Consider a formation of n spacecraft, i.e., $\mathcal{N} = \{1, \ldots, n\}$. According to Assumption 5, spacecraft are paired serially in the edge set. For convenience, it is assumed that spacecraft are numbered such that the edge set is given by

$$\mathcal{E} = \{(1,2), (2,3), \ldots, (n-1, n), (2,1), (3,2), \ldots, (n, n-1)\}. \tag{4.108}$$

The assignment set is given by (4.4) for an arbitrary assignment map satisfying Assumption 2. The desired relative attitudes Q_{ij}^d for $(i,j) \in \mathcal{E}$ are prescribed. Also, recall that the definition of error variables and their properties developed in the Proposition 4.1 of Section 4.2 are ready generalized to any $(i,j,k) \in \mathcal{A}$, and these

generalized variables become

$$e_{ij} = -Q_{ji}^d e_{ji}, \quad \|e_{ij}\| = \|e_{ji}\|, \tag{4.109}$$

$$\dot{\Psi}_{ij} = e_{ij} \cdot e_{\Omega_i} + e_{ji} \cdot e_{\Omega_j}, \tag{4.110}$$

$$\|\dot{e}_{ij}\| \leq (k_{ij}^{\alpha} + k_{ij}^{\beta})(\|e_{\Omega_i}\| + \|e_{\Omega_j}\|) + B^d \|e_{ij}\|, \tag{4.111}$$

$$\underline{\psi}_{ij} \|e_{ij}\|^2 \leq \Psi_{ij} \leq \overline{\psi}_{ij} \|e_{ij}\|^2 \tag{4.112}$$

where $\underline{\psi}_{ij}$ and $\overline{\psi}_{ij}$ are positive constants can be determined, the way to find out these two constants are addressed in the proof section of Proposition 4.1. Moreover, the desired absolute angular velocities Ω_i^d for $i \in \mathcal{N}$ are chosen such that

$$\Omega_{ij}^d(t) = \Omega_i^d(t) - Q_{ji}^d(t)\Omega_j^d(t) \quad \text{for } (i,j) \in \mathcal{E}. \tag{4.113}$$

Proposition 4.4. Consider the attitude dynamics of spacecraft given by (4.7), (4.8) for $i \in \{1, \ldots, n\}$, with the LOS measurements specified by (4.108) and (4.4). Desired relative attitudes are given by $Q_{ij}^d(t)$ for $(i,j) \in \mathcal{E}$. For positive constants $k_{ij}^{\alpha}, k_{ij}^{\beta}, k_{\Omega_i}$ with $k_{ij}^{\alpha} \neq k_{ij}^{\beta}$, $k_{ij}^{\alpha} = k_{ji}^{\alpha}$, $k_{ij}^{\beta} = k_{ji}^{\beta}$, and $p \in \{2, \ldots, n-1\}$, the control inputs are chosen as

$$u_1 = -e_{12} - k_{\Omega_1} e_{\Omega_1} + \hat{\Omega}_1^d J_1 (e_{\Omega_1} + \Omega_1^d) + J_1 \dot{\Omega}_1^d, \tag{4.114}$$

$$u_p = -\frac{1}{2}(e_{p,p-1} + e_{p,p+1}) - k_{\Omega_p} e_{\Omega_p} + \hat{\Omega}_p^d J_p (e_{\Omega_p} + \Omega_p^d) + J_p \dot{\Omega}_p^d, \tag{4.115}$$

$$u_n = -e_{n,n-1} - k_{\Omega_n} e_{\Omega_n} + \hat{\Omega}_n^d J_n (e_{\Omega_n} + \Omega_n^d) + J_n \dot{\Omega}_n^d. \tag{4.116}$$

Next, the desired relative attitude configuration is almost globally exponentially sta-

ble, and a (conservative) estimate to the region of attraction is given by

$$\sum_{i=1}^{n-1} \Psi_{i,i+1}(0) \leq \psi < 2 \min_{1\leq i\leq n-1}\{k^{\alpha}_{i,i+1}, k^{\beta}_{i,i+1}\}, \tag{4.117}$$

$$\lambda_{M_1}\|e_{\Omega_1}(0)\|^2 + 2\sum_{i=2}^{n-1}\lambda_{M_i}\|e_{\Omega_i}(0)\|^2 + \lambda_{M_n}\|e_{\Omega_n}(0)\|^2 \leq 2(\psi - \sum_{i=1}^{n-1}\Psi_{i,i+1}(0)), \tag{4.118}$$

where ψ is a positive constant satisfying $\psi < 2\min_{1\leq i\leq n-1}\{k^{\alpha}_{i,i+1}, k^{\beta}_{i,i+1}\}$.

Proof. The proof of this proposition has been carried out by the proof of Proposition of 4.3 with tedious extension, which is also very similar to the proof of Proposition 4.2. Here we still summarize the essential equations to show the framework.

The time-derivative of J_1e_1 and J_ne_n are specified as follows, which is consistent with (4.65)

$$J_1(\dot{e}_{\Omega_1}) = (J_1e_{\Omega_1} + J_1\Omega_1^d)^{\wedge}e_{\Omega_1} - e_{12} - k_{\Omega_1}e_{\Omega_1}, \tag{4.119}$$

$$J_n(\dot{e}_{\Omega_n}) = (J_ne_{\Omega_n} + J_n\Omega_n^d)^{\wedge}e_{\Omega_n} - e_{n,n-1} - k_{\Omega_n}e_{\Omega_n}, \tag{4.120}$$

while the time-derivative of J_p, for $p \in \{2, \ldots, n-1\}$ is

$$J_p(\dot{e}_{\Omega_p}) = (J_pe_{\Omega_p} + J_p\Omega_{p_d})^{\wedge}e_{\Omega_p} - \frac{1}{2}(e_{p,p-1} + e_{p,p+1}) - k_{\Omega_p}e_{\Omega_p}. \tag{4.121}$$

Define $\mathcal{U} = \mathcal{U}_e + \mathcal{U}_\Psi$ where

$$\mathcal{U}_e = \frac{1}{2}e_{\Omega_1}\cdot J_1e_{\Omega_1} + \frac{1}{2}e_{\Omega_n}\cdot J_ne_{\Omega_n} + \sum_{i=2}^{n-1} e_{\Omega_i}\cdot J_ie_{\Omega_i}, \tag{4.122}$$

$$\mathcal{U}_\Psi = \sum_{i=1}^{n-1}\Psi_{i,i+1}. \tag{4.123}$$

In view of (4.110) and (4.119) through (4.121), the differentiation of $\mathcal{U}$ with respect

to time is

$$\dot{\mathcal{U}} = \dot{\mathcal{U}}_e + \dot{\mathcal{U}}_\Psi = -k_{\Omega_1}\|e_{\Omega_1}\|^2 - k_{\Omega_n}\|e_{\Omega_n}\|^2 - 2\sum_{i=2}^{n-1} k_{\Omega_i}\|e_{\Omega_i}\|^2, \tag{4.124}$$

which shows U is non-decreasing. Then, the Lyapunov candidate is in the form

$$\mathcal{V} = \mathcal{U} + ce_{\Omega_1}\cdot e_{12} + ce_{\Omega_n}\cdot e_{n,n-1} + c\sum_{i=2}^{n-1} e_{\Omega_i}\cdot(e_{i,i-1} + e_{i,i+1}). \tag{4.125}$$

where c is a constant which will be determined later. From (4.112), it is straightforward to show that the Lyapunov function satisfies the inequality given by (4.69).

Furthermore, for $(i,j) \in \{(1,2),(n,n-1)\}$ the upper bound of $\dot{e}_{\Omega_i}\cdot e_{ij}$ is given by (4.74), We rewrite as follows:

$$\dot{e}_{\Omega_1}\cdot e_{12} = \frac{\lambda_{M_1}}{\lambda_{m_1}}(k_{12}^{\alpha} + k_{12}^{\beta})\|e_{\Omega_1}\|^2 + \frac{\lambda_{M_1}B^d + k_{\Omega_1}}{\lambda_{m_1}}\|e_{12}\|\|e_{\Omega_1}\| - \frac{1}{\lambda_{M_1}}\|e_{12}\|^2, \tag{4.126}$$

and

$$\begin{aligned}\dot{e}_{\Omega_n}\cdot e_{n,n-1} = {} & \frac{\lambda_{M_n}}{\lambda_{m_n}}(k_{n,n-1}^{\alpha} + k_{n,n-1}^{\beta})\|e_{\Omega_n}\|^2 + \frac{\lambda_{M_n}B^d + k_{\Omega_n}}{\lambda_{m_n}}\|e_{n,n-1}\|\|e_{\Omega_n}\| \\ & - \frac{1}{\lambda_{M_n}}\|e_{n,n-1}\|^2,\end{aligned} \tag{4.127}$$

while the rest term of $\dot{e}_{\Omega_i}\cdot e_{ij}$ are given by

$$\begin{aligned}\dot{e}_{\Omega_i}\cdot(e_{i,i-1} + e_{i,i+1}) \leq {} & \frac{\lambda_{M_i}}{\lambda_{m_i}}(\overline{k}_{i,i-1} + \overline{k}_{i,i+1})\|e_{\Omega_i}\|^2 + \frac{\lambda_{M_i}B^d + k_{\Omega_i}}{\lambda_{m_i}}\|e_{i,i-1} + e_{i,i+1}\|\|e_{\Omega_i}\| \\ & - \frac{1}{2\lambda_{M_i}}\|e_{i,i-1} + e_{i,i+1}\|^2.\end{aligned} \tag{4.128}$$

The summation of (4.124) and (4.126) through (4.128) is the time-derive of (4.125).

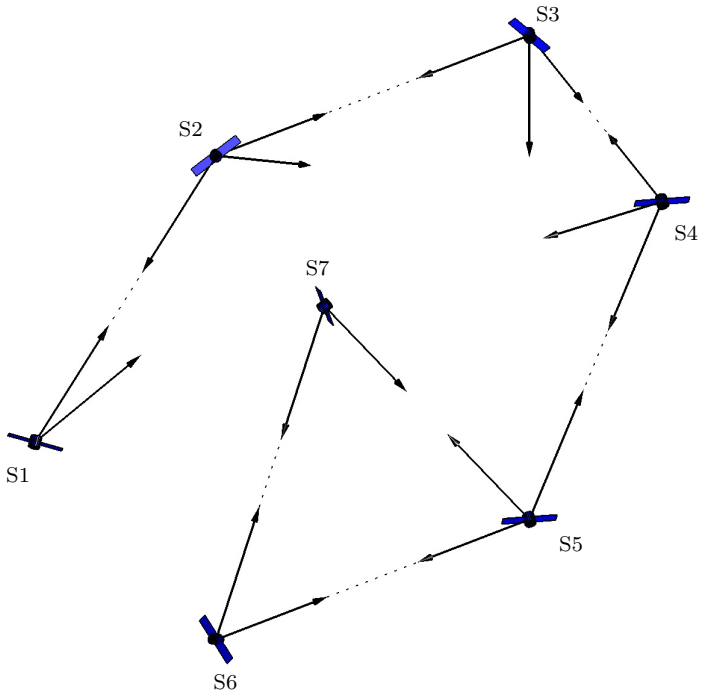

Figure 4.2: Relative attitude formation tracking for 7 spacecraft: the lines-of-sight measured by each spacecraft are denoted by arrows, and the dotted line between two spacecraft implies that they are paired at the edge set.

And it can be rearranged to the matrix form

$$\dot{\mathcal{V}} \leq -z_{12}^{\mathsf{T}} W_{12} z_{12} - z_{n,n-1}^{\mathsf{T}} W_{n,n-1} z_{n,n-1} - \sum_{i=2}^{n-1} z_{i,i-1,i+1}^{\mathsf{T}} W_{i,i-1,i+1} z_{i,i-1,i+1} - \sum_{i=1}^{n-1} \zeta_{i,i+1}^{\mathsf{T}} Z_{i,i+1} \zeta_{i,i+1}, \tag{4.129}$$

where $z_{i,i-1,i+1} = [\|e_{i,i-1} + e_{i,i+1}\|, \|e_{\Omega_i}\|]^{\mathsf{T}} \in \mathbb{R}^2$ and $\zeta_{i,i+1} = [\|e_{\Omega_i}\|, \|e_{\Omega_{i+1}}\|]^{\mathsf{T}}$. With analogous process from (4.79) through (4.81), it can be shown that if the constant c is sufficiently small, all the $\underline{M}$, $\overline{M}$, W, and Z matrices is positive definite. This directly implies that the Lyapunov function $\mathcal{V}$ is positive definite and decrescent and its time-derivative $\dot{\mathcal{V}}$ is negative definite. Thus we conclude the exponential stability of the desired equilibrium.

□

4.4 Numerical Example

Consider the formation of seven spacecraft illustrated at Figure 4.2. The corresponding edge is given by (4.108) with $n = 7$, and the assignment set is

$$\mathcal{A} = \{(1,2,3),(2,1,3),\ (2,3,4),(3,2,4),\ (3,4,5),(4,3,5),$$
$$(4,5,7),(5,4,7),\ (5,6,7),(6,5,7),\ (6,7,5),(7,6,5)\}.$$

The desired relative attitudes for Q_{34}^d and Q_{45}^d are given in terms of 3-2-1 Euler angles as $Q_{34}^d(t) = Q_{34}^d(\alpha(t), \beta(t), \gamma(t))$, $Q_{45}^d(t) = Q_{45}^d(\phi(t), \theta(t), \psi(t))$, where

$$\alpha(t) = \sin 0.5t,\ \beta(t) = 0.1,\ \gamma(t) = \cos t,$$
$$\phi(t) = 0,\ \theta(t) = -0.1 + \cos 0.2t,\ \psi(t) = 0.5 \sin 2t,$$

and $Q_{12}^d(t) = Q_{23}^d(t) = Q_{56}^d(t) = I$, $Q_{67}^d(t) = (Q_{45}^d(t))^{\mathsf{T}}$. It is chosen that $\Omega_4^d(t) = 0$, and other desired absolute angular velocities are selected to satisfy (4.113).

The initial attitudes for Spacecraft 3 and 6 are chosen as $R_3(0) = \exp(0.999\pi\hat{e}_1)$ and $R_6(0) = \exp(0.990\pi\hat{e}_2)$, where $e_1 = [1,0,0]^{\mathsf{T}}, e_2 = [0,1,0]^{\mathsf{T}} \in \mathbb{R}^3$. The initial attitudes for other spacecraft are chosen as the identity matrix. The resulting initial errors for the relative attitudes Q_{23} and Q_{67} are 0.99π rad $= 179.82°$. The initial angular velocity is chosen as zero for every spacecraft.

The inertia matrix is identical, i.e., $J_i = \mathrm{diag}[3,2,1]\,\mathrm{kgm}^2$ for all $i \in \mathcal{N}$. Controller gains are chosen as $k_{\Omega_i} = 7$, $k_{ij}^{\alpha} = 25$, and $k_{ij}^{\beta} = 25.1$ for any $(i,j) \in \mathcal{E}$.

The corresponding numerical results are illustrated at Figures 4.3. Tracking errors for relative attitudes and control inputs are shown at Figure 4.3, where the relative attitude error vectors are defined as $e_{Q_{ij}} = \frac{1}{2}((Q_{ij}^d)^{\mathsf{T}} Q_{ij} - Q_{ij}^{\mathsf{T}} Q_{ij}^d)^{\vee} \in \mathbb{R}^3$. These illustrate good convergence rates. In addition, the corresponding MATLAB code is attached in Appendix C.

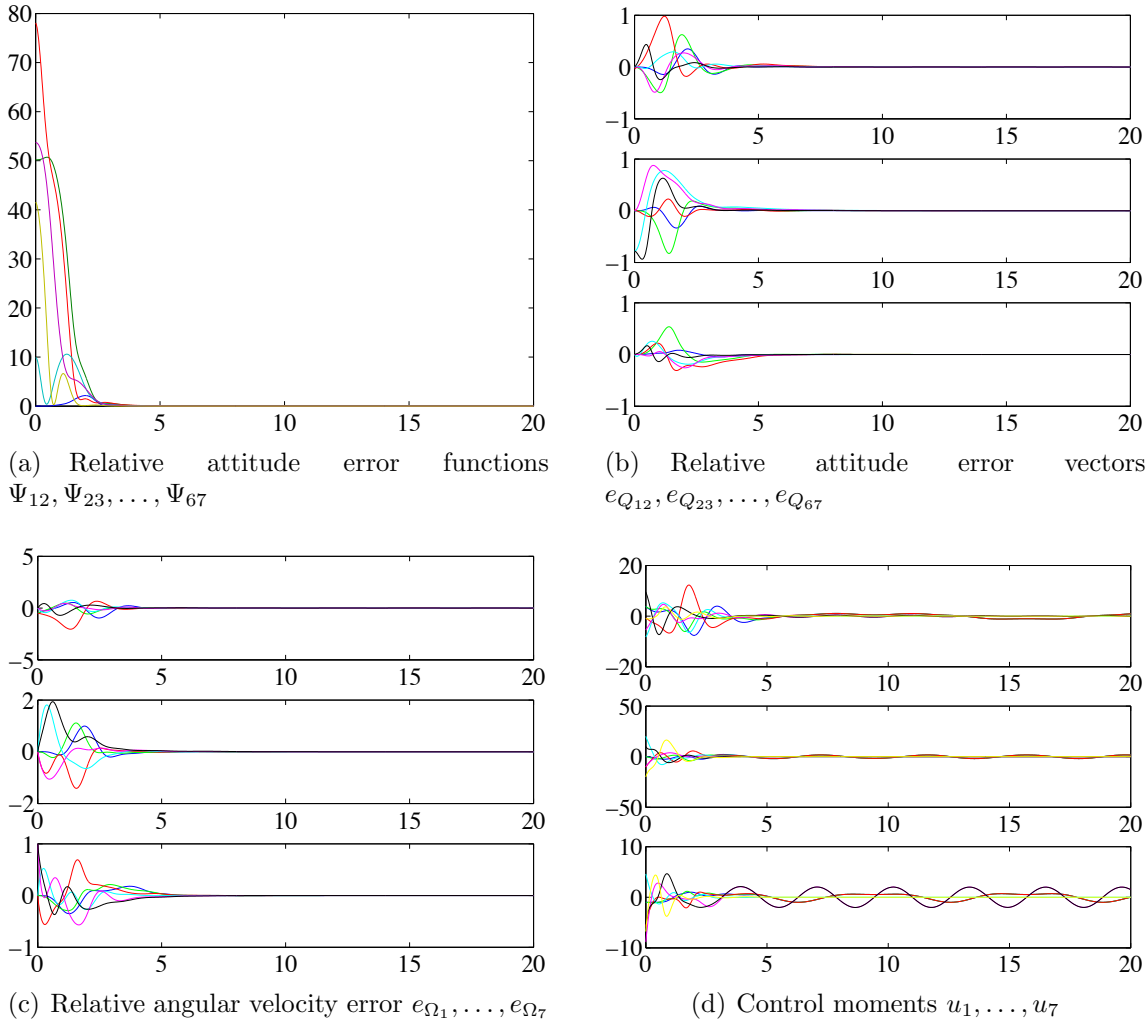

(a) Relative attitude error functions $\Psi_{12}, \Psi_{23}, \ldots, \Psi_{67}$

(b) Relative attitude error vectors $e_{Q_{12}}, e_{Q_{23}}, \ldots, e_{Q_{67}}$

(c) Relative angular velocity error $e_{\Omega_1}, \ldots, e_{\Omega_7}$

(d) Control moments $u_1, \ldots, u_7$

Figure 4.3: Numerical results for seven spacecrafts in formation (blue, green, red, cyan, magenta, and black in ascending order)

Chapter 5 Conclusions

5.1 Concluding Remarks

The current relative attitude control system is unique from the aspect that control inputs are directly expressed in terms of LOS measurements such that determining the full absolute attitude of spacecraft in formation is not required. Relative attitude are directly controlled, and it leads to higher accuracy and a relatively low-cost compare to other attitude determining sensors. Furthermore, the tracking command is allowed to be continuous function of time that gives the flexibility of the formation between each spacecrafts.

Developing attitude control system on $\mathsf{SO(3)}$ avoids complexities of using parameterization method such as Euler angle and quaternions. And even more remarkably, it avoids the singularities and ambiguities that occur in parameterization. Additionally, using unit vectors on S^2 to express LOS measurements is a simpler way to denote directions of spherical pendulum. This feature is more significant where there are multiple spacecraft in the system. Furthermore, the presented stability properties are valid globally fro all possible attitude configurations.

The relative attitude controller on $\mathsf{SO(3)}$ and PD controller on S^2 provide almost global exponential stability which is stronger than asymptotic stability offered by typical Lyapunov-based tracking controller. By definition, asymptotic stability implies attractivity only, i.e., the solution in the region of attraction will converge to equilibrium as time goes to infinity even though the rate of converge may be very

slow. Exponential stability offer a much higher rate of convergence [43]. The PID controller on S^2 does not have exponential stability since the error of integrator does not converge to zero, but it successfully remove the effect of fixed perturbation in the control system, in other words, the controlled system can still perform well even poor estimation of angular velocity is acquired.

5.2 Future Work

Vision-based spacecraft formation control on $\mathsf{SE}(3)$ This thesis explores relative attitude control with LOS measurements, however, the full formation includes not only relative attitude (rotation), but also relative positions (translation). It is possible to extend the vision-based control scheme presented in this thesis to full formation control. Specifically, previous work have shown that the dynamics of a spacecraft can globally expressed in the special Euclidean group, $\mathsf{SE}(3)$ [46], which is the semi-direct product of $\mathbb{R}^3$ and $\mathsf{SO}(3)$. Thus, using vision-based control on $\mathsf{SE}(3)$ for both rotational and translational motion is one of future directions.

Robust Spacecraft formation control The proposed relative attitude formation control system is actually a nonlinear PD controller. As the configuration error vector, e_{ij}, represents the proportional term and the angular velocity error vector ,e_{Ω_i}, corresponds to the derivative term. Based on the unique nonlinear PID controller on S^2 proposed in Chapter 2, it is reasonable to suggest that adding the integral term to the attitude control system of multiple spacecraft in the future to accomplish higher level of performance.

Spacecraft formation control with bounded inputs Throughout this thesis, we do not consider constraints of the control input, however, magnitude of control input may be constrained because the power source in not unlimited in the real

world. Thus, we may use saturation functions to generate bounded control inputs as a solution [47]. This will significantly increase practicability of the controller.

Bibliography

[1] D. P. Scharf, F. Y. Hadaegh, and S. R. Ploen, "A survey of spacecraft formation flying guidance and control. Part II: control," in *America Control Conference*, vol. 4, 2004, pp. 2976–2985.

[2] O. P. Lay, G. H. Blackwood, S. Dubovitsky, P. W. Gorham, and R. P. Linfield, "Design of the ST 3 formation flying interferometer," in *Working on the Fringe: Optical and IR Interferometry from Ground and Space ASP Conference Series*, vol. 194, 1999.

[3] E. S. Agency, "Darwin," October 2009. [Online]. Available: http://www.esa.int/esaSC/120382_index_0_m.html

[4] M. L. Mitchell, "CDGPS-based relative navigation for multiple spacecraft," Ph.D. dissertation, Massachusetts Institute of Technology, 2004.

[5] F. H. Bauer, K. Hartman, J. P. How, J. Bristow, D. Weidow, and F. Busse, "Enabling spacecraft formation flying through spaceborne GPS and enhanced automation technologies," in *ION-GPS Conference*, 1999, pp. 167–172.

[6] A. Khosravian and M. Namvarn, "Rigid body attitude control using a single vector measurement and gyro," *IEEE Transactions on Automatic Control*, vol. 57, no. 5, pp. 1273–1279, 2012.

[7] G. G. Scandaroli, P. Morlin, and G. Silveira, "A nonlinear observer approach for concurrent estimation of pose, IMU bias and camera-to-IMU rotation," in *IEEE/RSJ International Conference on Intelligent Robots and systems*, 2011, pp. 3335–33 341.

[8] G. N. DeSouza and A. C. Kak, "Vision for mobile robot navigation: a survey," *IEEE Transactions on Pattern Analysis and Machine Intelligence*, vol. 24, no. 2, pp. 237–267, 2002.

[9] J. A. Guerrero and R. Lozano, *Flight Formation Control*. Hoboken: John Wiley & Sons, 2012.

[10] T. Lee, "Relative attitude control of two spacecraft on SO(3) using line-of-sight observations," in *America Control Conference*, 2012, pp. 167–172.

[11] M. D. Shuster, "A survey of attitude representations," *The Journal of Astronautical Sciences*, vol. 41, no. 4, pp. 439–517, 1993.

[12] B. Zhang and S. Song, "Robust attitude coordination control of formation flying spacecraft under control input saturation," *International Journal of Innovative Computing, Information and Control*, vol. 7, no. 7, pp. 4223–4235, 2011.

[13] A. K. Bondhus, K. Y. Pettersen, and J. T. Gravdahl, "Leader/follower synchronization of satellite attitude without angular velocity measurements," in *IEEE Conference on Decision and Control, and the European Control Conference*, 2005, pp. 7270–7277.

[14] N. Chaturvedi, A. Sanyal, and N. McClamroch, "Rigid-body attitude control," *IEEE Control Systems Magazine*, vol. 31, no. 3, pp. 30–51, 2011.

[15] O. O. Gutirrez, C. A. Ibez, and H. Sossa, "Stabilization of the inverted spherical pendulum via Lyapunov approach," *Asian Journal of Control*, vol. 11, no. 6, pp. 587–594, 2009.

[16] K. Furuta, "Control of pendulum: from super mechano-system to human adaptive mechatronics," in *Proceedings of the 42nd IEEE onference on Decision and Control*, vol. 2, 2003, pp. 1498–1507.

[17] A. Shiriaev1, A. Pogromsky, H. Ludvigsen, and O. Egeland, "On global properties of passivity-based control of an inverted pendulum," *International Journal of Robust and Nonlinear Control*, pp. 283–200, 2000.

[18] T. Lee, M. Leok, and N. H. McClamroch, "Lagrangian mechanics and variational integrators on two-spheres," *International Journal for Numerical Methods in Engineering*, vol. 79, no. 9, pp. 1147–1174, 2009.

[19] J. Shen, A. K. Sanyal, N. A. Chaturvedi, D. Bernstein, and H. McClamroch, "Dynamics and control of a 3D rigid pendulum," in *IEEE Conference on Decision and Control*, vol. 1, 2004, pp. 323–328.

[20] N. A. Chaturvedi, F. Bacconi, A. K. Sanyal, D. Bernstein, and N. H. McClamroch, "Stabilization of a 3D rigid pendulum," in *America Control Conference*, vol. 5, 2005, pp. 3030–3035.

[21] A. D. Anderson, J. I. Sellers, and Y. Hashida, "Attitude determination and control system simulation and analysis for low-cost micro-satellites," in *America Control Conference*, vol. 5, 2004, pp. 2935–3949.

[22] F. Lizarralde and J. T. Wen, "Attitude control without angular velocity measurement: a passivity approach," *IEEE Transactions on Automatic Control*, vol. 41, no. 3, pp. 468–472, 1996.

[23] C. G. Mayhew, R. G. Sanfelice, and A. R. Teel, "Neural network-based distributed attitude coordination control for spacecraft formation flying with input saturation," *IEEE Transactions on Neural Networks and Learning Systems*, vol. 23, no. 7, pp. 1155–1162, 2012.

[24] ——, "Quaternion-based hybrid control for robust global attitude tracking," *IEEE Transactions on Automatic Control*, vol. 56, no. 11, pp. 2555–2566, 2011.

[25] S. P. Bhat and D. S. Bernstein, "A topological obstruction to continuous global stabilization of rotational motion and the unwinding phenomenon," *Systems and Control Letters*, vol. 39, no. 1, pp. 63–70, 2000.

[26] T. Lee, "Geometric tracking control of the attitude dynamics of a rigid body on SO(3)," in *America Control Conference*, 2011, pp. 1200–12 055.

[27] T. Lee, M. Leok, and N. H. McClamroch, "Stable manifolds of saddle equilibria for pendulum dynamics on S2 and SO(3)," in *Decision and Control and European Control Conference*, 2011, pp. 3915–3921.

[28] S. Bertrand, T. Hamel, H. Piet-Lahanier, and R. Mahony, "Attitude tracking of rigid bodies on the special orthogonal group with bounded partial state feedback," in *IEEE Conference on Decision and Control Conference*, 2009, pp. 2972–2977.

[29] R. Mahony, T. Hamel, and J. Pflimlin, "Nonlinear complementary filters on the special orthogonal group," *IEEE Transactions on Automatic Control*, vol. 53, no. 5, pp. 1200–1211, 2008.

[30] J. A. Fax and R. M. Murray, "Information flow and cooperative control of vehicle formations," *IEEE Transactions on Automatic Control*, vol. 49, no. 9, pp. 1465–1476, 2004.

[31] A. Jadbabaie, J. Lin, and A. S. Morse, "Coordination of groups of mobile autonomous agents using nearest neighbor rules," *IEEE Transactions on Automatic Control*, vol. 48, no. 6, pp. 2953–2958, 2003.

[32] W. Kang and H.-H. Yeh, "Co-ordinated attitude control of multi-satellite systems," *International Journal of Robust and Nonlinear Control*, vol. 12, pp. 185–205, 2002.

[33] T. Balch and R. C. Arkin, "Behavior-based formation control for multirobot teams," *IEEE Transactions on Robotics Automation*, vol. 14, no. 6, pp. 926–939, 1998.

[34] R. W. Beard, J. Lawton, and F. Y. Hadaegh, "A coordination architecture for spacecraft formation control," *IEEE Transactions on Control Systems and Technology*, vol. 9, no. 6, pp. 777–790, 2001.

[35] W. Ren and R. Beard, "Formation feedback control for multiple spacecraft via virtual structures," *IEE Proceedings-Control Theory and Applications*, vol. 151, no. 3, pp. 357–368, 2004.

[36] W. Ren and R. W. Beard, "Virtual structure based spacecraft formation control with formation feedback," in *AIAA Guidance, Navigation, and Control Conference and Exhibit*, 2002.

[37] Z.-H. Zhou, J. Yuan, W.-X. Zhang, and J.-P. Zhao, "Virtual-leader-follower structure and finite-time controller based cooperative control of multiple autonomous underwater vehicles," in *IEEE Control and Decision Conference*, 2012, pp. 3670–3675.

[38] P. Corke, *Robotics, Vision and Control: Fundamental Algorithms in MATLAB*. Berlin: Springer-Verlag, 2011.

[39] Y. Wang, W. Yan, and W. Yan, "A leader-follower formation control strategy for auvs based on line-of-sight guidance," in *IEEE International Conference on Mechatronics and Automation*, 2009, pp. 4863–4867.

[40] M. S. Andrle, J. L. Crassidis, R. Linares, Y. Cheng, and B. Hyun, "Deterministic relative attitude determination of three-vehicle formations," *Journal of Guidance, Control, and Dynamics*, vol. 32, no. 4, pp. 1077–1088, 2009.

[41] R. Linares, J. L. Crassidis, and Y. Cheng, "Constrained relative attitude determination for two-vehicle formations," *Journal of Guidance, Control, and Dynamics*, vol. 34, no. 2, pp. 543–553, 2011.

[42] D. E. Koditschek, "Application of a new lyapunov function to global adaptive attitude tracking," in *IEEE Conference on Decision and Control*, vol. 1, 1988, pp. 63–68.

[43] H. K. Khalil, *Nonlinear Systems*. Upper Saddle River: Prentice Hall, 2001.

[44] T. Fernando, J. Chandiramani, T. Lee, and H. Gutierrez, "Robust adaptive geometric tracking controls on $SO(3)$ with an application to the attitude dynamics of a quadrotor UAV," in *Decision and Control and European Control Conference*, 2011, pp. 7380–7385.

[45] F. Bullo and A. D. Lewis, *Geometric Control of Mechanical Systems*. New York-Heidelberg-Berlin: Springer Verlag, 2004.

[46] T. Lee, M. Leok, and N. H. McClamroch, "Geometric tracking control of a quadrotor uav on SE(3)," in *IEEE Conference on Decision and Control*, 2010, pp. 5420–5425.

[47] J. Moreno-Valenzuela, V. Santibez, and R. Campa, "On output feedback tracking control of robot manipulators with bounded torque input," *International Journal of Control, Automation, and Systems*, vol. 6, no. 1, pp. 76–85, 2008.

[48] G. Strang, *Linear Algebra and Its Applications*. Belmont: Brooks/Cole, 2006.

Appendix A Hat Map Identities

The hat map $\wedge : \mathbb{R}^3 \to \mathfrak{so}(3)$ transforms a vector in $\mathbb{R}^3$ to a 3×3 skew-symmetric matrix where $\mathfrak{so}(3)$ is the vector space of skew-symmetric matrices in $\mathbb{R}^{3\times 3}$ [14], and it is Lie algebra of $\mathsf{SO}(3)$:

$$\mathfrak{so}(3) = \{\hat{x} \in \mathbb{R}^{3\times 3} \mid \hat{x}^{\mathsf{T}} = -\hat{x}\}.$$

On the contrary, the inverse of the hat map is defined by the vee map $\vee : \mathfrak{so}(3) \to \mathbb{R}^3$.

To illustrate the idea, we first define $x, y \in \mathbb{R}^3$

$$x = \begin{bmatrix} x_1 \\ x_2 \\ x_3 \end{bmatrix}, \quad y = \begin{bmatrix} y_1 \\ y_2 \\ y_3 \end{bmatrix},$$

then the cross product of x and y can be expressed as

$$x \times y = \begin{bmatrix} x_2y_3 - x_3y_2 \\ x_3y_1 - x_1y_3 \\ x_1y_2 - x_2y_1 \end{bmatrix} = \begin{bmatrix} 0 & -x_3 & x_2 \\ x_3 & 0 & -x_1 \\ -x_2 & x_1 & 0 \end{bmatrix} \begin{bmatrix} y_1 \\ y_2 \\ y_3 \end{bmatrix} = \hat{x}y.$$

Thus, we have

$$\hat{x} = \begin{bmatrix} 0 & -x_3 & x_2 \\ x_3 & 0 & -x_1 \\ -x_2 & x_1 & 0 \end{bmatrix} = -\hat{x}^{\mathsf{T}} \in \mathfrak{so}(3). \tag{A.1}$$

There are few properties of the hat map are summarized as follows:

$$\hat{x}y = x \times y = -y \times x = -\hat{y}x, \tag{A.2}$$

$$\widehat{x \times y} = \hat{x}\hat{y} - \hat{y}\hat{x} = yx^{\mathsf{T}} - xy^{\mathsf{T}}, \tag{A.3}$$

$$R\hat{x}R^{\mathsf{T}} = (Rx)^{\wedge}, \tag{A.4}$$

$$x \cdot \hat{y}z = y \cdot \hat{z}x = z \cdot \hat{x}y, \tag{A.5}$$

$$\hat{x}\hat{y}z = x \times (y \times z) = (x \cdot z)y - (x \cdot y)z, \tag{A.6}$$

$$\hat{x}\hat{y}z - \hat{z}\hat{y}x = \hat{y}\hat{x}z, \tag{A.7}$$

$$\frac{1}{2}\mathrm{tr}[\hat{x}\hat{y}] = -x^{\mathsf{T}}y, \tag{A.8}$$

$$\mathrm{tr}[\hat{x}A] = \frac{1}{2}\mathrm{tr}[\hat{x}(A - A^{\mathsf{T}})] = -x^{\mathsf{T}}(A - A^{\mathsf{T}})^{\vee}, \tag{A.9}$$

for any $A \in \mathbb{R}^{3\times3}$, $R \in \mathsf{SO(3)}$. The sum of the diagonal entries of matrix A is equal to the sum of eigenvalues of A and it is defined as trace of A, denoted by $\mathrm{tr}[A]$.

Appendix B The Spectral Theorem

From Chapter 5 of [48], the spectral theorem states the fact that any real symmetric matrix $K \in \mathbb{R}^{n\times n}$ can be factored into $K = UGU^{\mathsf{T}}$. It's orthonormal eigenvectors are column vectors of the orthogonal matrix $U \in \mathbb{R}^{n\times n}$ and its eigenvalues are the elements of diagonal of $G \in \mathbb{R}^{n\times n}$ with every other elements are zero. The matrix form of the spectral theorem can be specified as

$$\begin{aligned} K = UGU^{\mathsf{T}} &= \begin{bmatrix} | & & | \\ x_1 & \cdots & x_n \\ | & & | \end{bmatrix} \begin{bmatrix} \lambda_1 & & \\ & \ddots & \\ & & \lambda_n \end{bmatrix} \begin{bmatrix} - & x_1^{\mathsf{T}} & - \\ & \vdots & \\ - & x_n^{\mathsf{T}} & - \end{bmatrix} \\ &= \lambda_1 x_1 x_1^{\mathsf{T}} + \lambda_2 x_2 x_2^{\mathsf{T}} + \cdots + \lambda_n x_n x_n^{\mathsf{T}}, \end{aligned} \tag{B.1}$$

where x_1, x_2,...$x_n \in \mathbb{R}^n$ and λ_1, λ_2,...$\lambda_n \in \mathbb{R}$ are the orthonormal eigenvectors and eigenvalues of a n by n symmetric matrix K, respectively.

Appendix C MATLAB Codes

The following is the MATLAB code for numerical simulation in Chapter 4.

```
function seven_spacecraft  %% Main function %%
filename='seven';
close all;
global J1 J2 J3 J4 J5 J6 J7
global s12 s21 s23 s32 s34 s43 s45 s54 s56 s65 s67 s76
global s13 s24 s35 s47 s57 s75
global kO1 kO2 kO3 kO4 kO5 kO6 kO7
global K12a K12b K23a K23b K34a K34b K45a K45b K56a K56b K67a K67b
global cc12 cc23 cc34 cc45 cc56 cc67
J1=[3 0 0; 0 2 0; 0 0 1];    %Inertia matrix
J2=J1; J3=J1; J4=J1; J5=J1; J6=J1; J7=J1;
s1=[-1 0.1 0]'; s2=[-0.5 0 1/sqrt(2)]'; s3=[0.5 0 1/sqrt(2)]';
s4=[1 0.1 0]'; s5=[0.5 0 -1/sqrt(2)]';  s6=[-0.5 0.0 -1/sqrt(2)]';
s7=[0 0.2 0]';
s12=(s2-s1)/norm(s2-s1); s13=(s3-s1)/norm(s3-s1);
s23=(s3-s2)/norm(s3-s2); s24=(s4-s2)/norm(s4-s2);
s34=(s4-s3)/norm(s4-s3); s35=(s5-s3)/norm(s5-s3);
s45=(s5-s4)/norm(s5-s4); s47=(s7-s4)/norm(s7-s4);
s56=(s6-s5)/norm(s6-s5); s57=(s7-s5)/norm(s7-s5);
s67=(s7-s6)/norm(s7-s6);

s21=-s12; s31=-s13;
s32=-s23; s42=-s24;
s43=-s34; s53=-s35;
s54=-s45; s74=-s47;
s65=-s56; s75=-s57; s76=-s67;
s123=cross(s12,s13); s213=cross(s21,s23); cc12=norm(s123)*norm(s213);
s234=cross(s23,s24); s324=cross(s32,s34); cc23=norm(s234)*norm(s324);
s345=cross(s34,s35); s435=cross(s43,s45); cc34=norm(s345)*norm(s435);
s457=cross(s45,s47); s547=cross(s54,s57); cc45=norm(s457)*norm(s547);
s567=cross(s56,s57); s657=cross(s65,s67); cc56=norm(s567)*norm(s657);
s675=cross(s67,s65); s765=cross(s76,s75); cc67=norm(s675)*norm(s765);

%k (w=3, eta=0.7, kO=2*eta*omega, ka=w^2)
```

```
w=5; eta=0.7;
kO1=2*w*eta;  kO2=2*w*eta;    kO3=2*w*eta;   kO4=2*w*eta;
kO5=2*w*eta;  kO6=2*w*eta;    kO7=2*w*eta;
K12a=w^2;     K12b=w^2+0.1;   K23a=w^2;      K23b=w^2+0.1;
K34a=w^2;     K34b=w^2+0.1;   K45a=w^2;      K45b=w^2+0.1;
K56a=w^2;     K56b=w^2+0.1;   K67a=w^2;      K67b=w^2+0.1;

tstart=0;
tend=20;
n=1001; %time step
tspan=linspace(tstart,tend,n);
%initial value of Omega1
OO1=[0 0 0].';  OO2=[0 0 0].'; OO3=[0 0 0].';  OO4=[0 0 0].';
OO5=[0 0 0].';  OO6=[0 0 0].'; OO7=[0 0 0].';
%initial value of R, it should still be a rotation matrix
RR1=[1 0 0 0 1 0 0 0 1].';
RR2=[1 0 0 0 1 0 0 0 1].';
RR3=reshape(expm(0.999*pi*hat([1 0 0])),9,1);
RR4=[1 0 0 0 1 0 0 0 1].';
RR5=[1 0 0 0 1 0 0 0 1].';
RR6=reshape(expm(0.999*pi*hat([0 1 0])),9,1);
RR7=[1 0 0 0 1 0 0 0 1].';

xinit=[OO1;OO2;OO3;OO4;OO5;OO6;OO7;RR1;RR2;RR3;RR4;RR5;RR6;RR7];
OdeOption=odeset('RelTol',1e-8,'AbsTol',1e-8);
[t,x]=ode45(@pid_SOTeom,tspan,xinit);

R1=zeros(3,3,n); R2=R1; R3=R1; R4=R1; R5=R1; R6=R1; R7=R1;
Q12d=R1;  Q23d=R1;  Q34d=R1;  Q45d=R1;  Q56d=R1;  Q67d=R1;
dQ12d=R1; dQ23d=R1; dQ34d=R1; dQ45d=R1; dQ56d=R1; dQ67d=R1;
u1=zeros(3,n); u2=u1; u3=u1; u4=u1; u5=u1; u6=u1; u7=u1;
Omega12d=u1; Omega23d=u1;  Omega34d=u1;  Omega45d=u1;  Omega56d=u1;
Omega67d=u1; dOmega12d=u1; dOmega23d=u1; dOmega34d=u1; dOmega45d=u1;
dOmega56d=u1; dOmega67d=u1;
eOM1=u1; eOM2=u1; eOM3=u1; eOM4=u1; eOM5=u1; eOM6=u1; eOM7=u1;
eQ12=u1; eQ23=u1; eQ34=u1; eQ45=u1; eQ56=u1; eQ67=u1;
Psi12=zeros(1,n); Psi23=Psi12; Psi34=Psi12; Psi45=Psi12;
Psi56=Psi12; Psi67=Psi12;

for k=1:n
    R1(:,:,k)=reshape(x(k,22:30),3,3);
    R2(:,:,k)=reshape(x(k,31:39),3,3);
    R3(:,:,k)=reshape(x(k,40:48),3,3);
    R4(:,:,k)=reshape(x(k,49:57),3,3);
    R5(:,:,k)=reshape(x(k,58:66),3,3);
```

```
    R6(:,:,k)=reshape(x(k,67:75),3,3);
    R7(:,:,k)=reshape(x(k,76:84),3,3);
    [Q12d(:,:,k) dQ12d(:,:,k) Omega12d(:,k) dOmega12d(:,k)...
        Q23d(:,:,k) dQ23d(:,:,k) Omega23d(:,k) dOmega23d(:,k)...
        Q34d(:,:,k) dQ34d(:,:,k) Omega34d(:,k) dOmega34d(:,k)...
        Q45d(:,:,k) dQ45d(:,:,k) Omega45d(:,k) dOmega45d(:,k)...
        Q56d(:,:,k) dQ56d(:,:,k) Omega56d(:,k) dOmega56d(:,k)...
        Q67d(:,:,k) dQ67d(:,:,k) Omega67d(:,k) dOmega67d(:,k)]...
        = desire(t(k));
    [u1(:,k) u2(:,k) u3(:,k) u4(:,k) u5(:,k) u6(:,k) u7(:,k)...
        Psi12(k) Psi23(k) Psi34(k) Psi45(k) Psi56(k) Psi67(k)...
        eOM1(:,k) eOM2(:,k) eOM3(:,k) eOM4(:,k) ...
        eOM5(:,k) eOM6(:,k) eOM7(:,k)...
        eQ12(:,k) eQ23(:,k) eQ34(:,k)...
        eQ45(:,k) eQ56(:,k) eQ67(:,k)...
        Omega1d(:,k) Omega2d(:,k) Omega3d(:,k) Omega4d(:,k)...
        Omega5d(:,k) Omega6d(:,k) Omega7d(:,k) dOmega1d(:,k)...
        dOmega2d(:,k) dOmega3d(:,k) dOmega4d(:,k) dOmega5d(:,k)...
        dOmega6d(:,k) dOmega7d(:,k)] = controller(t(k),x(k,:)');
end

W1=x(:,1:3);   W2=x(:,4:6);   W3=x(:,7:9);  W4=x(:,10:12);
W5=x(:,13:15); W6=x(:,16:18); W7=x(:,19:21);

figure;
plot(t,Psi12,t,Psi23,t,Psi34,t,Psi45,t,Psi56,t,Psi67);

figure;
for ff=1:3;
  subplot(3,1,ff);
  for aa=1:6;
    eval(['plot(t,eOM' num2str(aa) '(' num2str(ff) ',:));']);
    hold on;
  end
end

figure;
for ff=1:3;
  subplot(3,1,ff);
  for aa=1:5;
      eval(['plot(t,eQ' num2str(aa) num2str(aa+1)...
      '(' num2str(ff) ',:));']);
      hold on;
  end
end
```

```
save(filename);
evalin('base','clear all;')
evalin('base',['load ' filename ';']);  % load results to workspace
end

%% Second Function
function [dx] = pid_SOTeom(t,x) %% Sub function %%
global J1 J2 J3 J4 J5 J6 J7;
%angular velocity, Omega(BFF)
Om1=x(1:3);   Om2=x(4:6);   Om3=x(7:9);   Om4=x(10:12);
Om5=x(13:15); Om6=x(16:18); Om7=x(19:21);
%Omega1 hat
Om1h=hat(Om1); Om2h=hat(Om2); Om3h=hat(Om3); Om4h=hat(Om4);
Om5h=hat(Om5); Om6h=hat(Om6); Om7h=hat(Om7);
R1=reshape(x(22:30),3,3); %Rotation matrix
R2=reshape(x(31:39),3,3);
R3=reshape(x(40:48),3,3);
R4=reshape(x(49:57),3,3);
R5=reshape(x(58:66),3,3);
R6=reshape(x(67:75),3,3);
R7=reshape(x(76:84),3,3);
[u1 u2 u3 u4 u5 u6 u7]=controller(t,x);

%% Equation of Motion
dOm1=J1 (u1-cross(Om1,J1*Om1));
dOm2=J2 (u2-cross(Om2,J2*Om2));
dOm3=J3 (u3-cross(Om3,J3*Om3));
dOm4=J4 (u4-cross(Om4,J4*Om4));
dOm5=J5 (u5-cross(Om5,J5*Om5));
dOm6=J6 (u6-cross(Om6,J6*Om6));
dOm7=J7 (u7-cross(Om7,J7*Om7));
dR1=R1*Om1h; dR2=R2*Om2h; dR3=R3*Om3h; dR4=R4*Om4h;
dR5=R5*Om5h; dR6=R6*Om6h; dR7=R7*Om7h;
dR1a=reshape(dR1,9,1); dR2a=reshape(dR2,9,1);
dR3a=reshape(dR3,9,1); dR4a=reshape(dR4,9,1);
dR5a=reshape(dR5,9,1); dR6a=reshape(dR6,9,1);
dR7a=reshape(dR7,9,1);
dx=[dOm1;dOm2;dOm3;dOm4;dOm5;dOm6;dOm7;...
    dR1a;dR2a;dR3a;dR4a;dR5a;dR6a;dR7a];
end


%% Sub-sub-routine
function [Q12d dQ12d Omega12d dOmega12d Q23d dQ23d Omega23d ...
 dOmega23d Q34d dQ34d Omega34d dOmega34d Q45d dQ45d Omega45d...
```

```
 dOmega45d Q56d dQ56d Omega56d dOmega56d Q67d dQ67d Omega67d...
 dOmega67d]= desire(t)

Q12d=eye(3); dQ12d=zeros(3); Omega12d=[0 0 0]'; dOmega12d=[0 0 0]';
Q23d=eye(3); dQ23d=zeros(3); Omega23d=[0 0 0]'; dOmega23d=[0 0 0]';

% Euler angle: gamma beta alpha
alpha=sin(0.5*t); dalpha=0.5*cos(0.5*t); ddalpha=-(0.5^2)*sin(0.5*t);
beta=0.1;         dbeta=0;               ddbeta=0;
gamma=cos(t);     dgamma=-sin(t);        ddgamma=-cos(t);

[Q34d dQ34d Omega34d dOmega34d]=Eu2Rot(alpha,dalpha,ddalpha,...
beta,dbeta,ddbeta,gamma,dgamma,ddgamma);

alpha=0;             dalpha=0;              ddalpha=0;
beta=-0.1+cos(0.2*t); dbeta=-0.2*sin(0.2*t); ddbeta=-(0.2)^2*cos(0.2*t);
gamma=0.5*sin(2*t);   dgamma=0.5*2*cos(2*t); ddgamma=-0.5*2*2*sin(2*t);

[Q45d dQ45d Omega45d dOmega45d]=Eu2Rot(alpha,dalpha,ddalpha,...
beta,dbeta,ddbeta,gamma,dgamma,ddgamma);

Q56d=eye(3);  dQ56d=zeros(3); Omega56d=[0 0 0]';  dOmega56d=[0 0 0]';
Q67d=Q45d';   dQ67d=dQ45d';   Omega67d=-Q67d'*Omega45d;
dOmega67d=-dQ67d'*Omega45d-Q67d'*dOmega45d;
end

function [Q dQ W dW]=...
Eu2Rot(alpha,dalpha,ddalpha,beta,dbeta,ddbeta,gamma,dgamma,ddgamma)
e1=[1 0 0]'; e2=[0 1 0]'; e3=[0 0 1]';
he1=hat(e1); he2=hat(e2); he3=hat(e3); %e3 hat

ea=expm(gamma*he3);  eb=expm(beta*he2);  ec=expm(alpha*he1);
dea=(dgamma*he3)*ea; deb=(dbeta*he2)*eb; dec=(dalpha*he1)*ec;
ddea =(ddgamma*he3)*ea+(dgamma*he3)*dea;
ddeb =(ddbeta*he2)*eb+(dbeta*he2)*deb;
ddec =(ddalpha*he1)*ec+(dalpha*he1)*dec;

Q=ea*eb*ec;
dQ=dea*eb*ec + ea*deb*ec + ea*eb*dec;

ddQ1=ddea*eb*ec + dea*deb*ec + dea*eb*dec;
ddQ2=dea*deb*ec + ea*ddeb*ec + ea*deb*dec;
ddQ3=dea*eb*dec + ea*deb*dec + ea*eb*ddec;
ddQ =ddQ1+ddQ2+ddQ3;
```

```
W=vee(Q'*dQ);
dW=vee(dQ'*dQ+Q'*ddQ);
end

%% Controller
function [u1 u2 u3 u4 u5 u6 u7...
Psi12 Psi23 Psi34 Psi45 Psi56 Psi67...
eOM1 eOM2 eOM3 eOM4 eOM5 eOM6 eOM7...
eQ12 eQ23 eQ34 eQ45 eQ56 eQ67 ...
Omega1d Omega2d Omega3d Omega4d Omega5d Omega6d Omega7d ...
dOmega1d dOmega2d dOmega3d dOmega4d dOmega5d dOmega6d...
dOmega7d ] = controller(t,x)
global J1 J2 J3 J4 J5 J6 J7
global s12 s21 s23 s32 s34 s43 s45 s54 s56 s65 s67 s76
global s13 s24 s35 s47 s57 s75
global kO1 kO2 kO3 kO4 kO5 kO6 kO7
global K12a K12b K23a K23b K34a K34b K45a K45b K56a K56b K67a K67b
global VS MAGN BeaconLocs
global cc12 cc23 cc34 cc45 cc56 cc67

Om1=x(1:3); Om2=x(4:6); Om3=x(7:9); Om4=x(10:12); %Omega
Om5=x(13:15); Om6=x(16:18); Om7=x(19:21);
R1=reshape(x(22:30),3,3); %Rotation matrix
R2=reshape(x(31:39),3,3);
R3=reshape(x(40:48),3,3);
R4=reshape(x(49:57),3,3);
R5=reshape(x(58:66),3,3);
R6=reshape(x(67:75),3,3);
R7=reshape(x(76:84),3,3);
Q12=(R2.')*R1; Q23=(R3.')*R2; Q34=(R4.')*R3; %Q
Q45=(R5.')*R4; Q56=(R6.')*R5; Q67=(R7.')*R6;

[Q12d dQ12d Omega12d dOmega12d...
    Q23d dQ23d Omega23d dOmega23d Q34d dQ34d Omega34d dOmega34d...
    Q45d dQ45d Omega45d dOmega45d Q56d dQ56d Omega56d dOmega56d...
    Q67d dQ67d Omega67d dOmega67d] = desire(t);

b12=(R1')*s12; b13=(R1')*s13;
b21=(R2')*s21; b23=(R2')*s23; b24=(R2')*s24;
b32=(R3')*s32; b34=(R3')*s34; b35=(R3')*s35;
b43=(R4')*s43; b47=(R4')*s47;
b45=(R4')*s45;
b54=(R5')*s54; b56=(R5')*s56; b57=(R5')*s57;
b65=(R6')*s65; b67=(R6')*s67;
b75=(R7')*s75; b76=(R7')*s76;
```

```
b123=cross(b12,b13); b213=cross(b21,b23);
psi12a=1-dot(b21,(-Q12d*b12)); psi12b=1-(1/cc12)*dot(Q12d*b123,-b213);
Psi12=(K12a*psi12a)+(K12b*psi12b);

b234=cross(b23,b24); b324=cross(b32,b34);
psi23a=1-dot(b32,(-Q23d*b23)); psi23b=1-(1/cc23)*dot(Q23d*b234,-b324);
Psi23=(K23a*psi23a)+(K23b*psi23b);

b345=cross(b34,b35); b435=cross(b43,b45);
psi34a=1-dot(b43,(-Q34d*b34)); psi34b=1-(1/cc34)*dot(Q34d*b345,-b435);
Psi34=(K34a*psi34a)+(K34b*psi34b);

b457=cross(b45,b47);     b547=cross(b54,b57);
psi45a=1-dot(b54,(-Q45d*b45)); psi45b=1-(1/cc45)*dot(Q45d*b457,-b547);
Psi45=(K45a*psi45a)+(K45b*psi45b);

b567=cross(b56,b57);     b657=cross(b65,b67);
psi56a=1-dot(b65,(-Q56d*b56)); psi56b=1-(1/cc56)*dot(Q56d*b567,-b657);
Psi56=(K56a*psi56a)+(K56b*psi56b);

b675=cross(b67,b65);     b765=cross(b76,b75);
psi67a=1-dot(b76,(-Q67d*b67)); psi67b=1-(1/cc67)*dot(Q67d*b675,-b765);
Psi67=(K67a*psi67a)+(K67b*psi67b);

e12a = cross( ((Q12d.')*b21),b12 );  %e_12^alpha
e21a = cross( (Q12d*b12),b21 );      %e_21^alpha
e12b = cross( ( (1/cc12)*(Q12d.')*b213 ),b123 );  %e_12^beta
e21b = cross( ( (1/cc12)*Q12d*b123 ),b213 );      %e_21^beta
e12 = (K12a*e12a)+(K12b*e12b); %e_12
e21 = (K12a*e21a)+(K12b*e21b); %e_21

e23a = cross( ((Q23d.')*b32),b23 );  %e_23^alpha
e32a = cross( (Q23d*b23),b32 );
e23b = cross( ((1/cc23)*(Q23d.')*b324),b234 );  %e_23^beta
e32b = cross( ((1/cc23)*Q23d*b234),b324 );      %e_32^beta
e23 = (K23a*e23a)+(K23b*e23b); %e_23
e32 = (K23a*e32a)+(K23b*e32b); %e_32

e34a = cross( ((Q34d.')*b43),b34 );  %e_34^alpha
e43a = cross( (Q34d*b34),b43 );      %e_43^alpha
e34b = cross( ( (1/cc34)*(Q34d.')*b435 ),b345 );  %e_34^beta
e43b = cross( ( (1/cc34)*Q34d*b345 ),b435 );      %e_43^beta
e34 = (K34a*e34a)+(K34b*e34b); %e_34
e43 = (K34a*e43a)+(K34b*e43b); %e_43
```

```
e45a=cross(((Q45d.')*b54),b45);
e54a=cross((Q45d*b45),b54);
e45b=cross(((1/cc45)*(Q45d.')*b547),b457);
e54b=cross(((1/cc45)*Q45d*b457),b547);
e45 = (K45a*e45a)+(K45b*e45b);
e54 = (K45a*e54a)+(K45b*e54b);

e56a = cross( ((Q56d.')*b65),b56 );
e65a = cross( (Q56d*b56),b65 );
e56b = cross( ( (1/cc56)*(Q56d.')*b657 ),b567 );
e65b = cross( ( (1/cc56)*Q56d*b567 ),b657 );
e56 = (K56a*e56a)+(K56b*e56b);
e65 = (K56a*e65a)+(K56b*e65b);

e67a = cross( ((Q67d.')*b76),b67 );
e76a = cross( (Q67d*b67),b76 );
e67b = cross( ( (1/cc67)*(Q67d.')*b765 ),b675 );
e76b = cross( ( (1/cc67)*Q67d*b675 ),b765 );
e67 = (K67a*e67a)+(K67b*e67b);
e76 = (K67a*e76a)+(K67b*e76b);

Omega3d=Omega34d;   dOmega3d=dOmega34d;
Omega4d=[0 0 0]';   dOmega4d=[0 0 0]';
Omega2d=Q23d'*Omega3d;  dOmega2d=dQ23d'*Omega3d+Q23d'*dOmega3d;
Omega1d=Q12d'*Omega2d;  dOmega1d=dQ12d'*Omega2d+Q12d'*dOmega2d;
Omega5d=-Q45d*Omega45d; dOmega5d=-dQ45d*Omega45d-Q45d*dOmega45d;
Omega6d=Q56d*Omega5d;   dOmega6d=dQ56d*Omega5d+Q56d*dOmega5d;
Omega7d=Q67d*(Omega6d-Omega67d);
dOmega7d=dQ67d*(Omega6d-Omega67d)+Q67d*(dOmega6d-dOmega67d);
eOM1=Om1-Omega1d; eOM2=Om2-Omega2d; eOM3=Om3-Omega3d;
eOM4=Om4-Omega4d; eOM5=Om5-Omega5d; eOM6=Om6-Omega6d;
eOM7=Om7-Omega7d;

A1=cross(Omega1d, J1*(eOM1+Omega1d));
A2=cross(Omega2d, J2*(eOM2+Omega2d));
A3=cross(Omega3d, J3*(eOM3+Omega3d));
A4=cross(Omega4d, J4*(eOM4+Omega4d));
A5=cross(Omega5d, J5*(eOM5+Omega5d));
A6=cross(Omega6d, J2*(eOM6+Omega6d));
A7=cross(Omega7d, J7*(eOM7+Omega7d));
B1=J1*dOmega1d; B2=J2*dOmega2d; B3=J3*dOmega3d; B4=J4*dOmega4d;
B5=J5*dOmega5d; B6=J6*dOmega6d; B7=J7*dOmega7d;

u1=-e12-kO1*eOM1+A1+B1;          u7=-e76-kO7*eOM7+A7+B7;
```

```
u2=-(e21+e23)/2-kO2*eOM2+A2+B2; u3=-(e32+e34)/2-kO3*eOM3+A3+B3;
u4=-(e43+e45)/2-kO4*eOM4+A4+B4; u5=-(e54+e56)/2-kO5*eOM5+A5+B5;
u6=-(e65+e67)/2-kO6*eOM6+A6+B6;

eQ12=vee( 1/2*( (Q12d.')*Q12-(Q12.')*Q12d ) );
eQ23=vee( 1/2*( (Q23d.')*Q23-(Q23.')*Q23d ) );
eQ34=vee( 1/2*( (Q34d.')*Q34-(Q34.')*Q34d ) );
eQ45=vee( 1/2*( (Q45d.')*Q45-(Q45.')*Q45d ) );
eQ56=vee( 1/2*( (Q56d.')*Q56-(Q56.')*Q56d ) );
eQ67=vee( 1/2*( (Q67d.')*Q67-(Q67.')*Q67d ) );
end

function x=vee(X)
x=[X(3,2) X(1,3) X(2,1)]';
end

function Y=hat(y)
Y=[0 -y(3) y(2); y(3) 0 -y(1); -y(2) y(1) 0];
end
```